NSP-74-103
Revision 1
November 1982
30.2874.0103

MONTICELLO NUCLEAR GENERATING PLANT
PLANT UNIQUE ANALYSIS REPORT
VOLUME 3
VENT SYSTEM ANALYSIS

Prepared for:
Northern States Power Company

Prepared by:
NUTECH Engineers, Inc.
San Jose, California

Prepared by:

Dr. T. I. Hsu, P.E.
Project Engineer

Approved by:

I. D. McInnes, P.E.
Engineering Manager

Approved by:

T. J. Wenner, P.E.
Engineering Director

Issued by:

M. F. Aleksey
Project Manager

T. J. Mulford
Project Director

8212210333 821215
PDR ADOCK 05000263
P PDR

nutech ENGINEERS

REVISION CONTROL SHEET

TITLE: Monticello Nuclear Generating Plant
Plant Unique Analysis Report
Volume 3

REPORT NUMBER: NSP-74-103
Revision 1

J. C. Attwood/Senior Consultant	JCA INITIALS
A. J. Chao/Specialist	AJC INITIALS
H. K. Fatehi/Specialist	HKF INITIALS
T. I. Hsu/Senior Engineer	TIH INITIALS
S. Y. Kung/Consultant I	SYK INITIALS
I. D. McInnes/Principal Engineer	IDM INITIALS
K. A. Para/Technician II	KAP INITIALS
S. P. Quinn/Senior Technician	SPQ INITIALS
M. A. Rupersburg/Specialist	MAR INITIALS
J. K. Smith/Engineering Manager	JKS INITIALS
W. J. Steffey/Senior Engineer	WJS INITIALS

nutech ENGINEERS

REVISION CONTROL SHEET

(Continued)

TITLE: Monticello Nuclear Generating Plant
Plant Unique Analysis Report
Volume 3

REPORT NUMBER: NSP-74-103
Revision 1

EFFECTIVE PAGE(S)	REV	PREPARED	ACCURACY CHECK	CRITERIA CHECK	EFFECTIVE PAGE(S)	REV	PREPARED	ACCURACY CHECK	CRITERIA CHECK
3-vi	0	JKS	TIH	TIH	3-2.25	0	TIH	JKS	JKS
3-vii		JKS			3-2.26				
3-viii		JKS			3-2.27				
3-ix		JKS	TIH	TIH	3-2.28				
3-x		TIH	Kap	Kap	3-2.29				
3-xi					3-2.30				
3-xii		TIH	WJS	WJS	3-2.31				
3-xiii					3-2.32				
3-xiv					3-2.33				
3-xv					3-2.34				
3-1.1		JKS	TIH	TIH	3-2.35				
3-1.2					3-2.36				
3-1.3					3-2.37				
3-1.4					3-2.38				
3-1.5					3-2.39				
3-1.6					3-2.40				
3-1.7					3-2.41				
					3-2.42				
3-2.1					3-2.43				
3-2.2		WJS	TIH	JKS	3-2.44				
3-2.3					3-2.45				
3-2.4					3-2.46				
3-2.5					3-2.47				
3-2.6					3-2.48				
3-2.7					3-2.49				
3-2.8					3-2.50				
3-2.9					3-2.51				
3-2.10			JKS	TIH	3-2.52				
3-2.11					3-2.53				
3-2.12					3-2.54		Kap	TIH	TIH
3-2.13					3-2.55				
3-2.14					3-2.56				
3-2.15					3-2.57				
3-2.16					3-2.58		WJS		
3-2.17					3-2.59		WJS		
3-2.18					3-2.60		Kap	HKF	HKF
3-2.19					3-2.61			WJS	
3-2.20					3-2.62			WJS	
3-2.21					3-2.63			SYK	TIH
3-2.22					3-2.64		WJS		
3-2.23					3-2.65		WJS		
3-2.[illegible]	0	TIH		JKS	3-2.66	0	WJS		

QEP-001.4-0[illegible]

nutech ENGINEERS

REVISION CONTROL SHEET
(Continued)

TITLE: Monticello Nuclear Generating Plant
Plant Unique Analysis Report
Volume 3

REPORT NUMBER: NSP-74-103
Revision 1

EFFECTIVE PAGE(S)	REV	PREPARED	ACCURACY CHECK	CRITERIA CHECK	EFFECTIVE PAGE(S)	REV	PREPARED	ACCURACY CHECK	CRITERIA CHECK
3-2.67	0	KAP	WJS	SYK	3-2.108	0	TIH	JKS	JKS
3-2.68		HKF	SYK	HKF	3-2.109				
3-2.69			TIH	TIH	3-2.110				
3-2.70					3-2.111				
3-2.71					3-2.112		WJS	TIH	TIH
3-2.72					3-2.113		WJS	TIH	TIH
3-2.73		WJS			3-2.114		TIH	JKS	JKS
3-2.74		WJS			3-2.115				
3-2.75		KAP	WJS	SYK	3-2.116				
3-2.76			SYK	HKF	3-2.117				
3-2.77			WJS	TIH	3-2.118				
3-2.78			SYK	TIH	3-2.119				
3-2.79			WJS		3-2.120				
3-2.80			WJS		3-2.121				
3-2.81					3-2.122				
3-2.82			SYK		3-2.123				
3-2.83					3-2.124				
3-2.84					3-2.125				
3-2.85					3-2.126				
3-2.86					3-2.127				
3-2.87					3-2.128				
3-2.88			TIH		3-2.129				
3-2.89					3-2.130				
3-2.90		WJS			3-2.131				
3-2.91		WJS			3-2.132				
3-2.92		KAP	WJS		3-2.134				
3-2.93		TIH	JKS	JKS	3-2.135				
3-2.94					3-2.136		KAP	WJS	TIH
3-2.95					3-2.137				
3-2.96					3-2.138				
3-2.97					3-2.139		WJS	TIH	
3-2.98					3-2.140		KAP		
3-2.99					3-2.141			SYK	
3-2.100					3-2.142				
3-2.101		KAP	WJS	TIH	3-2.143				
3-2.102					3-2.144				
3-2.103					3-2.145				
3-2.104					3-2.146				
3-2.105			TIH	JKS	3-2.147				
3-2.106					3-2.148				
3-2.107					3-2.149				
	0					0			

QEP-001.4-00

nutech ENGINEERS

REVISION CONTROL SHEET
(Concluded)

TITLE: Monticello Nuclear Generating Plant Plant Unique Analysis Report Volume 3

REPORT NUMBER: NSP-74-103 Revision 1

EFFECTIVE PAGE(S)	REV	PREPARED	ACCURACY CHECK	CRITERIA CHECK
3-2.150	0	KAP	SYK	TIH
3-2.151		TIH	JKS	JKS
3-2.152				
3-2.153				
3-2.154				
3-2.155				
3-2.156		KAP	WJS	TIH
3-2.157		TIH	JKS	JKS
3-2.158				
3-2.159				
3-2.160				
3-2.161				
3-2.162				
3-2.163				
3-2.164		KAP	TIH	TIH
3-2.165		TIH	JKS	JKS
3-2.166				
3-2.167				
3-2.168				
3-2.169		WJS	TIH	TIH
3-2.170		TIH	JKS	JKS
3-2.171		TIH	JKS	JKS
3-2.172		AJC	TIH	TIH
3-2.173		HKF	IDM	
3-2.174			TIH	
3-2.175		MAR	SYK	
3-2.176		TIH	JKS	JKS
3-2.177		IDM	HKF	TIH
3-2.178		TIH	JKS	JKS
3-2.179		MAR	SYK	TIH
3-2.180		JCR	TIH	
3-2.181			KAP	
3-2.182				
3-2.183				JKS
3-2.184		TIH	JKS	
3-2.185				
3-2.186				
3-2.187				
3-2.188				
3-3.1	0			

EFFECTIVE PAGE(S)	REV	PREPARED	ACCURACY CHECK	CRITERIA CHECK
3-v	1	TIH	SYK	IDM
3-xv				
3-2.6				
3-2.16				
3-2.50				
3-2.51				
3-2.52				
3-2.53				
3-2.69				
3-2.70				
3-2.79				
3-2.123				
3-2.143				
3-2.144				
3-2.145				
3-2.146				
3-2.147				
3-2.148				
3-2.149				
3-2.150				
3-2.170				
3-2.171				
3-2.177				
3-3.1	1			

QEP-001.4-06

nutech ENGINEERS

ABSTRACT

The primary containment for the Monticello Nuclear Generating Plant was designed, erected, pressure-tested, and ASME Code N-stamped during the late 1960's for the Northern States Power Company by the Chicago Bridge and Iron Company. Since that time new requirements have been generated. These requirements affect the design and operation of the primary containment system and are defined in the Nuclear Regulatory Commission's Safety Evaluation Report NUREG-0661. The requirements to be addressed include an assessment of additional containment design loads postulated to occur during a loss-of-coolant accident or a safety relief valve discharge event, as well as an assessment of the effects that these postulated events have on the operational characteristics of the containment system.

This plant unique analysis report documents the efforts undertaken to address and resolve each of the applicable NUREG-0661 requirements, and demonstrates, in accordance with NUREG-0661 acceptance criteria, that the design of the primary containment system is adequate and that original design safety margins have been restored. The report is composed of the following five volumes.

- Volume 1 - GENERAL CRITERIA AND LOADS METHODOLOGY
- Volume 2 - SUPPRESSION CHAMBER ANALYSIS
- Volume 3 - VENT SYSTEM ANALYSIS
- Volume 4 - INTERNAL STRUCTURES ANALYSIS
- Volume 5 - SAFETY RELIEF VALVE DISCHARGE LINE PIPING ANALYSIS

Volume 3 documents the evaluation of the vent system and has been prepared by NUTECH Engineers, Incorporated (NUTECH), acting as an agent to the Northern States Power Company.

TABLE OF CONTENTS

			Page
ABSTRACT			3-vi
LIST OF ACRONYMS			3-viii
LIST OF TABLES			3-x
LIST OF FIGURES			3-xiii
3-1.0	INTRODUCTION		3-1.1
	3-1.1	Scope of Analysis	3-1.3
	3-1.2	Summary and Conclusions	3-1.5
3-2.0	VENT SYSTEM ANALYSIS		3-2.1
	3-2.1	Component Description	3-2.2
	3-2.2	Loads and Load Combinations	3-2.24
		3-2.2.1 Loads	3-2.25
		3-2.2.2 Load Combinations	3-2.93
	3-2.3	Analysis Acceptance Criteria	3-2.108
	3-2.4	Methods of Analysis	3-2.115
		3-2.4.1 Analysis for Major Loads	3-2.116
		3-2.4.2 Analysis for Asymmetric Loads	3-2.151
		3-2.4.3 Analysis for Local Effects	3-2.157
		3-2.4.4 Methods for Evaluating Analysis Results	3-2.165
	3-2.5	Analysis Results	3-2.170
		3-2.5.1 Discussion of Analysis Results	3-2.183
		3-2.5.2 Closure	3-2.186
3-3.0	LIST OF REFERENCES		3-3.1

LIST OF ACRONYMS

ADS	Automatic Depressurization System
ACI	American Concrete Institute
AISC	American Institute of Steel Construction
ASME	American Society of Mechanical Engineers
CDF	Cumulative Distribution Function
CO	Condensation Oscillation
DC	Downcomer
DC/VH	Downcomer/Vent Header
DBA	Design Basis Accident
DBE	Design Basis Earthquake
DLF	Dynamic Load Factor
FSAR	Final Safety Analysis Report
FSI	Fluid-Structure Interaction
FSTF	Full-Scale Test Facility
IBA	Intermediate Break Accident
LDR	Load Definition Report
LOCA	Loss-of-Coolant Accident
MJ	Miter Joint
MVA	Multiple Valve Actuation
NEP	Non-Exceedance Probability
NOC	Normal Operating Condition
NRC	Nuclear Regulatory Commission

LIST OF ACRONYMS
(Concluded)

NVB	Non-Vent Line Bay
OBE	Operating Basis Earthquake
PUA	Plant Unique Analysis
PUAAG	Plant Unique Analysis Application Guide
PUAR	Plant Unique Analysis Report
PULD	Plant Unique Load Definition
QSTF	Quarter-Scale Test Facility
RPV	Reactor Pressure Vessel
RSEL	Resultant-Static-Equivalent Load
SBA	Small Break Accident
SRSS	Square Root of the Sum of the Squares
SRV	Safety Relief Valve
SRVDL	Safety Relief Valve Discharge Line
SSE	Safe Shutdown Earthquake
SVA	Single Valve Actuation
TAP	Torus-Attached Piping
VB	Vent Line Bay
VH	Vent Header
VL	Vent Line
VL/VH	Vent Line/Vent Header

LIST OF TABLES

Number	Title	Page
3-2.2-1	Vent System Component Loading Information	3-2.55
3-2.2-2	Suppression Pool Temperature Response Analysis Results - Maximum Temperatures	3-2.56
3-2.2-3	Vent System Pressurization and Thrust Loads For DBA Event	3-2.57
3-2.2-4	Pool Swell Impact Loads for Vent Line	3-2.58
3-2.2-5	Pool Swell Impact, Froth Impingement, and Pool Fallback Loads for Vacuum Breaker System	3-2.59
3-2.2-6	Downcomer Longitudinal Bracing and Tie Rods Pool Swell Drag and Fallback Submerged Structure Load Distribution	3-2.60
3-2.2-7	Support Column LOCA Air and Water Clearing Submerged Structure Load Distribution	3-2.61
3-2.2-8	Downcomer LOCA Air Clearing Submerged Structure Load Distribution	3-2.62
3-2.2-9	Downcomer Longitudinal Bracing and Tie Rods LOCA Air Clearing Submerged Structure Load Distribution	3-2.63
3-2.2-10	IBA Condensation Oscillation Downcomer Loads	3-2.64
3-2.2-11	DBA Condensation Oscillation Downcomer Loads	3-2.65
3-2.2-12	IBA and DBA Condensation Oscillation Vent System Internal Pressures	3-2.66
3-2.2-13	Support Column DBA Condensation Oscillation Submerged Structure Load Distribution	3-2.67
3-2.2-14	Downcomer Longitudinal Bracing and Tie Rods DBA Condensation Oscillation Submerged Structure Load Distribution	3-2.68

LIST OF TABLES
(Continued)

Number	Title	Page
3-2.2-15	Maximum Downcomer Chugging Load Determination	3-2.69
3-2.2-16	Multiple Downcomer Chugging Load Magnitude Determination	3-2.70
3-2.2-17	Chugging Lateral Loads for Multiple Downcomers - Maximum Overall Effects	3-2.71
3-2.2-18	Chugging Lateral Loads on Two Downcomers - Maximum Local Effects	3-2.72
3-2.2-19	Load Reversal Histogram for Chugging Downcomer Lateral Load Fatigue Evaluation	3-2.73
3-2.2-20	Chugging Vent System Internal Pressures	3-2.74
3-2.2-21	Support Column Pre-Chug Submerged Structure Load Distribution	3-2.75
3-2.2-22	Downcomer Longitudinal Bracing and Tie Rods Pre-Chug Submerged Structure Load Distribution	3-2.76
3-2.2-23	Support Column Post-Chug Submerged Structure Load Distribution	3-2.77
3-2.2-24	Downcomer Longitudinal Bracing and Tie Rods Post-Chug Submerged Structure Load Distribution	3-2.78
3-2.2-25	Support Column SRV Discharge Submerged Structure Load Distribution	3-2.79
3-2.2-26	Downcomer SRV Discharge Submerged Structure Load Distribution	3-2.80
3-2.2-27	Downcomer Longitudinal Bracing and Tie Rods SRV Discharge Submerged Structure Load Distribution	3-2.81
3-2.2-28	Mark I Containment Event Combinations	3-2.101
3-2.2-29	Controlling Vent System Load Combinations	3-2.102

LIST OF TABLES
(Concluded)

Number	Title	Page
3-2.2-30	Enveloping Logic for Controlling Vent System Load Combinations	3-2.104
3-2.3-1	Allowable Stresses for Vent System Components and Component Supports	3-2.112
3-2.3-2	Allowable Displacements and Cycles for Vent Line Bellows	3-2.114
3-2.4-1	Vent System Frequency Analysis Results With Water Inside Downcomers	3-2.136
3-2.4-2	Vent System Frequency Analysis Results Without Water Inside Downcomer	3-2.137
3-2.5-1	Major Vent System Component Maximum Membrane Stresses for Governing Loads	3-2.172
3-2.5-2	Maximum Column Reactions for Governing Vent System Loads	3-2.173
3-2.5-3	Maximum Vent Line-Drywell Penetration Reactions for Governing Vent System Loads	3-2.174
3-2.5-4	Maximum Vent Line Bellows Displacements For Governing Vent System Loads	3-2.175
3-2.5-5	Maximum Vent System Stresses For Controlling Load Combinations	3-2.176
3-2.5-6	Maximum Vent Line-SRV Piping Penetration Stresses for Controlling Load Combinations	3-2.178
3-2.5-7	Maximum Vent Line Bellows Differential Displacements for Controlling Load Combinations	3-2.179
3-2.5-8	Maximum Fatigue Usage Factors For Vent System Components and Welds	3-2.180

LIST OF FIGURES

Number	Title	Page
3-2.1-1	Plan View of Containment	3-2.10
3-2.1-2	Elevation View of Containment	3-2.11
3-2.1-3	Suppression Chamber Section - Midbay Vent Line Bay	3-2.12
3-2.1-4	Suppression Chamber Section - Miter Joint	3-2.13
3-2.1-5	Suppression Chamber Section - Midbay Non-Vent Line Bay	3-2.14
3-2.1-6	Developed View of Suppression Chamber Segment	3-2.15
3-2.1-7	Vent Line Details - Upper End	3-2.16
3-2.1-8	SRV Penetration in Vent Line	3-2.17
3-2.1-9	Vent Line-SRV Piping Penetration Nozzle Details	3-2.18
3-2.1-10	Vent Line-Vent Header Intersection Details	3-2.19
3-2.1-11	Developed View of Downcomer Bracing System	3-2.20
3-2.1-12	Downcomer-to-Vent Header Intersection Details	3-2.21
3-2.1-13	Vent Header Support Column Ring Plate Details	3-2.22
3-2.1-14	Vent System Support Column Details	3-2.23
3-2.2-1	Vent System Internal Pressures For SBA Event	3-2.82
3-2.2-2	Vent System Internal Pressures for IBA Event	3-2.83
3-2.2-3	Vent System Internal Pressures for DBA Event	3-2.84
3-2.2-4	Vent System Temperatures for SBA Event	3-2.85

LIST OF FIGURES
(Continued)

Number	Title	Page
3-2.2-5	Vent System Temperatures for IBA Event	3-2.86
3-2.2-6	Vent System Temperatures for DBA Event	3-2.87
3-2.2-7	Downcomer Pool Swell Impact Loads	3-2.88
3-2.2-8	Pool Swell Impact Loads for Vent Header Deflectors at Selected Locations	3-2.89
3-2.2-9	Downcomer Longitudinal Bracing and Tie Rods	3-2.90
3-2.2-10	IBA and DBA Condensation Oscillation Downcomer Differential Pressure Load Distribution	3-2.91
3-2.2-11	Pool Acceleration Profile for Dominant Suppression Chamber Frequency at Midbay Location	3-2.92
3-2.2-12	Vent System SBA Event Sequence	3-2.105
3-2.2-13	Vent System IBA Event Sequence	3-2.106
3-2.2-14	Vent System DBA Event Sequence	3-2.107
3-2.4-1	Vent System 1/16 Segment Beam Model - Isometric View	3-2.138
3-2.4-2	Vent Line-Drywell Penetration Axisymmetric Finite Difference Model - View of Typical Meridian	3-2.139
3-2.4-3	Vent Line-Vent Header Intersection Finite Element Model	3-2.140
3-2.4-4	Vacuum Breaker Penetration Finite Element Model	3-2.141
3-2.4-5	Downcomer-Vent Header Intersection Finite Element Model - Isometric View	3-2.142
3-2.4-6	Harmonic Analysis Results for Support Column Submerged Structure Load Frequency Determination	3-2.143

LIST OF FIGURES
(Concluded)

Number	Title	Page
3-2.4-7	Harmonic Analysis Results for Downcomer Submerged Structure Load Frequency Determination	3-2.144
3-2.4-8	Harmonic Analysis Results for Tie Rods Submerged Structure Load Frequency Determination	3-2.145
3-2.4-9	Harmonic Analysis Results for Longitudinal Bracing Submerged Structure Load Frequency Determination	3-2.146
3-2.4-10	Harmonic Analysis Results for Condensation Oscillation Downcomer Load Frequency Determination	3-2.147
3-2.4-11	Harmonic Analysis Results for Condensation Oscillation Vent System Pressure Load Frequency Determination	3-2.148
3-2.4-12	Harmonic Analysis Results for Chugging Downcomer Lateral Load Frequency Determination	3-2.149
3-2.4-13	Harmonic Analysis Results for Chugging Vent System Pressure Load Frequency Determination	3-2.150
3-2.4-14	Vent System 180° Beam Model - Isometric View	3-2.156
3-2.4-15	SRV Piping-Vent Line Penetration Finite Element Model - Isometric View	3-2.164
3-2.4-16	Allowable Number of Stress Cycles For Vent System Fatigue Evaluation	3-2.169
3-2.5-1	Vent System Support Column Response Due to Pool Swell Impact Loads - Outside Column	3-2.181
3-2.5-2	Vent System Support Column Response Due to Pool Swell Impact Loads - Inside Column	3-2.182

3-1.0 INTRODUCTION

In conjunction with Volume 1 of the Plant Unique Analysis Report (PUAR), this volume documents the efforts undertaken to address the NUREG-0661 requirements which affect the Monticello vent system. The vent system PUAR is organized as follows.

- o INTRODUCTION
  - Scope of Analysis
  - Summary and Conclusions
- o VENT SYSTEM ANALYSIS
  - Component Description
  - Loads and Load Combinations
  - Analysis Acceptance Criteria
  - Methods of Analysis
  - Analysis Results

The INTRODUCTION section contains an overview of the scope of the vent system evaluation, as well as a summary of the conclusions derived from the comprehensive evaluation of the vent system. The VENT SYSTEM ANALYSIS section contains a comprehensive discussion of the vent system loads and load combinations and a description of the components of the vent system

affected by these loads. The section also contains a discussion of the methodology used to evaluate the effects of these loads, the associated evaluation results, and the acceptance limits to which the results are compared.

3-1.1 Scope of Analysis

The criteria presented in Volume 1 are used as the basis for the Monticello vent system evaluation. The modified vent system is evaluated for the effects of LOCA-related loads and SRV discharge-related loads defined by the NRC Safety Evaluation Report NUREG-0661 (Reference 1) and the "Mark I Containment Program Load Definition Report" (LDR) (Reference 2).

The LOCA and SRV discharge loads used in this evaluation are formulated using the methodology discussed in Volume 1 of this report. The loads are developed using the plant unique geometry, operating parameters, and test results contained in the Plant Unique Load Definition (PULD) report (Reference 3). The effects of increased suppression pool temperatures which occur during SRV discharge events are also evaluated. These temperatures are taken from the plant's suppression pool temperature response analysis. Other loads and methodology, such as the evaluation for seismic loads, are taken from the plant's Final Safety Analysis Report (FSAR) (Reference 4).

The evaluation includes performing a structural analysis of the vent system for the effects of LOCA and SRV discharge-related loads to confirm that the design of the vent system is adequate. Rigorous analytical techniques are used in this evaluation, including the use of detailed analytical models for computing the dynamic response of the vent system. Effects such as local penetration and intersection flexibilities are considered in the vent system analysis.

The results of the structural evaluation for each load are used to evaluate load combinations and fatigue effects for the vent system in accordance with the "Mark I Containment Program Structural Acceptance Criteria Plant Unique Analysis Application Guide" (PUAAG) (Reference 5). The analysis results are compared with the acceptance limits specified by the PUAAG and the applicable sections of the ASME Code (Reference 6).

3-1.2 Summary and Conclusions

The evaluation documented in this volume is based on the modified Monticello vent system described in Section 1-2.1. The overall load-carrying capacity of the modified vent system and its supports is substantially greater than that of the original suppression chamber design described in the plant's FSAR.

The loads considered in the original design of the vent system include dead weight loads, OBE and DBE loads, thrust loads, and pressure and temperature loads associated with normal operating conditions (NOC) and a postulated LOCA event. Additional loadings, which affect the design of the vent system, are postulated to occur during SBA, IBA, or DBA LOCA events and during SRV discharge events. These loadings are defined generically in NUREG-0661. These events result in impact and drag loads on vent system components above the suppression pool, in hydrodynamic internal pressure loadings on the vent system, in hydrodynamic drag loadings on the submerged components of the vent system, and in motion and reaction loadings caused by loads acting on structures attached to the vent system.

Section 1-4.0 discusses the methodology used to develop plant unique loadings for the vent system evaluation. Applying this methodology results in conservative values for each of the significant NUREG-0661 loadings which envelop those postulated to occur during an actual LOCA or SRV discharge event.

The LOCA and SRV discharge-related loads are grouped into event combinations using the NUREG-0661 criteria discussed in Section 1-3.2. The event sequencing and event combinations specified and evaluated envelop the actual events postulated to occur throughout the life of the plant.

Some of the loads contained in the postulated event combinations are major contributors to the total response of the vent system. These include pressurization and thrust loads, pool swell impact loads, condensation oscillation downcomer loads, and chugging downcomer lateral loads. Although considered in the evaluation, other loadings, such as internal pressure loads, temperature loads, seismic loads, froth impingement and fallback loads, submerged structure loads, and containment motion and reaction loads, have a lesser effect on the total response of the vent system.

The vent system evaluation is based on the NUREG-0661 acceptance criteria discussed in Section 1-3.2. These acceptance limits are at least as restrictive as those used in the original vent system design documented in the plant's FSAR. Use of these criteria ensures that the original vent system design margins have been restored.

The controlling event combinations for the vent system are those which include the loadings found to be major contributors to the response of the vent system. The evaluation results for these event combinations show that all of the vent system stresses and support reactions are within acceptable limits.

As a result, the modified vent system described in Section 1-2.1 is adequate to restore the margins of safety inherent in the original design of the vent system documented in the plant's FSAR. The intent of the NUREG-0661 requirements, as they affect the design adequacy and safe operation of the Monticello vent system, are considered to be met.

3-2.0 VENT SYSTEM ANALYSIS

Evaluations of each of the NUREG-0661 requirements which affect the design adequacy of the Monticello vent system are presented in the following sections. The criteria used in this evaluation are contained in Volume 1 of this report.

Section 3-2.1 describes the vent system components examined. Section 3-2.2 describes and presents the loads and load combinations for which the vent system is evaluated. Section 3-2.4 discusses the analysis methodology used to evaluate the effects of these loads and load combinations on the vent system. The acceptance limits to which the analysis results are compared, discussed, and presented are in Section 3-2.3. Section 3-2.5 presents the analysis results and the corresponding vent system design margins.

3-2.1 Component Description

The Monticello vent system is constructed from cylindrical shell segments joined together to form a manifold-like structure which connects the drywell to the suppression chamber. Figures 3-2.1-1 and 3-2.1-2 show the configuration of the vent system. The major components of the vent system include the vent lines, vent header, and downcomers. Figures 3-2.1-3 through 3-2.1-6 show the proximity of the vent system to other components of the containment.

The eight vent lines connect the drywell to the vent header in alternate mitered cylinders of the suppression chamber. The vent lines are nominally 1/4" thick and have an inside diameter of 6'9". The upper ends of the vent lines include a conical transition segment at the penetration to the drywell (Figure 3-2.1-7). The drywell shell around each vent line-drywell penetration varies from 3/4" to 1-1/4" thick and is reinforced with a 2-1/2" thick insert plate and 3" thick cylindrical nozzle. The vent lines are shielded from jet impingement loads at each vent line-drywell penetration location by jet deflectors which span the openings of the vent lines. The lower ends of the vent lines are con-

nected to the vent header in the manner of a penstock (Figure 3-2.1-8).

The SRV piping is routed from the drywell through the vent line and penetrates the vent lines inside the suppression chamber (Figures 3-2.1-7 through 3-2.1-10). The vent lines and SRV discharge piping lines are reinforced at each penetration location by a 2-1/2" thick insert plate and a 13-1/2" OD, 2-1/2" thick section of piping at each penetration. The vent line-SRV piping penetration assembly provides an effective means of transferring loads acting on the SRV piping to the vent line.

The vent header is a continuous assembly of mitered cylindrical shell segments joined together to form a ring header (Figure 3-2.1-1). The vent header is 1/4" thick and has an inside diameter of 4'9". At the vent line-vent header intersection, the vent header segments connect to a transition weldment that in turn connects to the vent line. Additional stiffening for the vent line-vent header intersection is provided by 1" thick plates attached to the transition weldment.

A total of 96 downcomers penetrate the vent header in pairs (Figures 3-2.1-1 and 3.2.1-11). Two downcomer pairs are located in each vent line bay and four pairs are located in each non-vent line bay. Each downcomer consists of an inclined segment which penetrates the vent header and a vertical segment which terminates below the surface of the suppression pool (Figure 3-2.1-12). The inclined segment is 3/8" thick and the vertical segment is 1/4" thick. Both segments have 1'11-1/2" inside diameters.

Full penetration welds connect the vent lines to the drywell, the vent lines to the vent header, and the downcomers to the vent header. As such, the connections of the major components of the vent system are capable of developing the full capacity of the associated major components themselves.

The intersections of the downcomers and the vent header are reinforced with a system of stiffener plates and bracing members (Figures 3-2.1-11 and 3-2.1-12). In the plane of the downcomers, the intersections are stiffened by a pair of 1/2" gusset plates located between each set of the downcomers and a pair of 2-1/2" pipe members at the bottom of each set of two downcomers. The gusset

plates are welded both to the tangent points of the downcomer legs and to the vent header. The pipe members are welded to the downcomer legs near the tangent points. The system of stiffener plates is designed to reduce local intersection stresses caused by loads acting in the plane of the downcomers. The system of pipe bracing ties the downcomer legs together in a pair; therefore, separation forces on the pair of downcomer legs will be taken as axial forces in the bracing.

In the direction normal to the plane of the downcomer pair, the intersections are braced by 2-1/2" diameter pipe members located on each side of the vent header (Figure 3-2.1-11). The ends of the horizontal pipe members are welded to the downcomers and the diagonals are connected to the horizontal members by means of gusset plates.

This bracing system provides an additional load path for the transfer of loads acting on the submerged portion of the downcomers and results in reduced local stresses in the downcomer-vent header intersection regions. The system of downcomer-vent header intersection stiffener plates and bracing members provides a redundant mechanism for the transfer of loads acting on the down-

comers, thus reducing the magnitude of loads passing directly through the intersection. The bracing also ties together several pairs of downcomers in the longitudinal direction, causing an increase in stiffness to the overall system that minimizes the dynamic effect of several loads, including SRV submerged structure loads. This also results in load sharing among the downcomers for both chugging lateral loads and SRV submerged structure loads.

A bellows assembly is provided at the penetration of the vent line to the suppression chamber (Figure 3-2.1-7). The bellows allows differential movement of the vent system and suppression chamber to occur without developing significant interaction loads. Each bellows assembly consists of a stainless steel bellows unit that is connected to a 1-3/4" thick nozzle. The bellows unit has a 7'3-3/4" inside diameter and contains five convolutions which connect to 1/2" thick cylindrical sleeves at each end. A 1-1/2" thick annular plate welded to the vent line connects to the upper end of the bellows assembly by full penetration welds. The lower end of the bellows assembly is a 1-3/4" thick nozzle, already described, which is connected to the suppression

chamber shell insert plate by full penetration welds. The overall length of the bellows assembly is 6'4-7/8".

Vent header deflectors are provided in both the vent line bays and the non-vent line bays (Figures 3-2.1-5, 3-2.1-6, and 3-2.1-12). The deflectors shield the vent header from pool swell impact loads which occur during the initial phase of a DBA event. The vent header deflectors are constructed from 14" diameter, Schedule 160 pipe with WT6 x 32.5 split tee sections attached to either side. The vent header deflectors are supported by 1" thick connection plates that are welded to the vent header collar plates near each miter joint. The vent header deflectors are designed to completely mitigate pool swell impact loads on the vent header.

The drywell/wetwell vacuum breakers are nominal 18" units and extend from mounting flanges attached to 1'8" OD, 1" thick nozzles. The nozzles penetrate the vent header at the vent line-vent header intersections (Figure 3-2.1-10). Additional support for the vacuum breakers at each vent line-vent header intersection location is provided by a system of three 1" thick stiffener plates around the nozzle. The vacuum breaker support system is designed to reduce local stresses at

the intersections of the vacuum breaker nozzles and the vent header.

The vent system is supported vertically by two column members at each miter joint location (Figures 3-2.1-4, 3-2.1-13 and 3-2.1-14). The support column members are constructed with 6" diameter, Schedule 80 pipe. Built-up clevis assemblies are attached to each end of the columns. The upper ends of each support column are connected to the 1" thick vent header collar plates by a 2-3/4" diameter pin. The collar plates are attached to the vent header with 5/16" fillet welds. The support column loads are transferred at the upper pin locations by 3/4" thick clevis plates and 3/4" thick reinforcing plates, which provide additional bearing capacity. The lower ends of each support column are attached to 1-1/2" thick ring girder pin plates with a 2-3/4" diameter pin and two 3/4" thick clevis plates. The support column assemblies are designed to transfer vertical loads acting on the vent system to the suppression chamber ring girders while simultaneously resisting drag loads on submerged structures.

The vent system is supported horizontally by the vent lines which transfer lateral loads acting on the vent

system to the drywell at the vent line-drywell penetration locations. The vent lines also provide additional vertical support for the vent system, although the vent system support columns provide primary vertical support. The support provided by the vent line bellows is negligible, since the relative stiffness of the bellows with respect to other vent system components is small.

The vent system also provides support for a portion of the SRV piping inside the vent line and suppression chamber (Figures 3-2.1-3 and 3-2.1-8). Loads acting on the SRV piping are transferred to the vent system by the penetration assembly on the vent line. Conversely, loads acting on the vent system cause motions to be transferred to the SRV piping at the same support locations.

The overall load-carrying capacities of the vent system components described in the preceding paragraphs are substantially greater than those of the original vent system design described in the plant's FSAR.

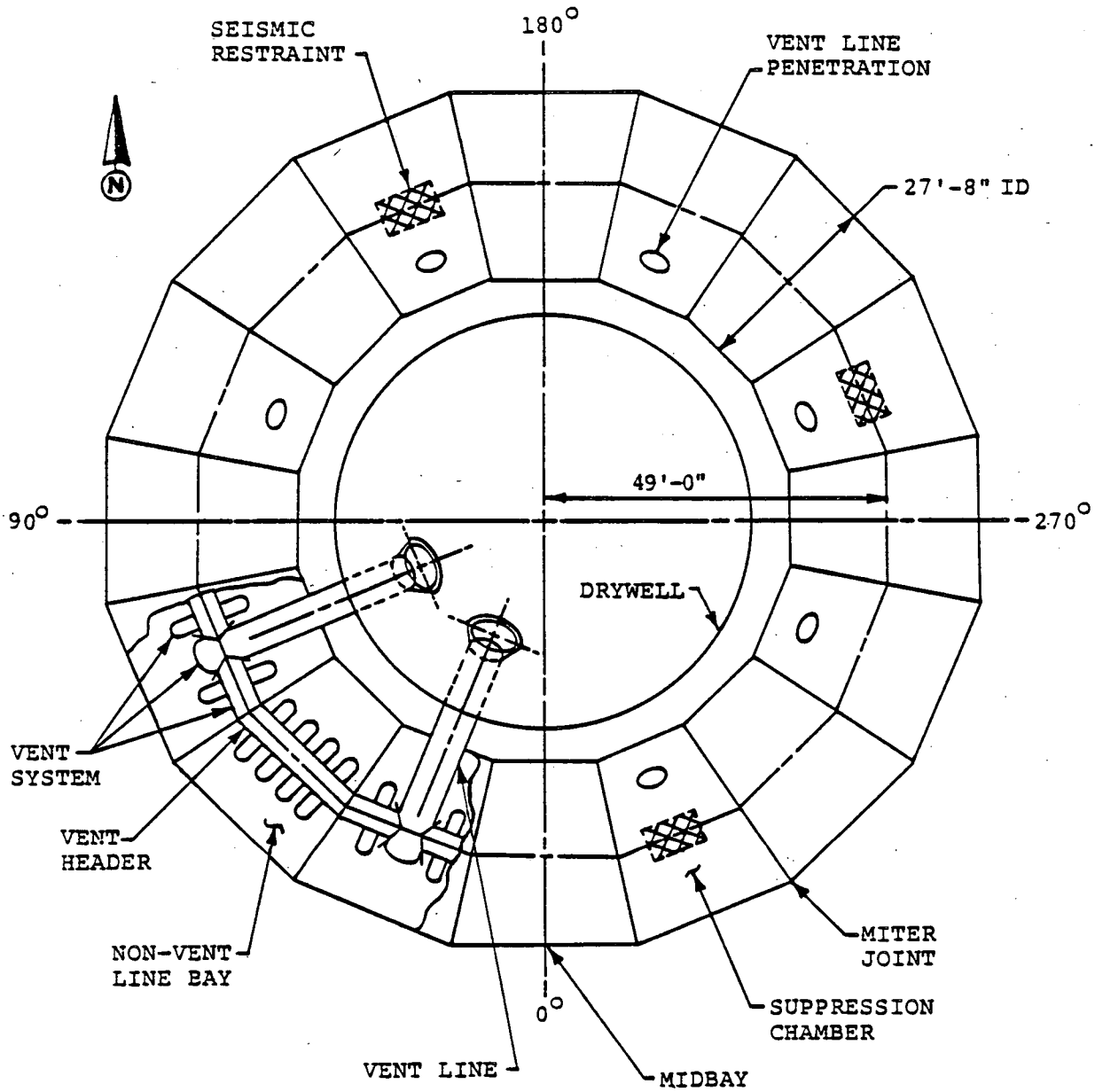

Figure 3-2.1-1

PLAN VIEW OF CONTAINMENT

nutech ENGINEERS

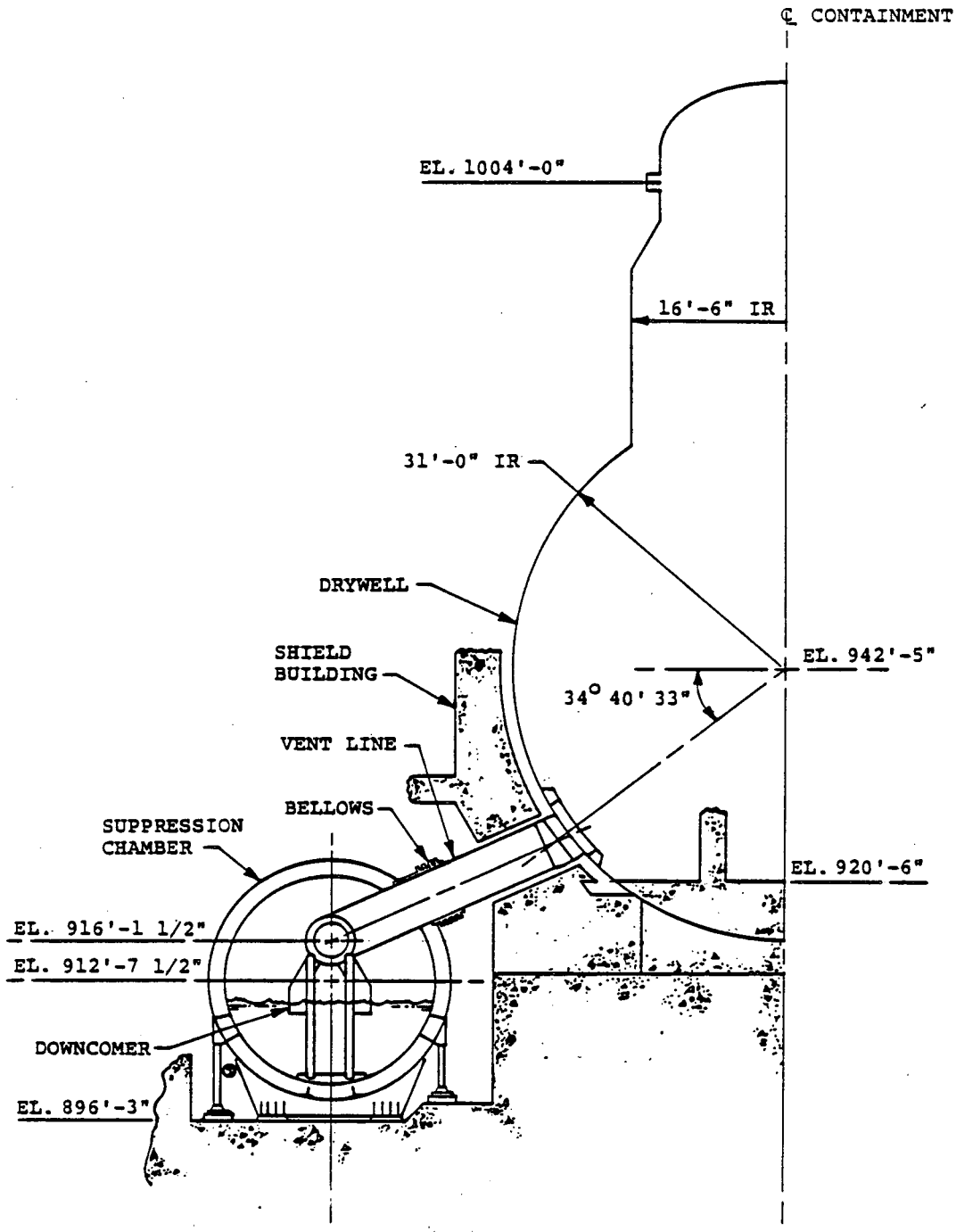

Figure 3-2.1-2

ELEVATION VIEW OF CONTAINMENT

nutech ENGINEERS

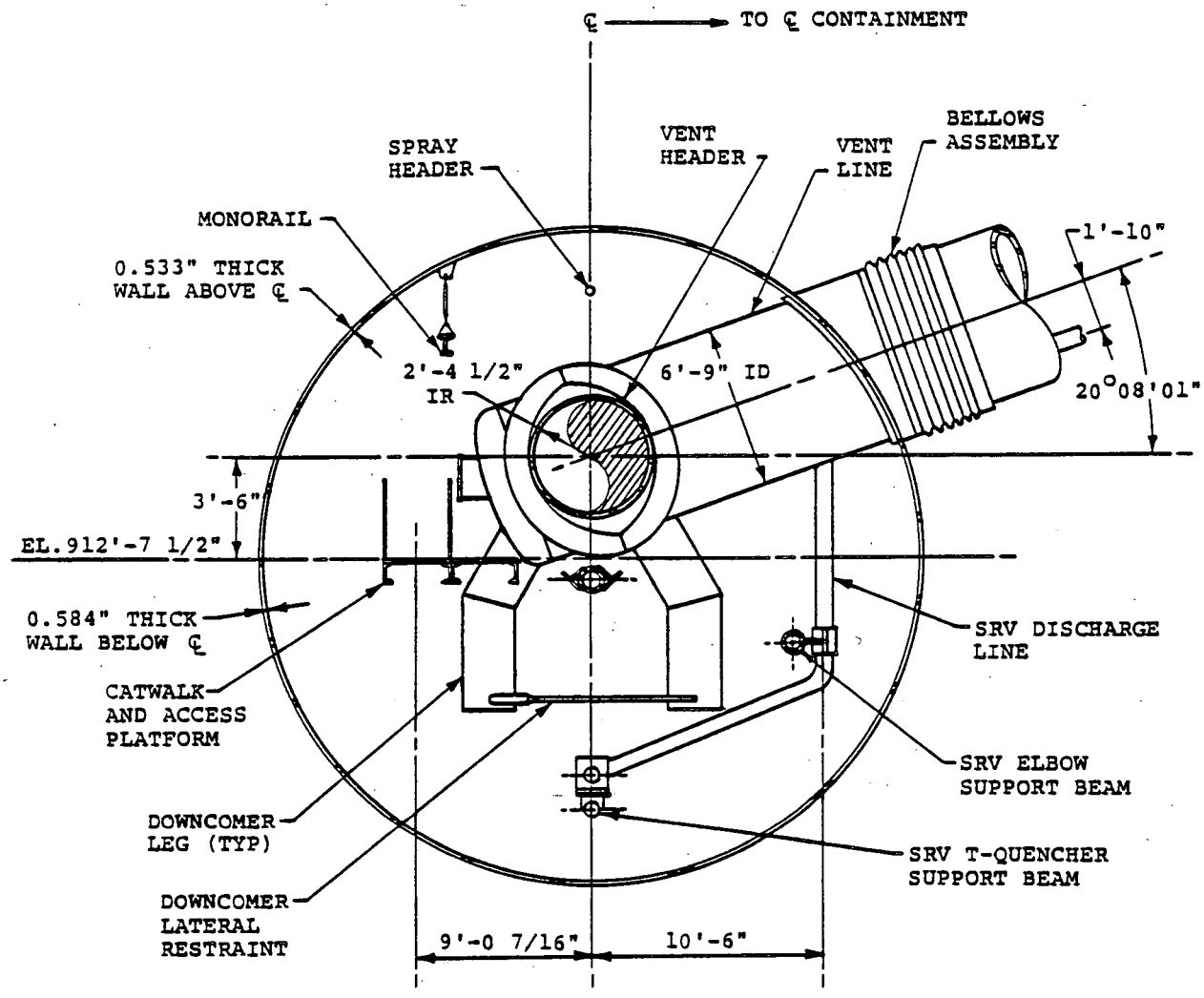

Figure 3-2.1-3

SUPPRESSION CHAMBER SECTION -

MIDBAY VENT LINE BAY

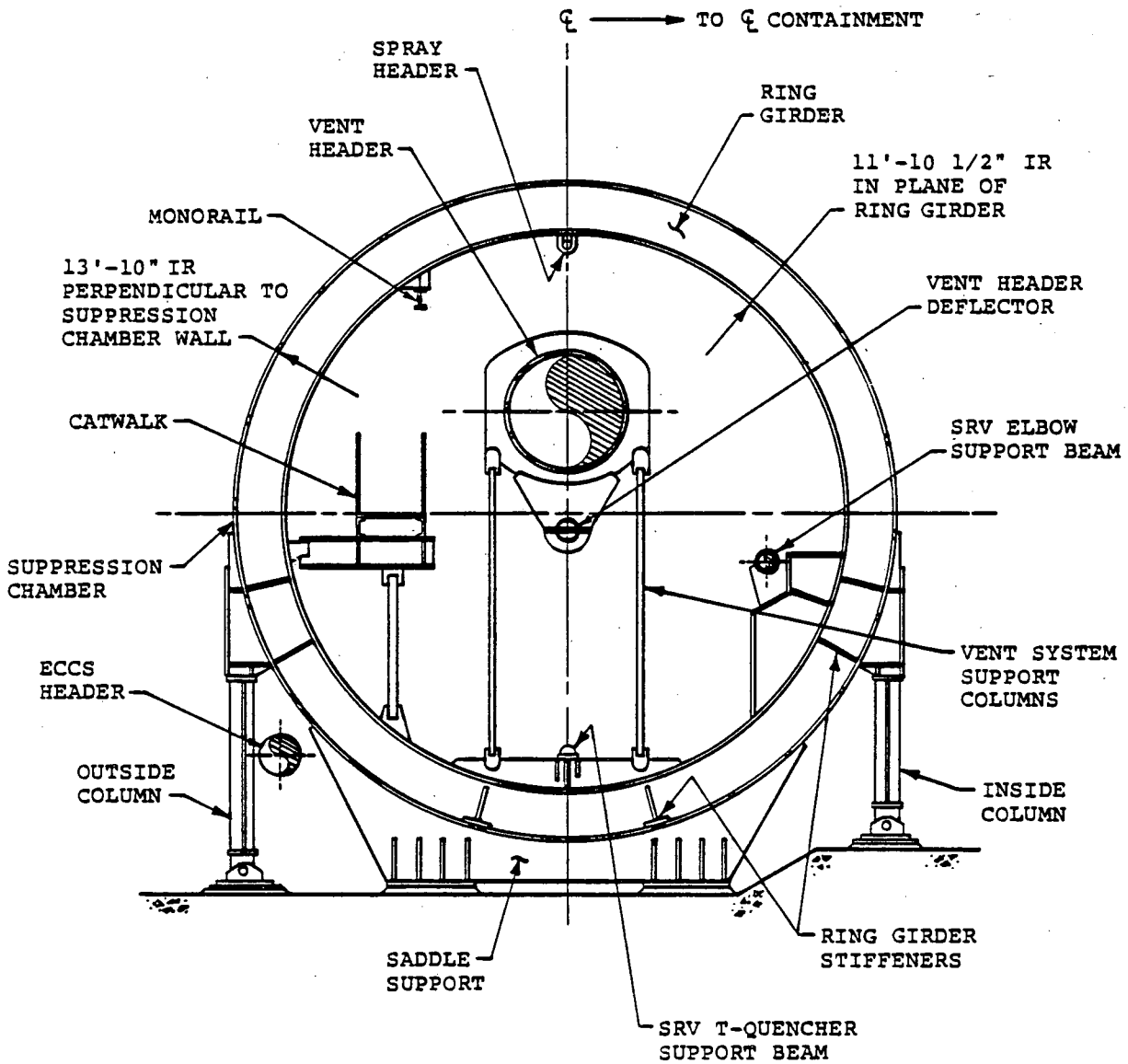

Figure 3-2.1-4

SUPPRESSION CHAMBER SECTION - MITER JOINT

nutech ENGINEERS

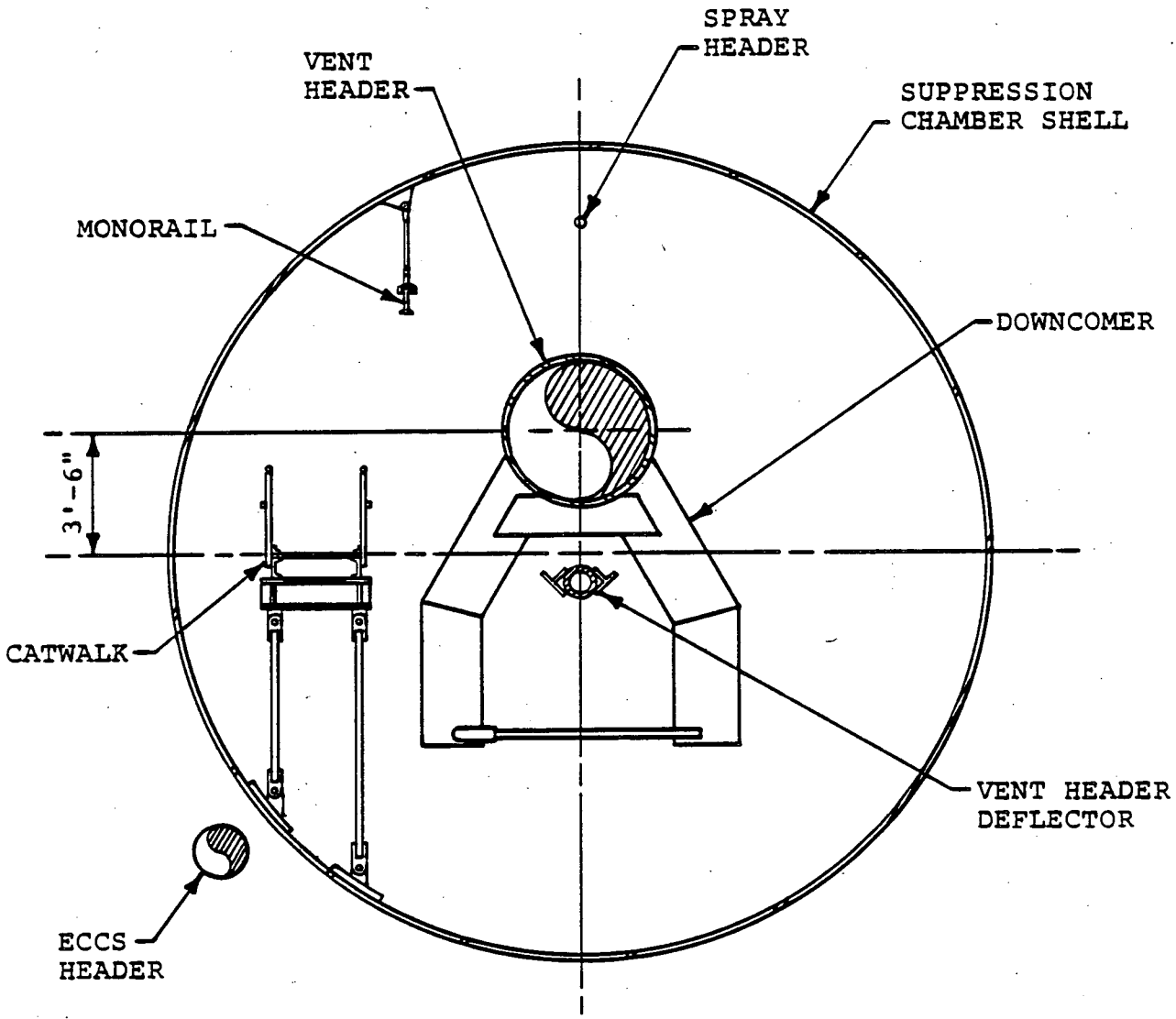

Figure 3-2.1-5

SUPPRESSION CHAMBER SECTION

MIDBAY NON-VENT LINE BAY

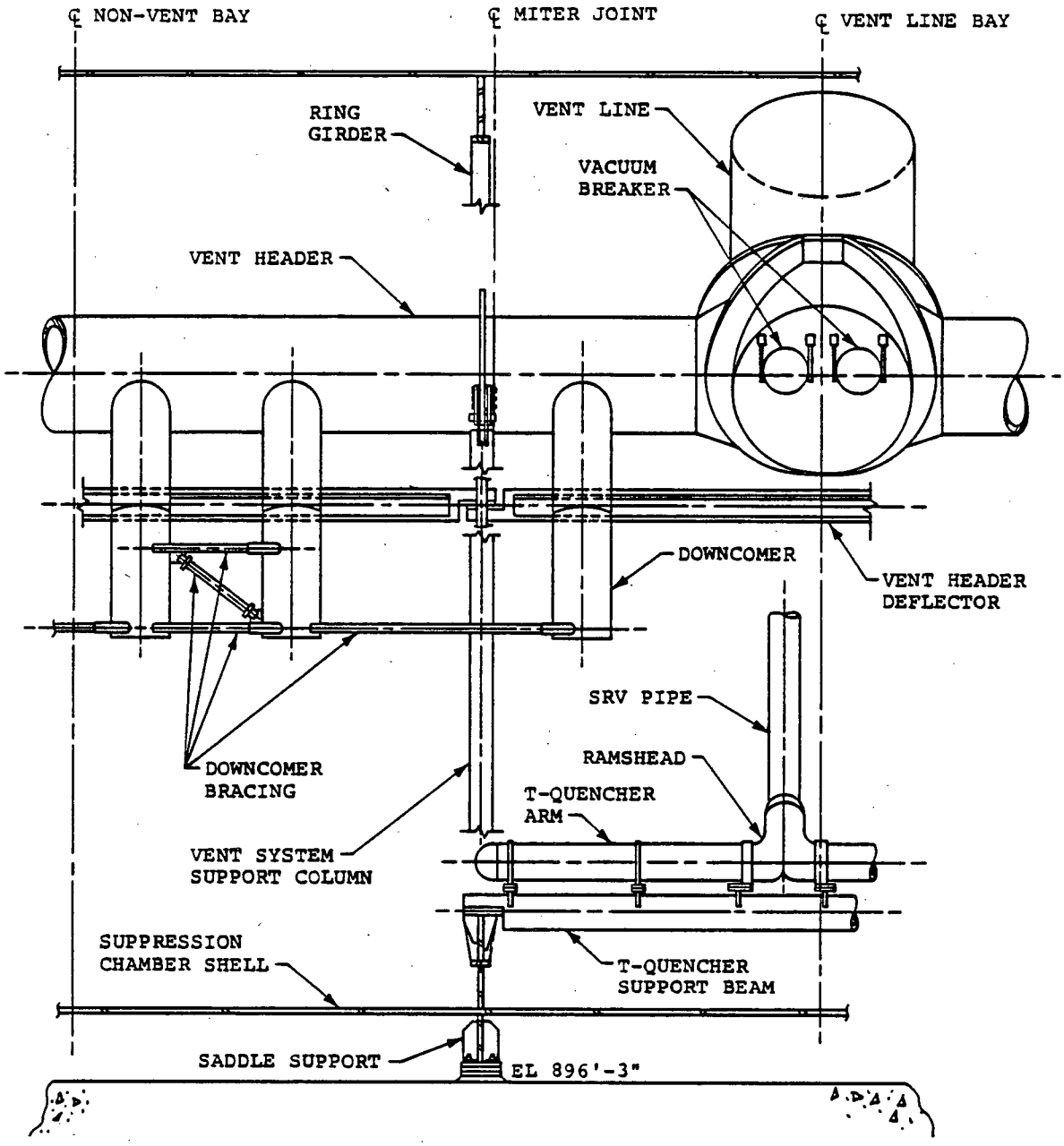

Figure 3-2.1-6

DEVELOPED VIEW OF SUPPRESSION CHAMBER SEGMENT

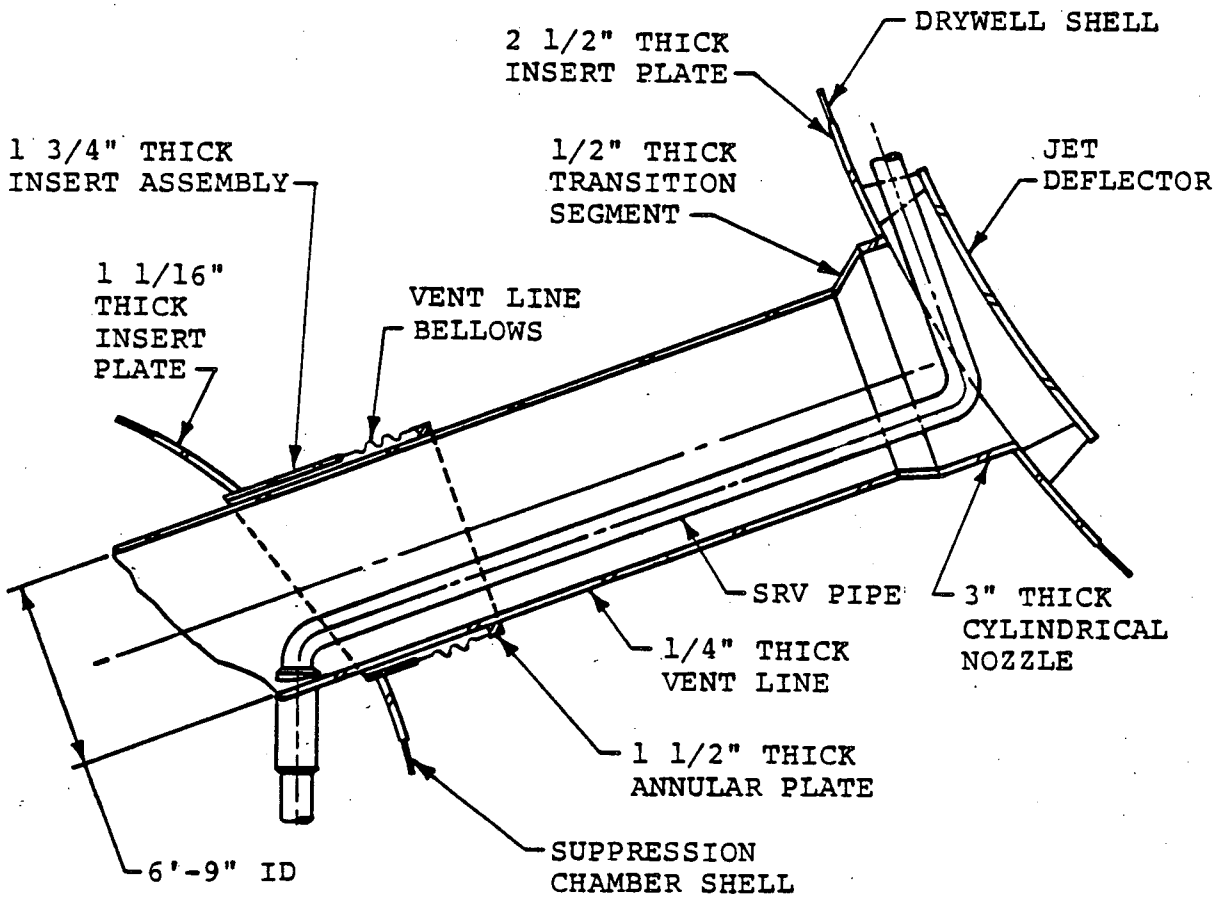

Figure 3-2.1-7

VENT LINE DETAILS - UPPER END

nutech ENGINEERS

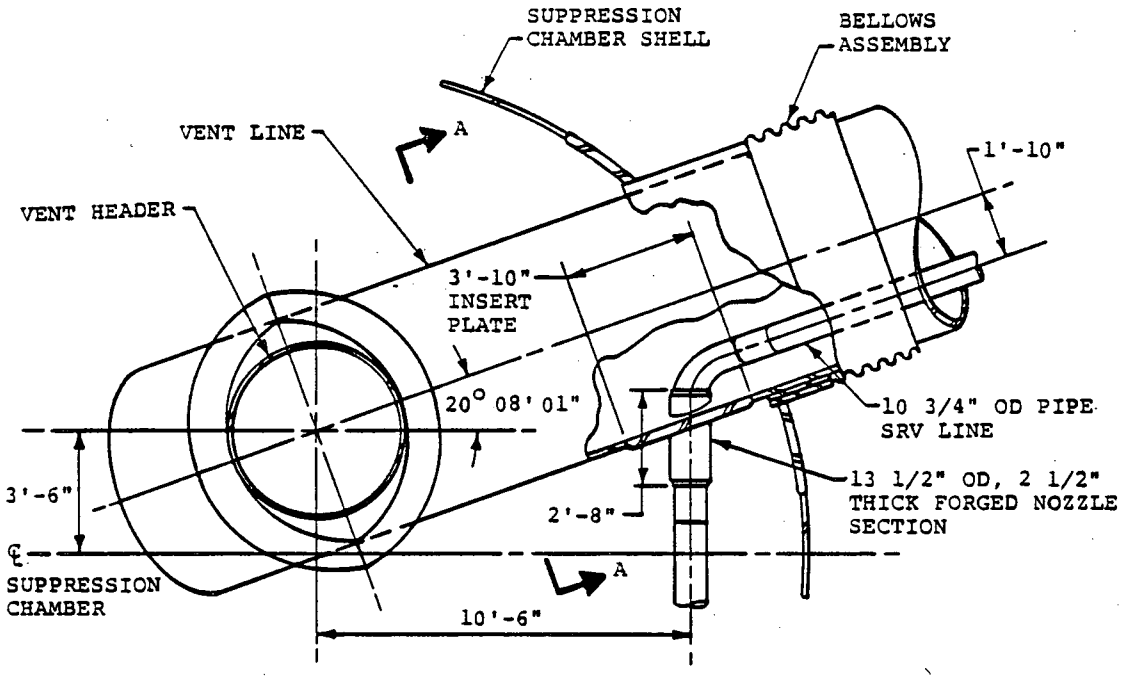

VENT LINE ELEVATION VIEW

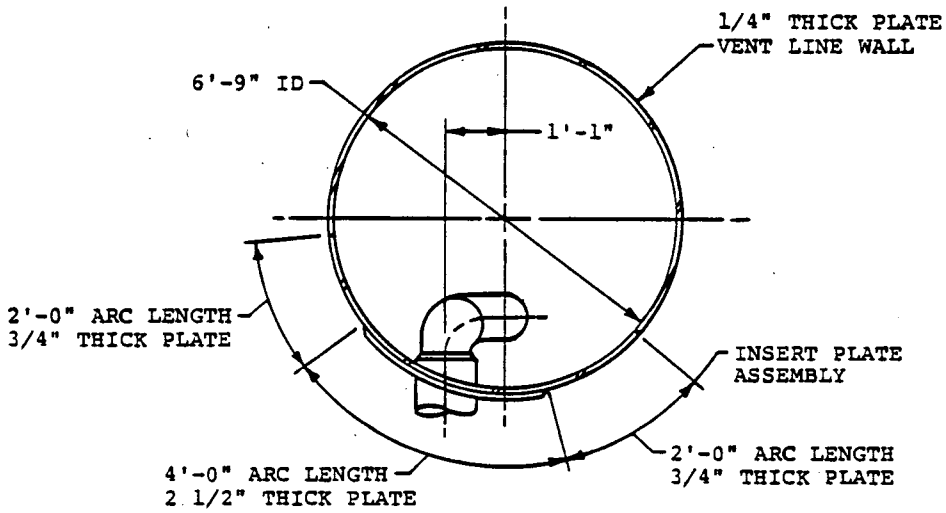

VIEW A-A

Figure 3-2.1-8

SRV PENETRATION IN VENT LINE

nutech ENGINEERS

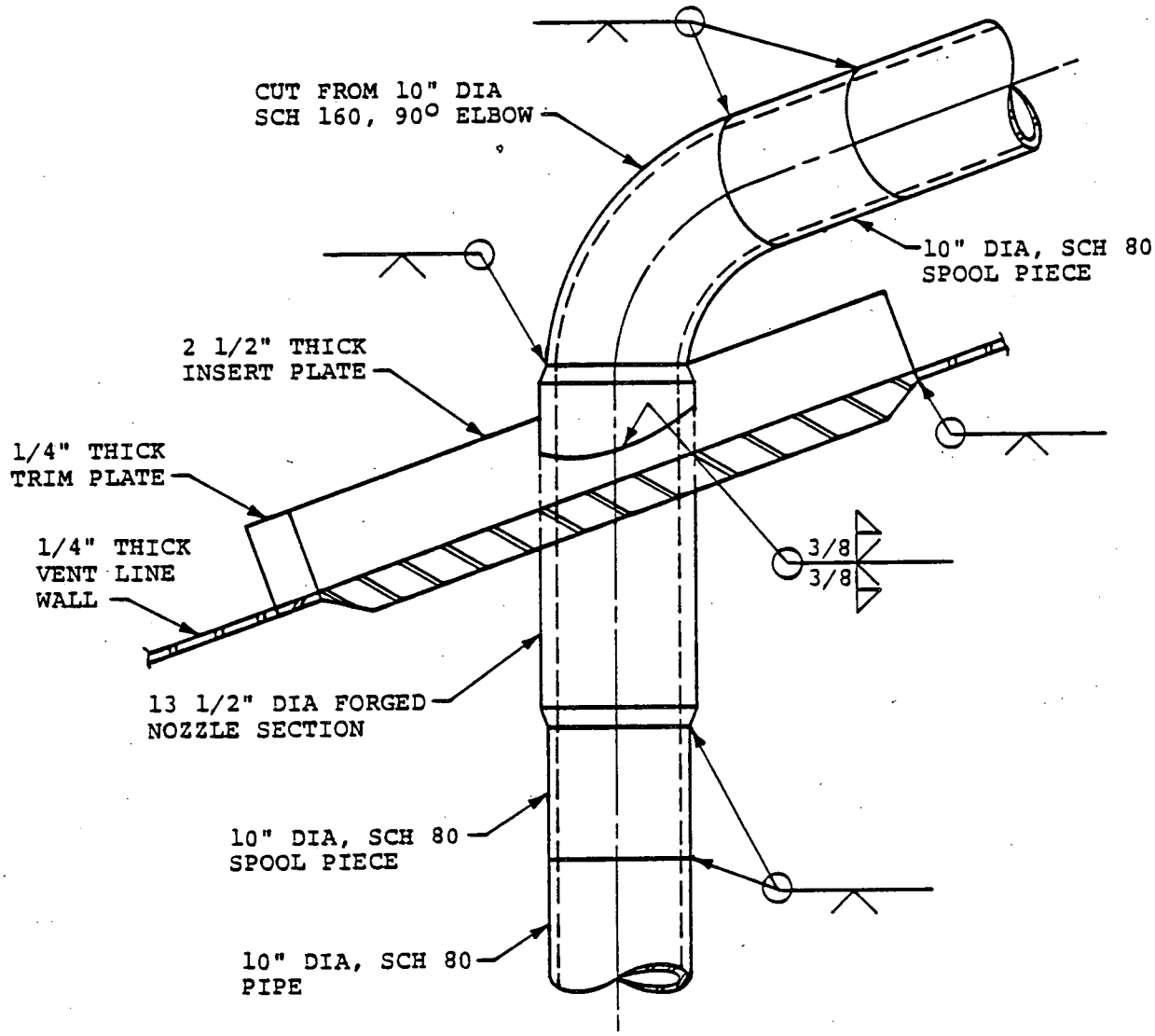

Figure 3-2.1-9

VENT LINE - SRV PIPING PENETRATION

NOZZLE DETAILS

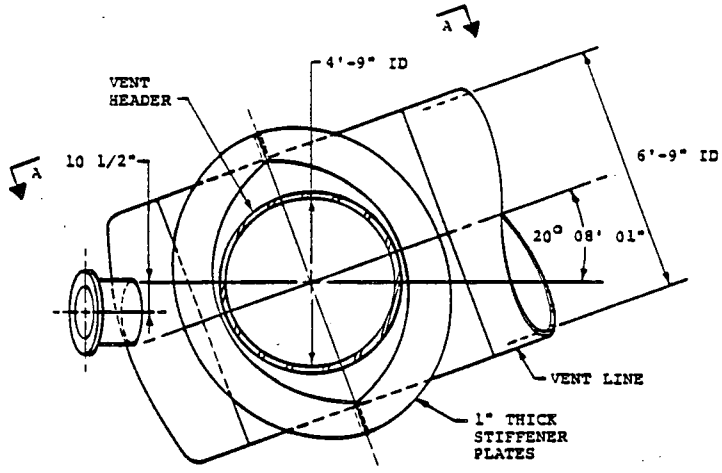

ELEVATION VIEW THROUGH VENT HEADER

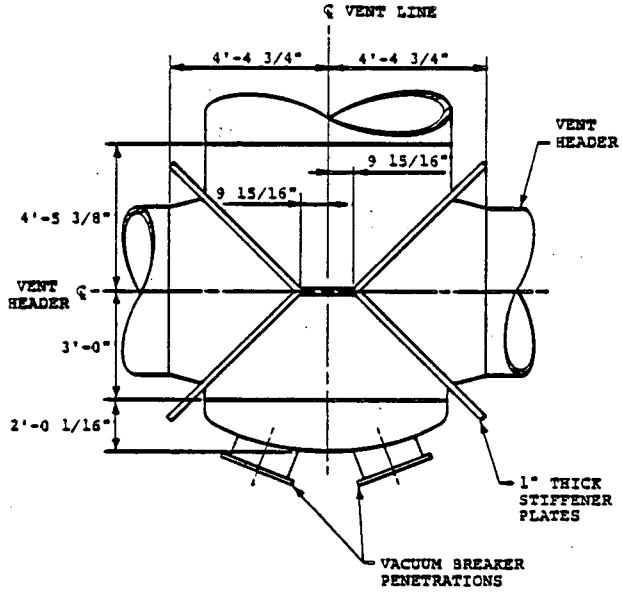

VIEW A-A

1. VACUUM BREAKERS NOT SHOWN FOR CLARITY.

Figure 3-2.1-10

VENT LINE-VENT HEADER INTERSECTION DETAILS

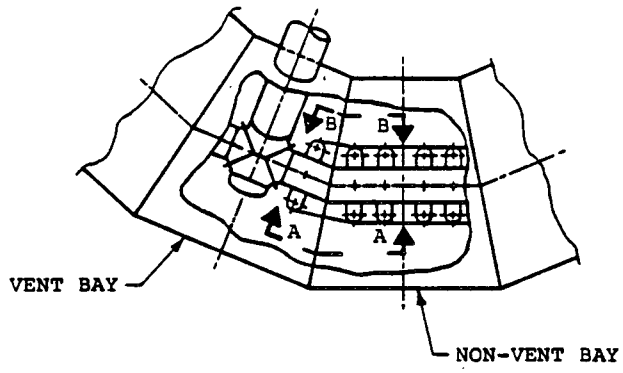

PARTIAL PLAN VIEW OF SUPPRESSION CHAMBER

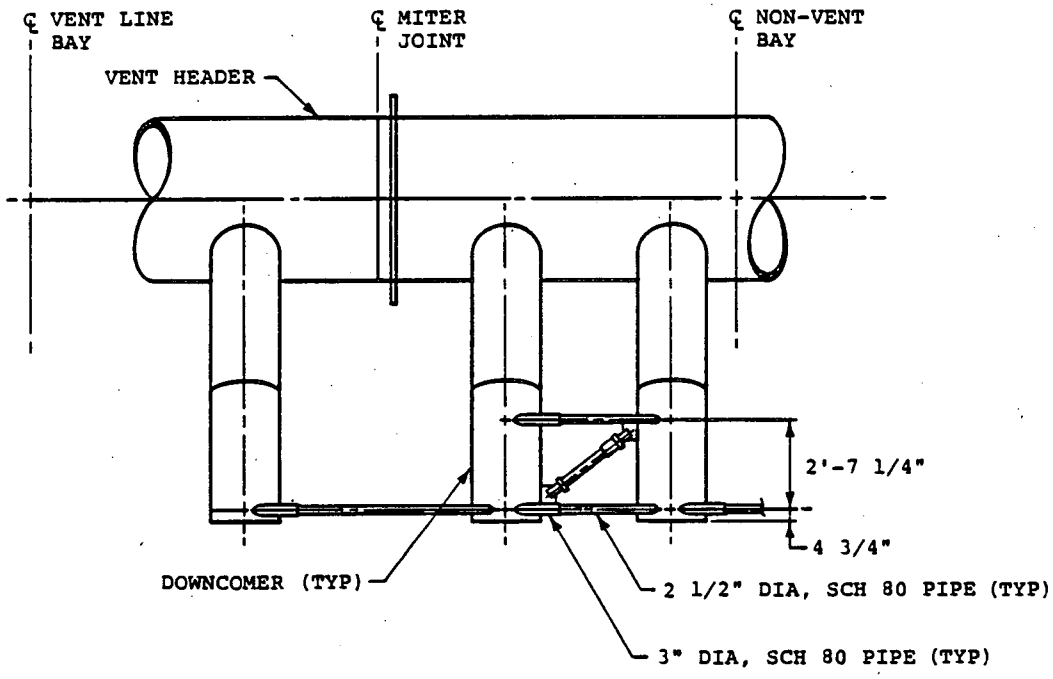

VIEW A-A

VIEW B-B (OPPOSITE HAND)

1. VENT HEADER DEFLECTOR AND VENT HEADER COLUMNS NOT SHOWN FOR CLARITY.

Figure 3-2.1-11

DEVELOPED VIEW OF
DOWNCOMER BRACING SYSTEM

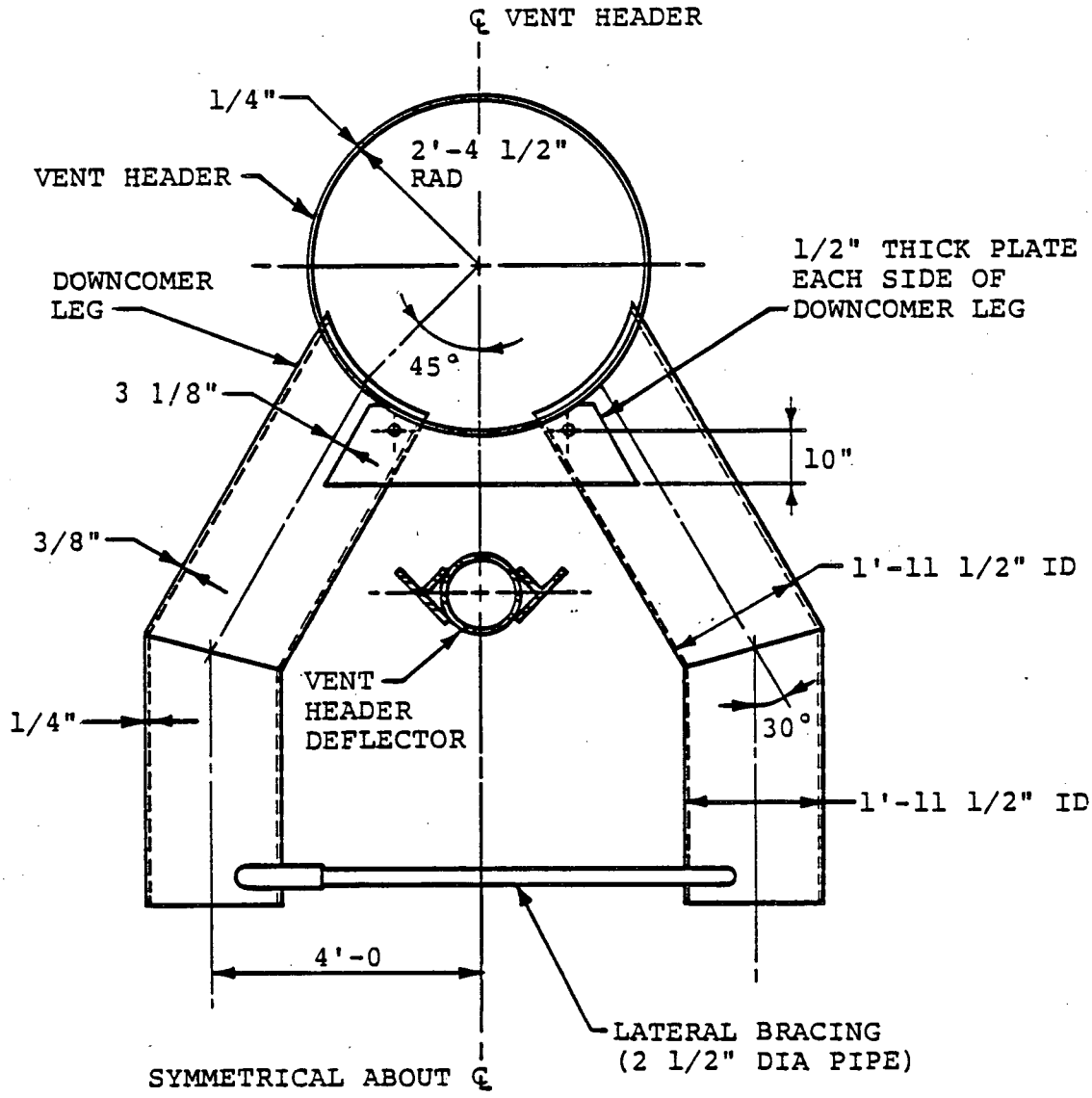

Figure 3-2.1-12

DOWNCOMER-TO-VENT HEADER INTERSECTION DETAILS

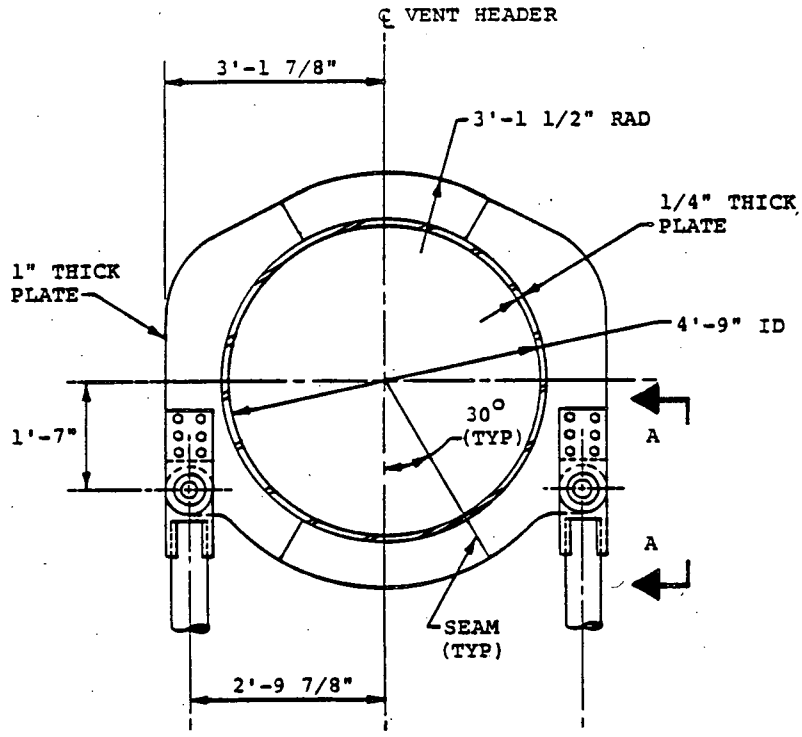

SECTION THROUGH VENT HEADER
AT RING PLATE

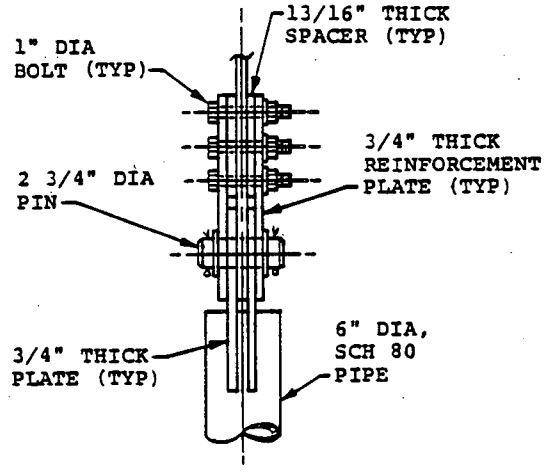

SECTION A-A

Figure 3-2.1-13

VENT HEADER SUPPORT COLUMN

RING PLATE DETAILS

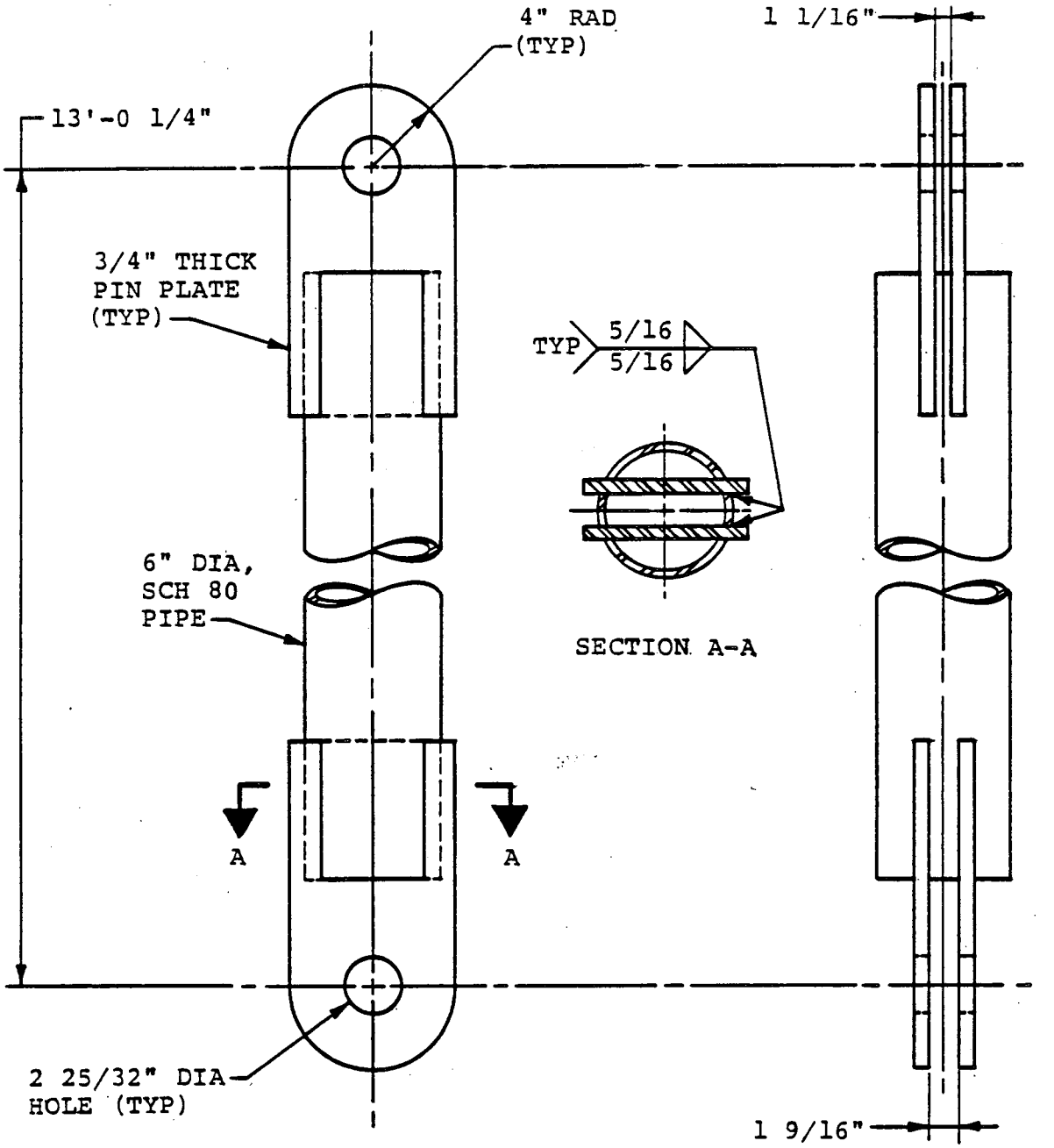

Figure 3-2.1-14

VENT SYSTEM SUPPORT COLUMN DETAILS

3-2.2 Loads and Load Combinations

The loads for which the Monticello vent system is evaluated are defined in NUREG-0661 on a generic basis for all Mark I plants. Section 1-4.0 discusses the methodology used to develop plant unique vent system loads for each load defined in NUREG-0661. The results of applying the methodology to develop specific values for each of the governing loads which act on the vent system are discussed and presented in Section 3-2.2.1.

Using the event combinations and event sequencing defined in NUREG-0661 and discussed in Sections 1-3.2 and 1-4.3, the controlling load combinations which affect the vent system are formulated. The controlling vent system load combinations are discussed and presented in Section 3-2.2.2.

3-2.2.1 Loads

The loads acting on the vent system are categorized as follows.

1. Dead Weight Loads
2. Seismic Loads
3. Pressure and Temperature Loads
4. Vent System Discharge Loads
5. Pool Swell Loads
6. Condensation Oscillation Loads
7. Chugging Loads
8. Safety Relief Valve Discharge Loads
9. Piping Reaction Loads
10. Containment Interaction Loads

Loads in categories 1 and 2 were considered in the original containment design as documented in the plant's FSAR. Category 3 pressure and temperature loads result from postulated LOCA and SRV discharge events. Loads in categories 4 through 7 result from postulated LOCA events; loads in category 8 result from SRV discharge events; loads in category 9 are reactions which result from loads acting on SRV piping systems; loads in category 10 are motions which result from loads acting on other containment-related structures.

Not all of the loads defined in NUREG-0661 are evaluated in detail since some are enveloped by others or have a negligible effect on the vent system. Only those loads which maximize the vent system response and lead to controlling stresses are fully evaluated and discussed. These loads are referred to as governing loads in subsequent discussions.

Table 3-2.2-1 shows the specific vent system components affected by each of the loadings defined in NUREG-0661. The table also lists the section in Volume 1 in which the methodology for developing values for each loading is discussed. The magnitudes and characteristics of each governing vent system load in each load category are identified and presented in the following paragraphs.

1. Dead Weight Loads

   a. Dead Weight of Steel: The weight of steel used to construct the modified vent system and its supports is considered. The nominal component dimensions and a density of steel of 490 lb/ft^3 are used in this calculation.

2. Seismic Loads

a. OBE Loads: The vent system is subjected to horizontal and vertical accelerations during an Operating Basis Earthquake (OBE). This loading is taken from the original design basis for the containment documented in the plant's FSAR. The OBE loads have a maximum horizontal spectral acceleration of 0.23g and a maximum vertical spectral acceleration of 0.153g.

b. SSE Loads: The vent system is subjected to horizontal and vertical accelerations during a Safe Shutdown Earthquake (SSE). This loading is taken from the original design basis for the containment documented in the plant's FSAR, termed a Design Basis Earthquake (DBE) (Reference 4). The SSE loads have a maximum horizontal spectral acceleration of 0.46g and a maximum vertical spectral acceleration of 0.307g.

3. Pressure and Temperature Loads

a. Normal Operating Internal Pressure Loads: The vent system is subjected to internal pressure

loads during Normal Operating Conditions. This loading is taken from the original design basis for the containment documented in the PULD report.

b. LOCA Internal Pressure Loads: The vent system is subjected to internal pressure loads during a small break accident (SBA), an intermediate break accident (IBA), and a design basis accident (DBA) event. The procedure used to develop LOCA internal pressures for the containment is discussed in Section 1-4.1.1. Figures 3-2.2-1 through 3-2.2-3 present the resulting vent system internal pressure transients and pressure magnitudes at key times during the SBA, IBA, and DBA events.

The vent system internal pressures for each event are conservatively assumed to be equal to the corresponding drywell internal pressures; reductions due to losses are negligible. The net internal pressures acting on the components of the vent system inside the

suppression chamber are extracted as the difference in pressures between the vent system and suppression chamber.

The pressures specified are assumed to act uniformly over the vent line, vent header, and downcomer shell surfaces. The external or secondary containment pressure for the vent system components outside the suppression chamber for all events is assumed to be zero. The effects of internal pressure on the vent system for the DBA event are included in the pressurization and thrust loads discussed in load case 4a.

c. Normal Operating Temperature Loads: The vent system is subjected to the thermal expansion loads associated with normal operating conditions. This loading is taken from the original design basis for the containment documented in the plant's FSAR. The range of normal operating temperatures for the vent system with a concurrent SRV discharge event is 65° to 150°F. The temperature of the SRV

piping with a concurrent SRV discharge event is conservatively taken as 375°F.

Additional normal operating temperatures for the vent system inside the suppression chamber are taken from the suppression pool temperature response analysis. Table 3-2.2-2 provides a summary of the resulting vent system temperatures.

d. LOCA Temperature Loads: The vent system is subjected to thermal expansion loads associated with the SBA, IBA, and DBA events. The procedure used to develop LOCA containment temperatures is discussed in Section 1-4.1.1. Figures 3-2.2-4 through 3-2.2-6 present the resulting vent system temperature transients and temperature magnitudes at key times during the SBA, IBA, and DBA events.

Additional vent system SBA event temperatures are taken from the suppression pool temperature response analysis. Table 3-2.2-2 summarizes the resulting vent system temperatures. The greater of the temperatures specified in

Figure 3-2.2-4 and Table 3-2.2-2 is used in evaluating the effects of SBA event temperatures.

The temperatures of the major components of the vent system, such as the vent line, vent header, and downcomers, are conservatively assumed to be equal to the corresponding drywell temperatures for the SBA, IBA and DBA events.

The temperatures of the external components of the vent system, such as the support columns, downcomer bracing, vent header deflectors, vacuum breaker penetration supports, and associated ring plates and stiffeners, are assumed equal to the corresponding suppression chamber temperatures for each event.

The temperatures specified are assumed representative of the major component and external component metal temperatures throughout the vent system. The temperature of the SRV piping is 375°F for those SBA, IBA, and DBA events which include SRV discharge loads. The

ambient or initial temperature of the vent system for all events is assumed equal to the arithmetic mean of the minimum and maximum vent system operating temperatures.

4. Vent System Discharge Loads

a. Pressurization and Thrust Loads: The vent system is subjected to dynamic pressurization and thrust loads during a DBA event. The procedure used to develop vent system pressurization and thrust forces applied to the unaffected areas of the major components of the vent system is discussed in Section 1-4.1.2. Table 3-2.2-3 shows the resulting maximum forces for each of the major component unreacted areas at key times during the DBA event.

The vent system discharge loads shown include the effects of a zero drywell/wetwell pressure differential. The vent system discharge loads specified for the DBA event include the effects of DBA internal pressure loads as

discussed in load case 3a. The vent system discharge loads which occur during the SBA or IBA events are negligible.

5. Pool Swell Loads

a. Vent System Impact and Drag Loads: During the initial phase of a DBA event, transient impact and drag pressures are postulated to act on major components of the vent system above the suppression pool. The major components affected are the vent line inside the suppression chamber below the maximum bulk pool height and the inclined portion of the downcomers. The vent headers in the vent line bay and in the non-vent line bay are shielded from pool swell impact loads by the vent header deflectors.

The procedure used to develop the transient forces and the spatial distribution of pool swell impact loads on these components is discussed in Section 1-4.1.4. Table 3-2.2-4 and Figures 3-2.2-7 and 3-2.2-8 summarize the resulting magnitudes and distribution of pool swell impact loads on the vent line, down-

comers, and vent header deflector. The results shown are based on plant unique QSTF test data contained in the PULD (Reference 3) and include the effects of the main vent orifice tests. Pool swell loads do not occur during the SBA and IBA events.

b. Impact and Drag Loads on Other Structures: During the initial phase of a DBA event, transient impact and drag pressures are postulated to act on non-major components of the vent system. The components affected are the vacuum breaker and vacuum breaker penetration. The downcomer tie rods, the downcomer longitudinal bracing members, and the SRV piping and supports are also subjected to the drag loads during this phase of a DBA event.

The procedure used to develop the transient forces and the spatial distribution of pool swell impact and drag loads on these components is discussed in Section 1-4.1.4. Tables 3-2.2-5 and 3-2.2-6 and Figure 3-2.2-9 summarize the resulting magnitudes and distribution of pool swell impact and drag

pressures on the vacuum breaker, the vacuum breaker penetration, the downcomer tie rods, and the downcomer longitudinal bracings. The pool swell drag loads on the SRV piping and supports located beneath the level of the vent line are presented in Volume 5 of this report. The results shown are based on plant unique QSTF test data contained in the PULD which are used to determine the impact velocities and arrival times. Pool swell loads do not occur during the SBA and IBA events.

c. Froth Impingement and Fallback Loads: During the initial phase of a DBA event, transient impingement pressures are postulated to act on components of the vent system located in specified regions above the rising suppression pool. The impacted components located in both Regions I and II are the vacuum breaker and vacuum breaker penetration.

The procedure used to develop the transient forces and spatial distribution of froth impingement and fall back loads on these components is discussed in Section 1-4.1.4.

Table 3-2.2-5 summarizes the resulting magnitudes and distribution of froth impingement and fallback pressures on the vacuum breaker and vacuum breaker penetration. Pool swell loads do not occur during the SBA and IBA events.

d. Pool Fallback Loads: During the later portion of the pool swell event, transient drag pressures are postulated to act on selected components of the vent system located between the maximum bulk pool height and the downcomer exit. The components affected are the downcomer longitudinal bracing members and the SRV piping and supports located beneath the level of the vent line. The procedure used to develop transient drag pressures and spatial distribution of pool fallback loads on these components is discussed in Section 1-4.1.4.

Table 3-2.2-6 summarizes the resulting magnitudes and distribution of pool fallback loads on the downcomer longitudinal bracing members. (The pool fallback loads on the SRV piping and supports located beneath the level

of the vent line are presented in Volume 5 of this report). The results shown include the effects of maximum pool displacements measured in plant unique QSTF tests. Pool swell loads do not occur during the SBA and IBA events.

e. LOCA Water Clearing Submerged Structure Loads: Water jet drag loads are postulated to act on the submerged components of the vent system during the water clearing phase of a DBA event. The components affected are the vent system support columns. The procedure used to develop the transient forces and spatial distribution of LOCA water clearing loads on these components is discussed in Section 1.4.1.5. Table 3-2.2-7 shows the resulting magnitudes and distribution of LOCA water clearing loads acting on the support columns.

f. LOCA Air Clearing Submerged Structure Loads: Transient drag pressures are postulated to act on the submerged components of the vent system during the air clearing phase of a DBA event. The components affected are the downcomers, the downcomer tie rods, the downcomer

longitudinal bracing members, the support columns, and the submerged portion of the SRV piping. The procedure used to develop the transient forces and spatial distribution of DBA air clearing drag loads on these components is discussed in Section 1-4.1.6.

Tables 3-2.2-7, 3-2.2-8, and 3-2.2-9 show the resulting magnitudes and distribution of drag pressures acting on the vent system support columns, the downcomers, the downcomer tie rods, and the downcomer longitudinal bracing members for the controlling DBA air clearing load case. (The controlling DBA air clearing loads on the submerged portion of the SRV piping are presented in Volume 5 of this report). The results shown include the effects of velocity drag, acceleration drag, and interference effects. The LOCA air clearing submerged structure loads which occur during an SBA or IBA event are negligible.

6. Condensation Oscillation Loads

a. IBA Condensation Oscillation Downcomer Loads: Harmonic internal pressure loads are postulated to act on the downcomers during the

condensation oscillation phase of an IBA event. The procedure used to develop the harmonic pressures and spatial distribution of IBA condensation oscillation downcomer loads is discussed in Section 1-4.1.7. The loading consists of a uniform internal pressure component acting on all downcomers and a differential internal pressure component acting on one downcomer in a downcomer pair. Table 3-2.2-10 shows the resulting pressure amplitudes and associated frequency range for each of the three harmonics in the IBA condensation oscillation downcomer loading. Figure 3-2.2-10 shows the corresponding distribution of differential downcomer internal pressure loadings.

The IBA condensation oscillation downcomer load harmonic in the range of the dominant downcomer frequency for the uniform and the differential pressure components is applied at the dominant downcomer frequency. The remaining two downcomer load harmonics are applied at frequencies which are multiples of the dominant frequency. The results of the three

harmonics for the uniform and differential IBA condensation oscillation downcomer load components are combined by absolute sum.

b. DBA Condensation Oscillation Downcomer Loads: Harmonic internal pressure loads are postulated to act on the downcomers during the condensation oscillation phase of a DBA event. The procedure used to develop the harmonic pressures and spatial distribution of DBA condensation oscillation downcomer loads is the same as that discussed for IBA condensation oscillation downcomer loads in load case 6a. Table 3-2.2-11 shows the resulting pressure amplitudes and associated frequency range for each of the three harmonics in the DBA condensation oscillation downcomer loading. Figure 3-2.2-10 shows the corresponding distribution of differential downcomer internal pressure loadings.

c. IBA Condensation Oscillation Vent System Pressure Loads: Harmonic internal pressure loads are postulated to act on the vent system during the condensation oscillation phase of an

IBA event. The components affected are the vent line, the vent header, and the downcomers. The procedure used to develop the harmonic pressures and spatial distribution of IBA condensation oscillation vent system pressures is discussed in Section 1-4.1.7. Table 3-2.2-12 shows the resulting pressure amplitudes and associated frequency range for the vent line and vent header. The loading is applied at the frequency within a specified range which maximizes the vent system response.

The effects of IBA condensation oscillation vent system pressures on the downcomers are included in the IBA condensation oscillation downcomer loads discussed in load case 6a. An additional static internal pressure of 1.55 psi is applied uniformly to the vent line, vent header, and downcomers to account for the effects of downcomer submergence. The IBA condensation oscillation vent system pressures act in conjunction with the IBA containment internal pressures discussed in load case 3a.

d. DBA Condensation Oscillation Vent System Pressure Loads: Harmonic internal pressure loads are postulated to act on the vent system during the condensation oscillation phase of a DBA event. The components affected are the vent line, vent header, and downcomers. The procedure used to develop the harmonic pressures and spatial distribution of the DBA condensation oscillation vent system pressures is the same as that discussed for the IBA in load case 6c. Table 3-2.2-12 shows the resulting pressure amplitudes and associated frequency range for the vent line and vent header. The effects of DBA condensation oscillation vent system pressures on the downcomers are included in the DBA condensation oscillation downcomer loads discussed in load case 6b. The DBA condensation oscillation vent system pressures act in addition to the DBA vent system pressurization and thrust loads discussed in load case 4a.

e. IBA Condensation Oscillation Submerged Structure Loads: Harmonic pressure loads are postulated to act on the submerged components

of the vent system during the condensation oscillation phase of an IBA event. In accordance with NUREG-0661, the submerged structure loads specified for pre-chug are used in lieu of IBA condensation oscillation submerged structure loads. Pre-chug submerged structure loads are discussed in load case 7c.

f. DBA Condensation Oscillation Submerged Structure Loads: Harmonic drag pressures are postulated to act on the submerged components of the vent system during the condensation oscillation phase of a DBA event. The components affected are the downcomer tie rods, the downcomer longitudinal bracing members, the support columns, and the submerged portions of the SRV piping. The procedure used to develop the harmonic forces and spatial distribution of DBA condensation oscillation drag loads on these components is discussed in Section 1-4.1.7.

Loads are developed for the case with the average source strength at all downcomers and the case with twice the average source

strength at the nearest downcomer. The results of these two cases are evaluated to determine the controlling loads.

Tables 3-2.2-13 and 3-2.2-14 show the resulting magnitudes and distribution of drag pressures acting on the support columns, the downcomer tie rods, and the downcomer longitudinal bracing members for the controlling DBA condensation oscillation drag load case. The controlling DBA condensation oscillation drag loads on the submerged portion of the SRV piping are presented in Volume 5 of this report. The effects of DBA condensation oscillation submerged structure loads on the downcomers are included in the loads discussed in load case 6b.

The results in Tables 3-2.2-13 and 3-2.2-14 include the effects of velocity drag, acceleration drag, torus shell FSI acceleration drag, interference effects, and acceleration drag volumes. Figure 3-2.2-11 shows a typical pool acceleration profile from which the FSI accelerations are derived. The results of

each harmonic in the loading are combined using the methodology discussed in Section 1-4.1.7.

7. Chugging Loads

a. Chugging Downcomer Lateral Loads: Lateral loads are postulated to act on the downcomers during the chugging phase of an SBA, IBA, and DBA event. The procedure used to develop chugging downcomer lateral loads is discussed in Section 1-4.1.8. The maximum lateral load acting on any one downcomer in any direction is obtained using the maximum downcomer lateral load and chugging pulse duration measured at FSTF, the frequency of the tied downcomers for FSTF, and the plant unique downcomer frequency calculated for Monticello. Table 3-2.2-15 summarizes this information. The resulting ratio of Monticello to the FSTF dynamic load factors (DLF) is used in subsequent calculations to determine the magnitude of multiple downcomer loads and to determine the load magnitude used for evaluating fatigue. Section 3-2.4.1 discusses the method-

ology used to determine the plant unique downcomer frequency.

The magnitude of chugging lateral loads acting on multiple downcomers simultaneously is determined using the methodology described in Section 1-4.1.8. The methodology involves calculation of the probability of exceeding a given downcomer load magnitude once per LOCA as a function of the number of downcomers loaded. The chugging load magnitudes (Table 3-2.2-16) are determined using the resulting non-exceedance probabilities and the ratio of the DLF's from the maximum downcomer load calculation. The distributions of chugging downcomer lateral loads considered are those cases which maximize both local and overall effects in the vent system. Tables 3-2.2-17 and 3-2.2-18 summarize these distributions.

The maximum downcomer lateral load magnitude used for evaluating fatigue is obtained using both the maximum downcomer lateral load measured at FSTF with a 95% NEP and the ratio of DLF's from maximum downcomer load calcula-

tions. The stress reversal histograms provided for FSTF are converted to plant unique stress reversal histograms using the postulated plant unique chugging duration (Table 3-2.2-19).

b. Chugging Vent System Pressures: Transient and harmonic internal pressures are postulated to act on the vent system during the chugging phase of an SBA, IBA, and DBA event. The components affected are the vent line, the vent header, and the downcomers. The procedure used to develop chugging vent system pressures is discussed in Section 1-4.1.8. The load consists of a gross vent system pressure oscillation component, an acoustic vent system pressure oscillation component, and an acoustic downcomer pressure oscillation component. Table 3-2.2-20 shows the resulting pressure magnitudes and characteristics of the chugging vent system pressure loading. The three load components are evaluated individually and are not combined.

The overall effects of chugging vent system pressures on the downcomers are included in the loads discussed in load case 7a. The downcomer pressures (Table 3-2.2-20) are used to evaluate downcomer hoop stresses. The chugging vent system pressures act in addition to the SBA and IBA containment internal pressures discussed in load case 3a and the DBA pressurization and thrust loads discussed in load case 4a.

c. Pre-Chug Submerged Structure Loads: During the chugging phase of an SBA, IBA, or DBA event, harmonic drag pressures associated with the pre-chug portion of a chugging cycle are postulated to act on the submerged components of the vent system. The components affected are the downcomer tie rods, the downcomer longitudinal bracing members, the support columns, and the submerged portion of the SRV piping. The procedure used to develop the harmonic forces and spatial distribution of pre-chug drag loads on these components is discussed in Section 1-4.1.8.

Loads are developed for the case with the average source strength at all downcomers and the case with twice the average source strength at the nearest downcomer. The results of these two cases are evaluated to determine the controlling loads. Tables 3-2.2-21 and 3-2.2-22 show the resulting magnitudes and distribution of drag pressures acting on the support columns, the downcomer tie rods, and the downcomer longitudinal bracing members for the controlling pre-chug drag load case. The controlling pre-chug drag loads on the submerged portion of the SRV piping are presented in Volume 5 of this report. The effects of pre-chug submerged structure loads on the downcomers are included in the loads discussed in Load Case 7a.

The results shown include the effects of velocity drag, acceleration drag, torus shell FSI acceleration drag, interference effects, and acceleration drag volumes. Figure 3-2.2-11 shows a typical pool acceleration profile from which the FSI accelerations are derived.

d. Post-Chug Submerged Structure Loads: During the chugging phase of an SBA, IBA, or DBA event, harmonic drag pressures associated with the post-chug portion of a chug cycle are postulated to act on the submerged components of the vent system. The components affected are the downcomer tie rods, the downcomer longitudinal bracing members, the support columns, and the submerged portion of the SRV piping. Section 1-4.1.8 discusses the procedure used to develop the harmonic forces and spatial distribution of pre-chug drag loads on these components.

Loads are developed for the cases with the maximum source strength at the nearest two downcomers acting both in-phase and out-of-phase. The results of these cases are evaluated to determine the controlling loads. Tables 3-2.2-23 and 3-2.2-24 shows the resulting magnitudes and distribution of drag pressures acting on the support columns, the downcomer tie rods, and the downcomer longitudinal bracing members for the controlling post-chug drag load case. The controlling post-chug drag loads on the submerged portion

of the SRV piping are presented in Volume 5 of this report. The effects of post-chug submerged structure loads acting on the downcomers are included in the chugging downcomer lateral loads discussed in Load Case 7a.

The results shown include the effects of velocity drag, acceleration drag, torus shell FSI acceleration drag, interference effects, and acceleration drag volumes. Figure 3-2.2-11 shows a typical pool acceleration profile from which the FSI accelerations are derived. The results of each harmonic are combined using the methodology described in Section 1-4.1.8.

8. Safety Relief Valve Discharge Loads

a. SRV Discharge Water Clearing Submerged Structure Loads: Water jet loads from the quencher arm holes are postulated to act on the submerged components of the vent system during the water clearing phase of an SRV discharge event. The quencher water jet does not reach the downcomers and longitudinal bracings. The components affected are the vent system support columns. The procedure used to develop the transient forces and

spatial distribution of the SRV discharge water clearing loads on these components is discussed in Section 1.4.2.4. Table 3-2.2-25 provides the resulting magnitudes and distribution of SRV water clearing loads acting on the support columns.

b. SRV Discharge Air Clearing Submerged Structure Loads: Transient drag pressures are postulated to act on the submerged components of the vent system during the air clearing phase of an SRV discharge event. The components affected are the downcomers, the downcomer tie rods, the downcomer longitudinal bracing members, support columns, the submerged portion of the SRV piping, and the SRV piping support. The procedure used to develop the transient forces and spatial distribution of the SRV discharge air clearing drag loads on these components is discussed in Section 1-4.2.4.

Loads are developed for the case with four bubbles from quenchers located in the bay containing the structure or either of the adjacent bays. A calibration factor is applied to the resulting downcomer loads

developed using the methodology discussed in Section 1-4.2.4. Tables 3-2.2-25, 3-2.2-26, and 3-2.2-27 show the magnitudes and distribution of drag pressures acting on the support columns, the downcomers, the downcomer tie rods, and the downcomer longitudinal bracings for the controlling SRV discharge drag load case.

These results include the effects of velocity drag, acceleration drag, interference effects, and acceleration drag volumes.

9. Piping Reaction Loads

a. SRV Piping Reaction Loads: Reaction loads affect the vent system because of loads acting on the drywell and wetwell SRV piping systems. These reaction loads occur at the vent line-SRV piping penetration. The SRV piping reaction loads consist of those caused by motions of the vent system and loads acting on the drywell and wetwell portions of the SRV piping systems. Loads acting on the SRV piping systems are pressurization and thrust loads, submerged structure loads, and other operating or design basis loads.

The effects of the SRV piping reaction loads on the vent system are included in the vent system analysis. These reaction loads were taken from the analysis of the SRV piping system that is described in Volume 5 of this report.

10. Containment Interaction Loads

a. Containment Structure Motions: Loads acting on the drywell, suppression chamber and vent system cause interaction effects between these structures. The interaction effects result in vent system motions applied at the attachment points of the vent system to the drywell and the suppression chamber. The effects of these motions on the vent system are considered in the vent system analysis.

The values of the loads presented in the preceding paragraphs envelop those which could occur during the LOCA and SRV discharge events postulated. An evaluation for the effects of the above loads results in conservative estimates of the vent system responses and leads to bounding values of vent system stresses.

Table 3-2.2-1

VENT SYSTEM COMPONENT LOADING INFORMATION

VOLUME 3 LOAD DESIGNATION			PUAR SECTION REFERENCE	COMPONENT PART LOADED										REMARKS
CATEGORY	LOAD TYPE	CASE NUMBER		DRYWELL PENETRATION	VENT LINE	VENT LINE BELLOWS	VENT HEADER	VENT HEADER DEFLECTOR	DOWNCOMERS	DOWNCOMER TIE ROD	DOWNCOMER LONGITUDINAL BRACING	SUPPORT COLUMNS	VACUUM BREAKER	
DEAD WEIGHT LOADS	DEAD WEIGHT OF STEEL	1a	1-3.1	X	X	X	X	X	X	X	X	X	X	AS-MODIFIED GEOMETRY
SEISMIC	OBE	2a	1-3.1	X	X	X	X	X	X	X	X	X	X	0.23g HORIZONTAL, 0.153g VERTICAL
	SSE	2b	1-3.1	X	X	X	X	X	X	X	X	X	X	0.46g HORIZONTAL, 0.307g VERTICAL
PRESSURE AND TEMPERATURE	NORMAL OPERATING INTERNAL PRESSURE	3a	1-3.1	X	X	X	X		X					-0.1 TO 1.0 psi
	LOCA INTERNAL PRESSURE	3b	1-4.1.1	X	X	X	X		X					SBA, IBA, & DBA PRESSURES
	NORMAL OPERATING TEMPERATURE	3c	1-3.1	X	X	X	X	X	X	X	X	X	X	65°TO 150°F
	LOCA TEMPERATURE	3d	1-4.1.1	X	X	X	X	X	X	X	X	X	X	SBA, IBA, & DBA TEMPERATURES
VENT SYSTEM DISCHARGE	PRESSURIZATION AND THRUST	4a	1-4.1.2		X		X		X					FORCES ON UNREACTED AREAS
POOL SWELL	VENT SYSTEM IMPACT AND DRAG	5a	1-4.1.4.1		X			X	X					HEADER SHIELDED BY DEFLECTORS
	IMPACT AND DRAG LOADS ON OTHER STRUCTURES	5b	1-4.1.4.2							X	X		X	COMPONENTS BELOW MAXIMUM POOL HEIGHT
	FROTH IMPINGEMENT & FALLBACK	5c	1-4.1.4.3										X	TWO REGIONS SPECIFIED
	POOL FALLBACK	5d	1-4.1.4.4								X			MAJOR COMPONENTS NOT AFFECTED
	LOCA WATER CLEARING SUBMERGED STRUCTURE	5e	1-4.1.5									X		EFFECTS ON SUPPORT COLUMNS
	LOCA AIR CLEARING SUBMERGED STRUCTURE	5f	1-4.1.6						X	X	X	X		PRIMARILY LOCAL EFFECTS
CONDENSATION OSCILLATION	IBA CO, DOWNCOMER LOADS	6a	1-4.1.7.2						X					UNIFORM & DIFFERENTIAL COMPONENTS
	DBA CO, DOWNCOMER LOADS	6b	1-4.1.7.2						X					UNIFORM & DIFFERENTIAL COMPONENTS
	IBA CO, VENT SYSTEM PRESSURE	6c	1-4.1.7.2	X	X		X							DOWNCOMER PRESSURES INCLUDED IN 6a
	DBA CO, VENT SYSTEM PRESSURE	6d	1-4.1.7.2	X	X		X							DOWNCOMER PRESSURES INCLUDED IN 6b
	IBA CO, SUBMERGED STRUCTURE	6e	1-4.1.7.3							X	X	X		DOWNCOMER LOADS INCLUDED IN 6a
	DBA CO, SUBMERGED STRUCTURE	6f	1-4.1.7.3							X	X	X		DOWNCOMER LOADS INCLUDED IN 6b
CHUGGING	CHUGGING, DOWNCOMER LATERAL LOADS	7a	1-4.1.8.2						X					RSEL BASED ON FSTF
	CHUGGING, VENT SYSTEM PRESSURES	7b	1-4.1.8.2	X	X		X		X					THREE LOADING ALTERNATES
	PRE-CHUG, SUBMERGED STRUCTURES	7c	1-4.1.8.3							X	X	X		DOWNCOMER LOADS INCLUDED IN 7a
	POST-CHUG, SUBMERGED STRUCTURES	7d	1-4.1.8.3							X	X	X		DOWNCOMER LOADS INCLUDED IN 7a
SRV DISCHARGE	WATER CLEARING, SUBMERGED STRUCTURES	8a	1-4.2.4									X		EFFECTS ON SUPPORT COLUMNS
	AIR CLEARING, SUBMERGED STRUCTURES	8b	1-4.2.4						X	X	X	X		PRIMARILY LOCAL EFFECTS
PIPING REACTION	SRV PIPING REACTION	9a	VOLUME 5		X									REACTIONS ON VENT LINE
CONTAINMENT INTERACTION	CONTAINMENT STRUCTURE MOTIONS	10a	VOLUME 2	X		X						X		DRYWELL & TORUS MOTIONS

nutech ENGINEERS

Table 3-2.2-2

SUPPRESSION POOL TEMPERATURE RESPONSE ANALYSIS RESULTS - MAXIMUM TEMPERATURES

CONDITION	CASE NUMBER (1)	NUMBER OF SRV's ACTUATED	MAXIMUM BULK POOL TEMPERATURE (°F)
NORMAL OPERATING	1A	0	155.0
	1B	1	168.0
	2A	3	166.0
	2B	1	146.0
	2C	3	156.0
SBA EVENT	3A	3 (ADS)	164.0
	3B	3	155.0

(1) SEE SECTION 1-5.1 FOR DESCRIPTION OF SRV DISCHARGE EVENTS CONSIDERED.

Table 3-2.2-3

VENT SYSTEM PRESSURIZATION AND THRUST LOADS FOR DBA EVENT

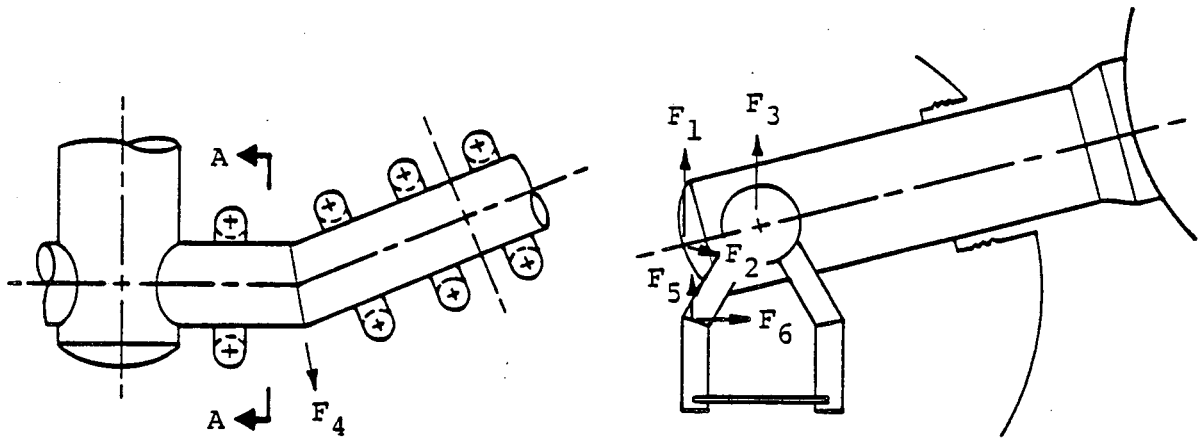

PLAN

SECTION A-A

KEY DIAGRAM

TIME DURING DBA EVENT (sec)	MAXIMUM COMPONENT FORCE MAGNITUDE (kips)					
	F_1	F_2	F_3	F_4	F_5	F_6
POOL SWELL 0.0 TO 1.5	-64.0	-152.0	58.0	24.0	1.2	-3.9
CONDENSATION OSCILLATION 5.0 TO 35.0	-28.0	-69.0	26.0	12.0	0.5	-1.4

1. LOADS SHOWN INCLUDE THE EFFECTS OF THE DBA INTERNAL PRESSURES IN FIGURE 3-2.2-3.
2. VALUES SHOWN ARE EQUAL TO PRODUCT OF PENETRATION UNREACTED AREA AND DBA INTERNAL PRESSURE.

Table 3-2.2-4

POOL SWELL IMPACT LOADS FOR VENT LINE

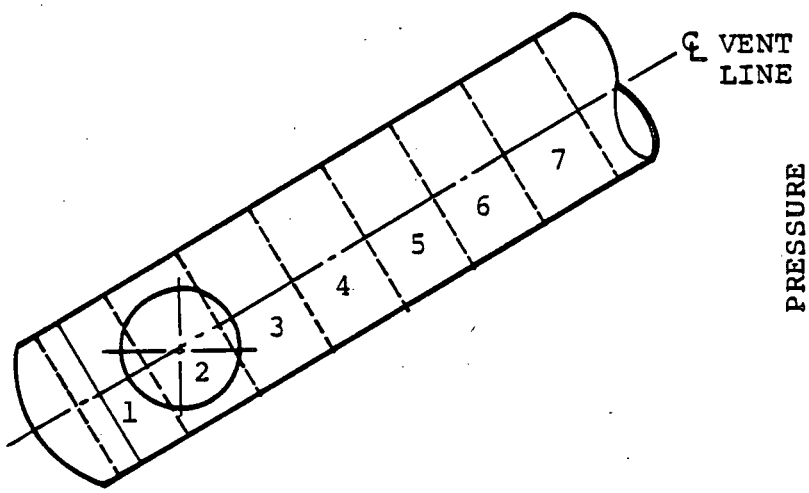

KEY DIAGRAM

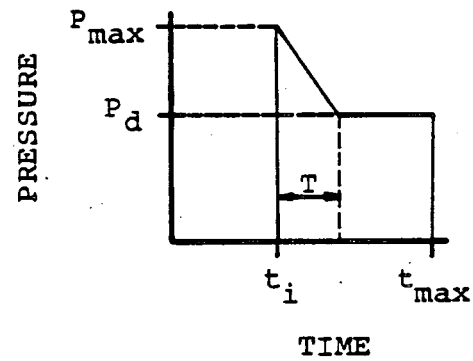

PRESSURE TRANSIENT

SEGMENT NUMBER	TIME (msec)			PRESSURE (psi)	
	IMPACT (t_i)	IMPACT DURATION (T)	MAXIMUM POOL HEIGHT (t_{max})	IMPACT (P_{max})	DRAG (P_d)
1	403	29.3	530	35.9	9.50
5	444	31.0	530	32.1	9.96
6	474	36.5	530	23.2	4.27

1. FOR STRUCTURE GEOMETRY, SEE FIGURES 3-2.1-3 AND 3-2.1-10.
2. PRESSURES SHOWN ARE APPLIED TO VERTICAL PROJECTED AREAS IN A DIRECTION NORMAL TO VENT LINE SURFACE.
3. LOADS ARE SYMMETRIC WITH RESPECT TO VERTICAL CENTERLINE OF VENT LINE.

Table 3-2.2-5

POOL SWELL IMPACT, FROTH IMPINGEMENT, AND POOL FALLBACK LOADS FOR VACUUM BREAKER SYSTEM

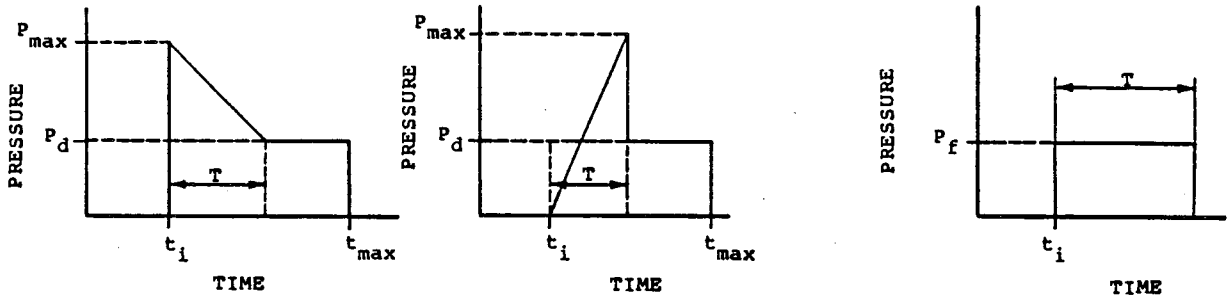

CYLINDRICAL STRUCTURES FLAT STRUCTURES

POOL SWELL PRESSURE TRANSIENTS

FROTH IMPINGEMENT PRESSURE TRANSIENT

ITEM	POOL SWELL IMPACT					FROTH IMPINGEMENT		
	TIME (msec)			PRESSURE (psi)		TIME (msec)		PRESSURE (psi)
	ARRIVAL TIME	IMPACT DURATION	MAXIMUM POOL HEIGHT	IMPACT	DRAG	ARRIVAL TIME	DURATION	FROTH PRESSURE
	(t_i)	(T)	(t_{max})	(P_{max})	(P_d)	(t_i)	(T)	(P_f)
VACUUM BREAKER	452	11.00	530	32.83	6.27	382	80.0	9.87
NOZZLE	440	4.02	530	44.50	8.70	382	80.0	9.87
GUSSET PLATE 1	470	2.85	530	66.53	7.62	N/A	N/A	N/A
GUSSET PLATE 2	440	2.26	530	106.30	9.33	N/A	N/A	N/A

1. VACUUM BREAKER IS IN FROTH REGION I.
2. PRESSURES SHOWN ARE APPLIED TO VERTICAL PROJECTED AREAS IN DIRECTION NORMAL TO STRUCTURE.

Table 3-2.2-6

DOWNCOMER LONGITUDINAL BRACING AND TIE RODS

POOL SWELL DRAG AND FALLBACK SUBMERGED STRUCTURE

LOAD DISTRIBUTION

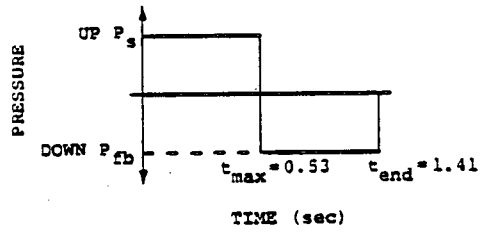

BRACING MEMBER	SEGMENT NUMBER	PRESSURE MAGNITUDE (psi)	
		P_s	P_{fb}
1	8 10 12 14	21.79 21.44 20.76 20.30	-6.66 -6.59 -6.53 -6.50
2	8 10 12 14	17.50 16.30 15.67 15.38	-6.21 -6.21 -6.21 -6.21
3	7 15 25 33	18.35 15.76 12.09 9.62	-6.14 -6.06 -5.86 -5.71
4	N/A	N/A	N/A(5)
5	N/A	N/A	N/A(5)
6 TIE ROD	1 2	20.54 3.65	N/A(6) N/A(6)

1. SEGMENT NUMBERS REPRESENT NODALIZATION OF STRUCTURES FOR LOAD CALCULATIONS.
2. FOR STRUCTURE GEOMETRY AND MEMBER DESIGNATIONS SEE FIGURES 3-2.1-11 AND 3-2.2-9.
3. PRESSURES SHOWN ARE APPLIED TO VERTICAL PROJECTED AREAS IN DIRECTION NORMAL TO STRUCTURE.
4. LOADS ARE SYMMETRIC WITH RESPECT TO VERTICAL CENTERLINE OF VENT HEADER.
5. BRACING MEMBERS 4 AND 5 ARE SHIELDED BY VENT HEADER AND BRACING MEMBER 2.
6. TIE RODS WILL EXPERIENCE NEGLIGIBLE FALLBACK LOADS.

Table 3-2.2-7

SUPPORT COLUMN LOCA AIR AND WATER CLEARING SUBMERGED STRUCTURE LOAD DISTRIBUTION

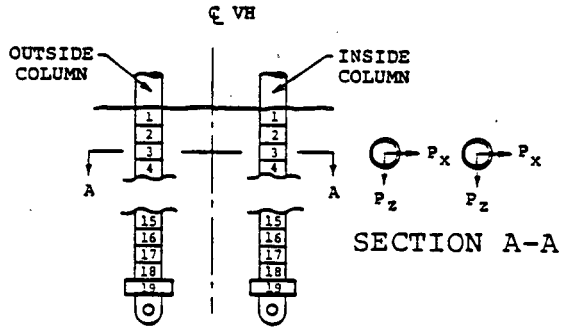

ELEVATION VIEW - MITER JOINT

SEGMENT NUMBER	PRESSURE MAGNITUDE (psi)			
	INSIDE COLUMN		OUTSIDE COLUMN	
	P_x	P_z	P_x	P_z
1	-0.12	-0.04	-0.04	-0.04
2	-0.34	-0.08	-0.10	-0.10
3	-0.62	-0.14	-0.16	-0.16
4	-1.00	-0.22	-0.20	-0.24
5	-1.52	-0.34	-0.24	-0.34
6	-2.22	-0.50	-0.26	-0.46
7	-3.08	-0.74	-0.26	-0.60
8	22.20	17.20	25.96	35.74
9	21.48	16.96	25.98	35.74
10	21.40	16.90	25.94	17.46
11	22.02	17.06	25.90	17.52
12	22.96	17.30	25.84	17.58
13	23.88	17.50	25.78	17.66
14	24.64	17.64	25.72	17.74
15	25.20	17.72	25.68	17.82
16	28.82	20.02	25.32	17.92
17	29.56	20.06	25.12	18.16
18	30.06	20.06	25.04	18.34
19	27.44	14.78	22.14	13.14

1. LOADS SHOWN INCLUDE DLF'S OF 2.0.

TABLE 3-2.2-8

DOWNCOMER LOCA AIR CLEARING SUBMERGED STRUCTURE LOAD DISTRIBUTION

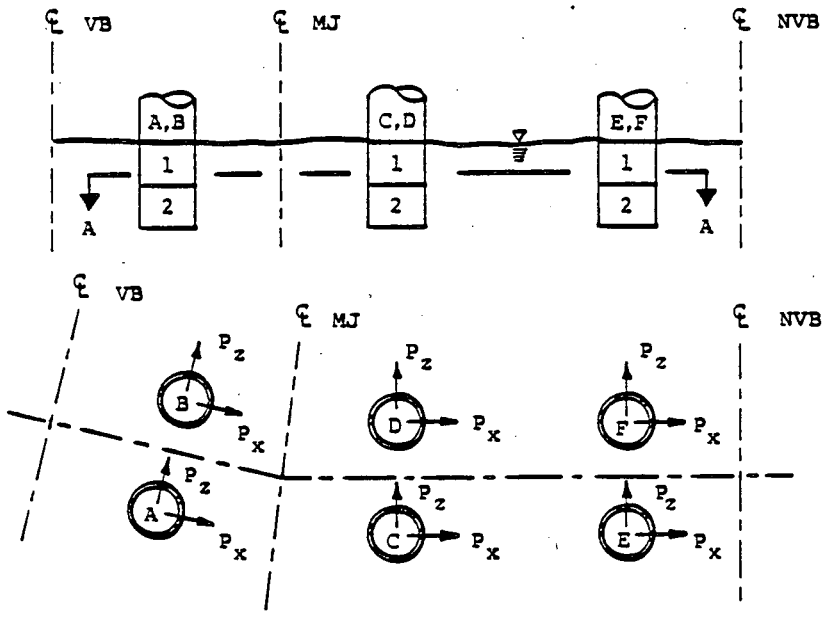

SECTION A-A

ITEM		SEGMENT NUMBER	PRESSURE MAGNITUDE (psi) (1)	
			P_x	P_z
DOWNCOMER	A	1	0.39	0.44
		2	1.36	1.14
	B	1	0.39	0.44
		2	1.36	1.14
	C	1	0.39	0.44
		2	1.36	1.14
	D	1	0.39	0.44
		2	1.36	1.14
	E	1	-0.36	-0.75
		2	-1.25	-2.09
	F	1	-0.36	0.68
		2	-1.32	1.91

(1) LOADS SHOWN INCLUDE DLF'S OF 2.0.

Table 3-2.2-9

DOWNCOMER LONGITUDINAL BRACING AND TIE RODS
LOCA AIR CLEARING SUBMERGED STRUCTURE
LOAD DISTRIBUTION

BRACING MEMBER (1)	SEGMENT NUMBER (2)	PRESSURE MAGNITUDE (psi) (3)		
		P_x	P_y	P_z
1	8	3.30	-8.38	0.00
	10	4.17	-10.03	0.00
	12	6.10	-13.69	0.00
	14	8.38	-17.35	0.00
2	5	3.35	-8.61	0.00
	8	2.06	-5.94	0.00
	12	2.26	-6.43	0.00
	19	4.17	-8.85	0.00
3	3	-2.10	-5.64	0.00
	10	-1.01	-3.23	0.00
	20	-3.94	-8.18	0.00
	30	-11.60	-20.51	0.00
4	5	0.30	-6.81	0.00
	8	0.26	-6.20	0.00
	12	0.26	-6.22	0.00
	19	0.31	-6.64	0.00
5	4	1.05	-3.01	-3.01
	8	0.59	-2.55	-2.55
	12	0.33	-2.47	-2.47
	16	0.05	-4.68	-4.68
6 TIE ROD	1	0.00	-8.81	1.41
	2	0.00	-4.24	0.00

(1) REFER TO FIGURE 3-2.2-9 FOR BRACING MEMBER DESIGNATION AND AXIS ORIENTATION.

(2) THE SEGMENTS SELECTED GIVE A REPRESENTATIVE DISTRIBUTION OF PRESSURE MAGNITUDE.

(3) LOADS SHOWN INCLUDE DLF'S OF 2.0.

Table 3-2.2-10

IBA CONDENSATION OSCILLATION

DOWNCOMER LOADS

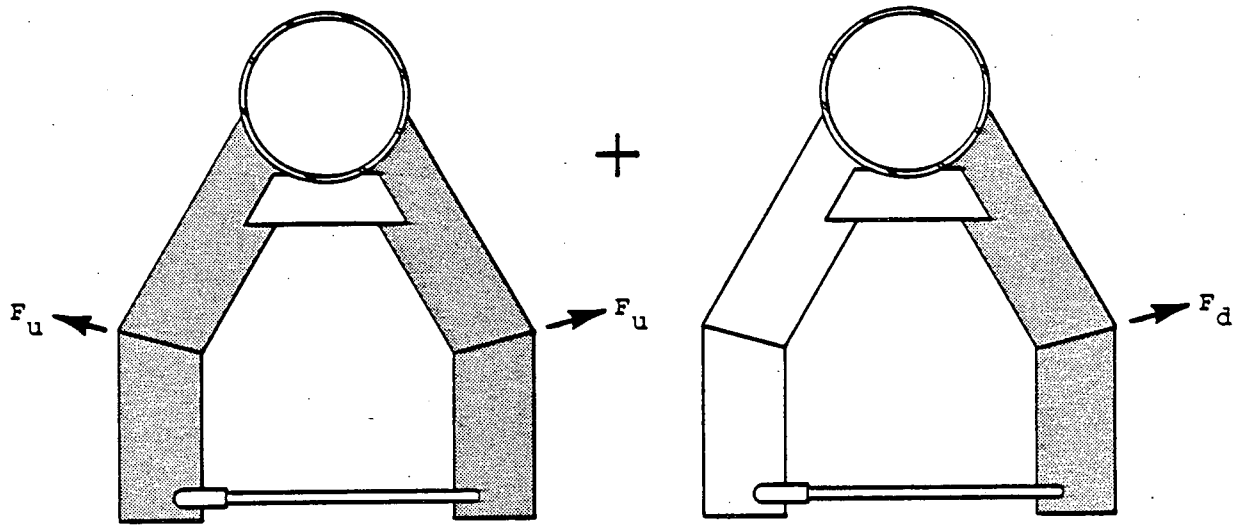

UNIFORM PRESSURE

DIFFERENTIAL PRESSURE

FREQUENCY INTERVAL (Hz)	DOWNCOMER LOAD AMPLITUDES (1)			
	UNIFORM (F_u)		DIFFERENTIAL (F_d) (2)	
	PRESSURE (psi)	FORCE (lb)	PRESSURE (psi)	FORCE (lb)
6.0 - 10.0	1.10	246.97	0.20	44.90
12.0 - 20.0	0.80	179.62	0.20	44.90
18.0 - 30.0	0.20	44.90	0.20	44.90

(1) EFFECTS OF UNIFORM AND DIFFERENTIAL PRESSURES SUMMED TO OBTAIN TOTAL LOAD.

(2) SEE FIGURE 3-2.2-10 FOR DOWNCOMER DIFFERENTIAL PRESSURE LOAD DISTRIBUTION.

Table 3-2.2-11

DBA CONDENSATION OSCILLATION

DOWNCOMER LOADS

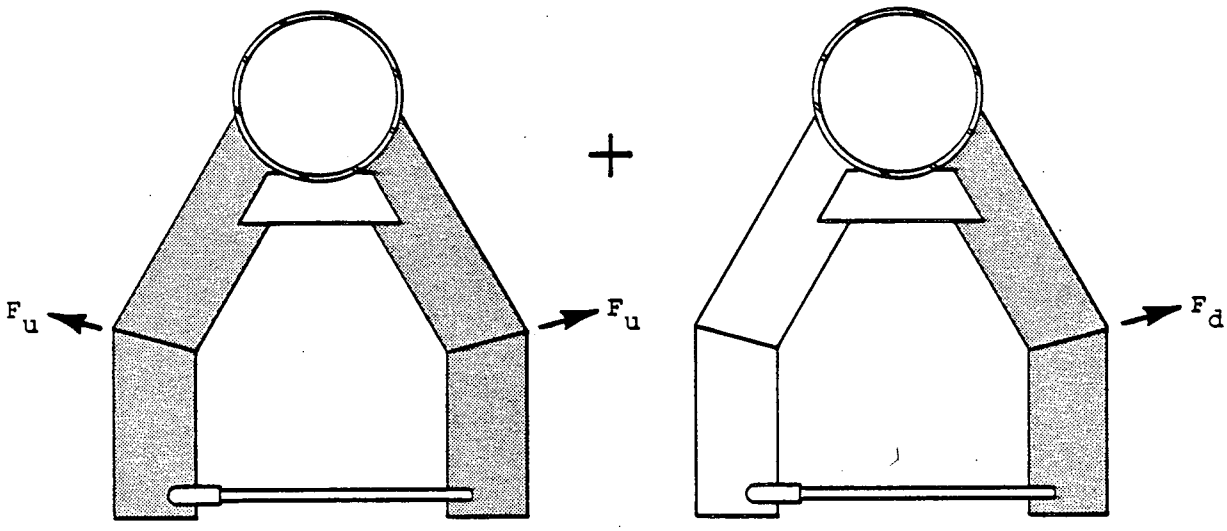

UNIFORM PRESSURE

DIFFERENTIAL PRESSURE

FREQUENCY INTERVAL (Hz)	DOWNCOMER LOAD AMPLITUDES (1)			
	UNIFORM (F_u)		DIFFERENTIAL (F_d) (2)	
	PRESSURE (psi)	FORCE (lb)	PRESSURE (psi)	FORCE (lb)
4.0 - 8.0	3.60	808.27	2.85	639.88
8.0 - 16.0	1.30	291.88	2.60	583.75
12.0 - 24.0	0.60	134.71	1.20	269.42

(1) EFFECTS OF UNIFORM AND DIFFERENTIAL PRESSURES SUMMED TO OBTAIN TOTAL LOAD.

(2) SEE FIGURE 3-2.2-10 FOR DOWNCOMER DIFFERENTIAL PRESSURE LOAD DISTRIBUTION.

Table 3-2.2-12

IBA AND DBA CONDENSATION OSCILLATION
VENT SYSTEM INTERNAL PRESSURES

LOAD CHARACTERISTICS	COMPONENT LOAD			
	VENT LINE		VENT HEADER	
	IBA	DBA	IBA	DBA
TYPE	SINGLE HARMONIC	SINGLE HARMONIC	SINGLE HARMONIC	SINGLE HARMONIC
MAGNITUDE (psi)	± 2.5	± 2.5	± 2.5	± 2.5
DISTRIBUTION	UNIFORM	UNIFORM	UNIFORM	UNIFORM
FREQUENCY RANGE (Hz)	6-10	4-8	6-10	4-8

1. DOWNCOMER CO INTERNAL PRESSURE LOADS ARE INCLUDED IN TABLES 3-2.2-10 AND 3-2.2-11.

2. LOADS SHOWN ACT IN ADDITION TO VENT SYSTEM INTERNAL PRESSURES IN FIGURES 3-2.2-2 AND 3-2.2-3.

3. AN ADDITIONAL STATIC INTERNAL PRESSURE OF 1.55 psi IS APPLIED TO THE ENTIRE VENT SYSTEM TO ACCOUNT FOR NOMINAL SUBMERGENCE OF DOWNCOMERS.

Table 3-2.2-13

SUPPORT COLUMN DBA CONDENSATION OSCILLATION SUBMERGED STRUCTURE LOAD DISTRIBUTION

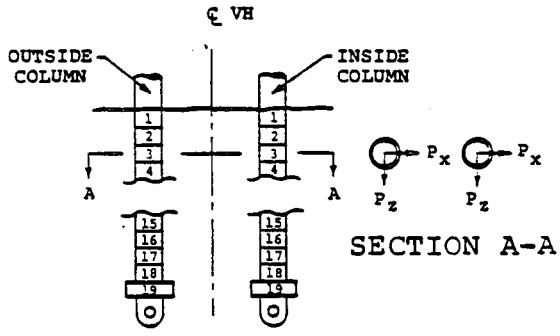

ELEVATION VIEW - MITER JOINT

SEGMENT NUMBER	PRESSURE MAGNITUDE (psi)			
	INSIDE COLUMN		OUTSIDE COLUMN	
	P_x	P_z	P_x	P_z
1	0.49	-0.39	-0.08	-0.36
2	1.54	-1.21	-0.25	-1.10
3	2.80	-2.20	-0.43	-1.88
4	4.38	-3.44	-0.61	-2.71
5	6.32	-4.97	-0.80	-3.54
6	8.40	-6.60	-0.96	-4.28
7	9.98	-7.84	-1.08	-4.77
8	10.30	-8.09	-1.11	-4.90
9	7.29	-5.72	-0.96	-4.23
10	5.82	-4.56	-0.86	-3.75
11	0.39	-0.31	-0.07	-0.33
12	1.22	-0.96	-0.23	-1.00
13	2.22	-1.74	-0.39	-1.71
14	3.47	-2.72	-0.56	-2.46
15	5.01	-3.93	-0.73	-3.22
16	12.19	-9.58	-5.42	-24.02
17	14.49	-11.38	-6.05	-26.80
18	14.95	-11.74	-6.23	-27.54
19	13.41	-10.52	-5.95	-26.14

1. LOADS SHOWN INCLUDE DLF'S, BUT DO NOT INCLUDE FSI EFFECTS.

Table 3-2.2-14

DOWNCOMER LONGITUDINAL BRACING AND TIE RODS
DBA CONDENSATION OSCILLATION SUBMERGED STRUCTURE
LOAD DISTRIBUTION

BRACING MEMBER (1)	SEGMENT NUMBER (2)	PRESSURE MAGNITUDE (psi)		
		P_x	P_y	P_z
1	8	-1.28	-1.40	0.00
	10	-1.82	-1.67	0.00
	12	-3.37	-2.43	0.00
	14	-5.83	-3.50	0.00
2	6	-1.07	-1.28	0.00
	8	-7.83	-1.14	0.00
	12	-8.82	-1.18	0.00
	19	-5.77	-3.45	0.00
3	6	0.38	-0.72	0.00
	10	0.31	-0.68	0.00
	20	1.10	-0.99	0.00
	30	3.95	-2.18	0.00
4	6	-0.13	-1.98	0.00
	8	-0.12	-1.93	0.00
	12	-0.12	-1.93	0.00
	19	-0.15	-2.10	0.00
5	8	-0.32	-1.02	-0.77
	10	-0.25	-1.09	-0.82
	12	-0.18	-1.11	-0.84
	14	-0.12	-1.12	-0.84
6 TIE ROD	1	0.00	-3.07	2.86
	2	0.00	-1.09	0.03

(1) REFER TO FIGURE 3-2.2-9 FOR BRACING MEMBER DESIGNATION AND AXIS PRIENTATION.

(2) THE SEGMENTS SELECTED GIVE A REPRESENTATIVE DISTRIBUTION OF PRESSURE MAGNITUDE.

(3) LOADS SHOWN INCLUDE DLF'S.

Table 3-2.2-15

MAXIMUM DOWNCOMER CHUGGING LOAD DETERMINATION

MAXIMUM CHUGGING LOAD FOR SINGLE DOWNCOMER
FSTF
MAXIMUM LOAD MAGNITUDE: $P_1 = 3.046$ kips
TIED DOWNCOMER FREQUENCY: $f_1 = 2.9$ Hz
PULSE DURATION: $t_d = 0.003$ sec
DYNAMIC LOAD FACTOR: $DLF_1 = \pi f_1 t_d = 0.027$
MONTICELLO
DOWNCOMER FREQUENCY: $f = 11.11$ Hz (1)
DYNAMIC LOAD FACTOR: $DLF = \pi f t_d = 0.105$
MAXIMUM LOAD MAGNITUDE (IN ANY DIRECTION):
P_{max} (2) $= P_1 \left(\frac{DLF}{DLF_1}\right) = (3.046)\ (3.878) = 11.81$ kips

(1) SEE FIGURE 3-2.4-12 FOR FREQUENCY DETERMINATION.

(2) MAXIMUM CHUGGING LOAD MAGNITUDE FOR STRESS EVALUATION IN THE DOWNCOMER BRACING IS

$$F_{max} = \frac{3.046 \text{ kips}}{\pi \times 11.11 \times 0.003} = 29.10 \text{ kips.}$$

Table 3-2.2-16

MULTIPLE DOWNCOMER CHUGGING LOAD MAGNITUDE DETERMINATION

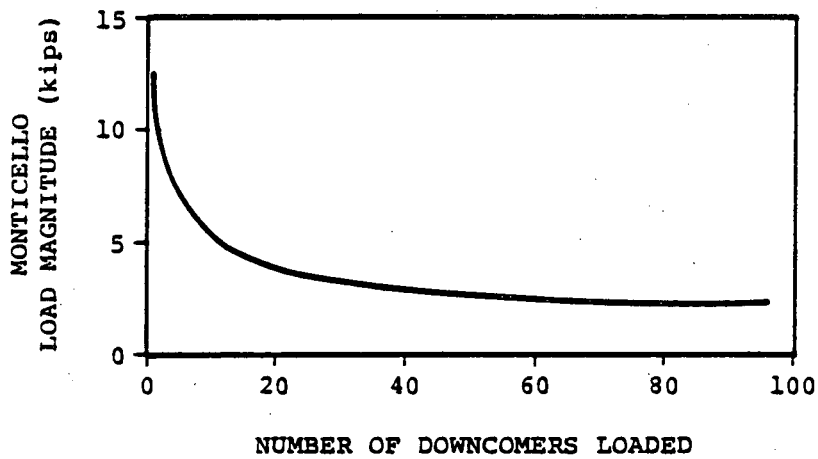

CHUGGING LOADS FOR MULTIPLE DOWNCOMERS (kips)				
NUMBER OF DOWNCOMBRS	NUMBER OF CHUGS	PROBABILITY OF EXCEEDANCE	FSTF LOAD PER DOWNCOMBR	MONTICELLO LOAD PER DOWNCOMER
6	412	2.42×10^{-3}	1.67	6.48
12	825	1.21×10^{-3}	1.20	4.65
24	1605	6.06×10^{-4}	0.91	3.53
48	3301	3.03×10^{-4}	0.68	2.64
96	6602	1.52×10^{-4}	0.57	2.21

FSTF

CHUGGING DURATION: $T_{c_1} = 512$ sec

NUMBER OF DOWNCOMERS: $n_{dc_1} = 8$

NUMBER OF CHUGS: $N_{c_1} = 313$

MONTICELLO

CHUGGING DURATION: $T_c = 900$ sec

NUMBER OF DOWNCOMERS: $n_{dc} = 2$ TO 96

NUMBER OF CHUGS: $N_c = \frac{N_{c_1}}{T_{c_1} \times n_{dc_1}} \times T_c \times n_{dc}$

PROBABILITY OF EXCEEDANCE: $P_{ex} = 1/N_c$

Table 3-2.2-17

CHUGGING LATERAL LOADS FOR MULTIPLE DOWNCOMERS – MAXIMUM OVERALL EFFECTS

LOAD CASE NUMBER	NUMBER OF DOWNCOMERS LOADED	LOAD DESCRIPTION	LOAD(1) MAGNITUDE (kips)
1	96	ALL DOWNCOMERS, PARALLEL TO MC PLANE, SAME DIRECTION, MAXIMIZE OVERALL LATERAL LOAD	2.21
2	96	ALL DOWNCOMERS, PARALLEL TO ONE VL, SAME DIRECTION, MAXIMIZE OVERALL LATERAL LOAD	2.21
3	96	ALL DOWNCOMERS, PARALLEL TO VH, SAME DIRECTION, MAXIMIZE VL BENDING	2.21
4	96	ALL DOWNCOMERS PERPENDICULAR TO VH, SAME DIRECTION, MAXIMIZE VH TORQUE	2.21
5	12	DOWNCOMERS CENTERED ON ONE VL, PERPENDICULAR TO VH, OPPOSING DIRECTIONS, MAXIMIZE VL BENDING	4.65
6	12	DOWNCOMERS CENTERED ON ONE VL, PERPENDICULAR TO VH, SAME DIRECTIONS, MAXIMIZE VL AXIAL LOADS	4.65
7	12	ALL DOWNCOMERS BETWEEN TWO VL'S, PERPENDICULAR TO VH, SAME DIRECTION MAXIMIZE VH BENDING	4.65
8-10	4	NVB DOWNCOMERS NEAR MITER, PARALLEL TO VH, PERMUTATE DIRECTIONS, MAXIMIZE DC BRACING LOADS	8.01

(1) MAGNITUDES OBTAINED FROM TABLE 3-2.2-16.

Table 3-2.2-18

CHUGGING LATERAL LOADS ON TWO DOWNCOMERS - MAXIMUM LOCAL EFFECTS

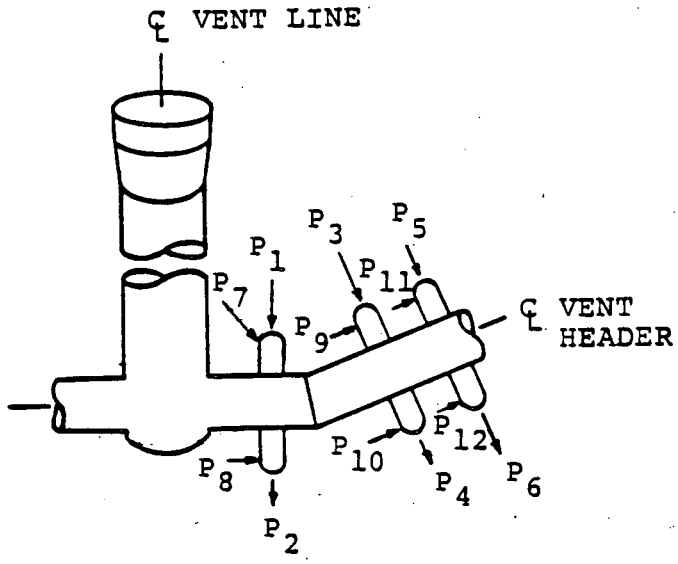

KEY DIAGRAM-PLAN VIEW

DOWNCOMER LOAD CASES FOR MAXIMUM LOCAL EFFECTS					
LOAD CASE NUMBER	ACTIVE (1) LOADS (P_i)	LOAD (2) MAGNITUDE (kips)	LOAD CASE NUMBER	ACTIVE (2) LOADS (P_i)	LOAD (2) MAGNITUDE (kips)
11	$+P_1$, $-P_2$	10.74	17	$-P_9$, $+P_{10}$	10.74
12	$+P_1$, $+P_2$	10.74	18	$+P_9$, $+P_{10}$	10.74
13	$-P_7$, $+P_8$	10.74	19	$+P_5$, $-P_6$	10.74
14	$+P_7$, $+P_8$	10.74	20	$+P_5$, $+P_6$	10.74
15	$+P_3$, $-P_4$	10.74	21	$-P_{11}$, $+P_{12}$	10.74
16	$+P_3$, $+P_4$	10.74	22	$+P_{11}$, $+P_{12}$	10.74

(1) SIGNS DESIGNATE DIRECTION.

(2) MAGNITUDES OBTAINED FROM TABLE 3-2.2-16.

Table 3-2.2-19

LOAD REVERSAL HISTOGRAM FOR CHUGGING DOWNCOMER LATERAL LOAD FATIGUE EVALUATION

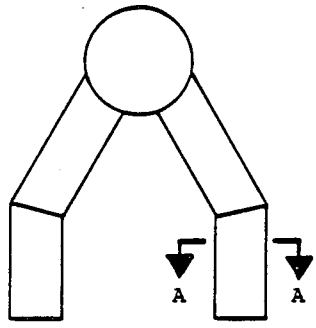

ELEVATION VIEW

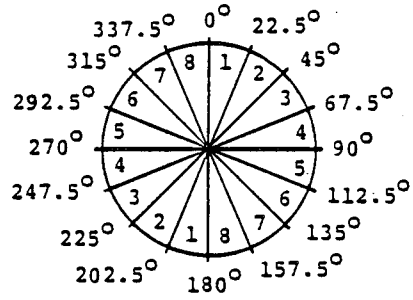

SECTION A-A

KEY DIAGRAM

PERCENT OF MAXIMUM LOAD RANGE (2)	ANGULAR SECTOR LOAD REVERSALS (cycles) (1)							
	1	2	3	4	5	6	7	8
5-10	4706	2573	2839	3076	3168	2673	2563	4629
10-15	2696	1206	1100	1104	1096	1052	1163	2545
15-20	1399	727	653	572	709	708	679	1278
20-25	676	419	452	377	370	398	368	621
25-30	380	250	252	225	192	255	197	334
30-35	209	187	139	121	97	114	162	208
35-40	157	62	84	86	62	60	90	150
40-45	113	53	28	39	48	44	58	86
45-50	83	33	32	26	18	23	33	67
50-55	65	26	14	11	9	7	16	40
55-60	51	26	11	5	11	11	23	28
60-65	44	9	2	4	0	5	9	26
65-70	32	16	7	5	0	2	9	21
70-75	12	9	11	5	0	4	7	19
75-80	26	4	2	0	2	4	7	18
80-85	7	5	2	0	0	0	0	12
85-90	4	11	0	0	0	0	5	11
90-95	7	4	0	0	2	0	0	9
95-100	2	5	0	0	0	2	4	7

(1) VALUES SHOWN ARE FOR CHUGGING DURATION OF 900 SECONDS.

(2) THE MAXIMUM SINGLE DOWNCOMER LOAD MAGNITUDE RANGE USED FOR FATIGUE IS 3.936 x 3.878 = 15.3 kips (SEE TABLE 3-2.2-15).

Table 3-2.2-20

CHUGGING VENT SYSTEM INTERNAL PRESSURES

LOAD TYPE		LOAD DESCRIPTION	COMPONENT LOAD MAGNITUDE (psi)		
NUMBER	DESCRIPTION		VENT LINE	VENT HEADER	DOWN-COMER
1	GROSS VENT SYSTEM PRESSURE OSCILLATION	TRANSIENT PRESSURE UNIFORM DISTRIBUTION	±2.5	±2.5	±5.0
2	ACOUSTIC VENT SYSTEM PRESSURE OSCILLATION	SINGLE HARMONIC IN 6.9 TO 9.5 Hz RANGE UNIFORM DISTRIBUTION	±2.5	±3.0	±3.5
3	ACOUSTIC DOWNCOMER PRESSURE OSCILLATION	SINGLE HARMONIC IN 40.0 TO 50.0 Hz RANGE. UNIFORM DISTRIBUTION	N/A	N/A	±13.0

1. DOWNCOMER LOADS SHOWN USED FOR HOOP STRESS CALCULATIONS ONLY.
2. LOADS SHOWN ACT IN ADDITION TO INTERNAL PRESSURES IN FIGURES 3-2.2-2 AND 3-2.2-3.

FORCING FUNCTION FOR LOAD TYPE 1

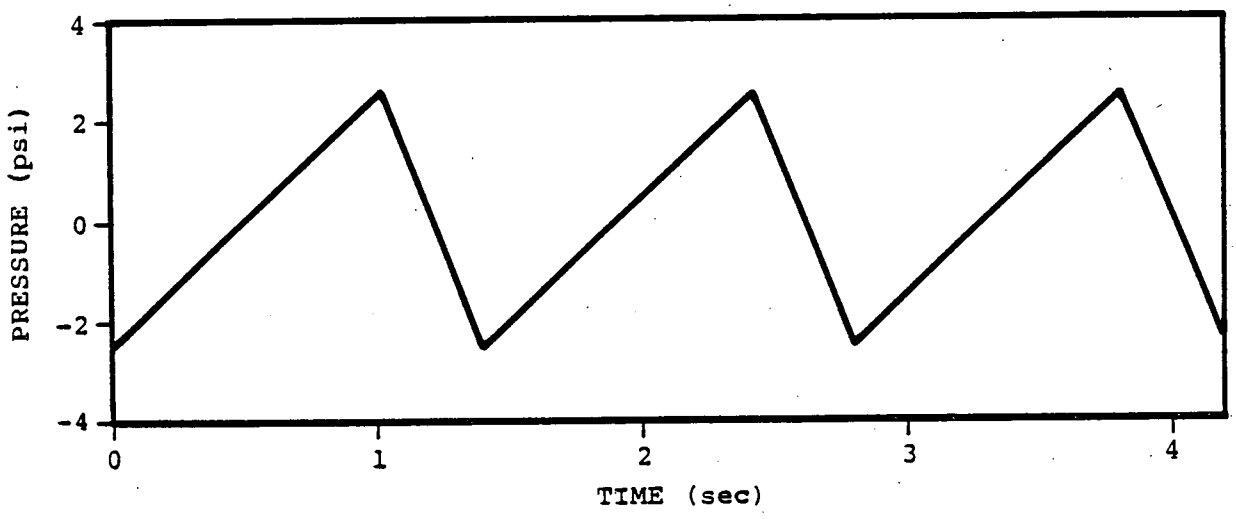

Table 3-2.2-21

SUPPORT COLUMN PRE-CHUG SUBMERGED STRUCTURE

LOAD DISTRIBUTION

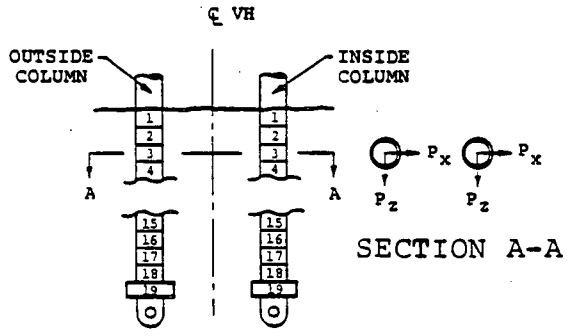

ELEVATION VIEW - MITER JOINT

SEGMENT NUMBER	PRESSURE MAGNITUDE (psi)			
	INSIDE COLUMN		OUTSIDE COLUMN	
	P_x	P_z	P_x	P_z
1	0.04	-0.04	-0.01	-0.04
2	0.13	-0.14	-0.02	-0.13
3	0.23	-0.25	-0.03	-0.22
4	0.36	-0.39	-0.05	-0.31
5	0.51	-0.57	-0.07	-0.41
6	0.68	-0.76	-0.08	-0.49
7	0.81	-0.90	-0.09	-0.55
8	0.84	-0.93	-0.09	-0.56
9	0.59	-0.66	-0.08	-0.48
10	0.47	-0.52	-0.07	-0.43
11	0.03	-0.04	-0.01	-0.04
12	0.10	-0.11	-0.02	-0.11
13	0.18	-0.20	-0.03	-0.20
14	0.28	-0.31	-0.05	-0.28
15	0.41	-0.45	-0.06	-0.37
16	0.99	-1.10	-0.44	-2.75
17	1.18	-1.30	-0.49	-3.07
18	1.22	-1.34	-0.51	-3.15
19	1.09	-1.20	-0.48	-2.99

1. LOADS SHOWN INCLUDE DLF'S, BUT DO NOT INCLUDE FSI EFFECTS.

Table 3-2.2-22

DOWNCOMER LONGITUDINAL BRACING AND TIE RODS

PRE-CHUG SUBMERGED STRUCTURE

LOAD DISTRIBUTION

BRACING MEMBER (1)	SEGMENT NUMBER (2)	PRESSURE MAGNITUDE (psi)		
		P_x	P_y	P_z
1	8	-0.18	-0.19	0.00
	10	-0.25	-0.23	0.00
	12	-0.47	-0.33	0.00
	14	-0.81	-0.47	0.00
2	6	-0.15	-0.17	0.00
	8	-0.11	-0.15	0.00
	12	-0.12	-0.16	0.00
	19	-0.80	-0.47	0.00
3	6	0.05	-0.10	0.00
	10	0.04	-0.09	0.00
	20	0.15	-0.13	0.00
	30	0.55	-0.30	0.00
4	6	-0.02	-0.27	0.00
	8	-0.02	-0.26	0.00
	12	-0.02	-0.26	0.00
	19	-0.02	-0.28	0.00
5	8	-0.044	-0.14	-0.10
	10	-0.034	-0.15	-0.11
	12	-0.025	-0.15	-0.11
	14	-0.017	-0.15	-0.11
6 TIE ROD	1	0.00	-0.40	0.37
	2	0.00	-0.14	0.00

(1) REFER TO FIGURE 3-2.2-9 FOR BRACING MEMBER DESIGNATION AND AXIS ORIENTATION.

(2) THE SEGMENTS SELECTED GIVE A REPRESENTATIVE DISTRIBUTION OF PRESSURE MAGNITUDE.

(3) LOADS SHOWN INCLUDE DLF'S.

Table 3-2.2-23

SUPPORT COLUMN POST-CHUG SUBMERGED STRUCTURE

LOAD DISTRIBUTION

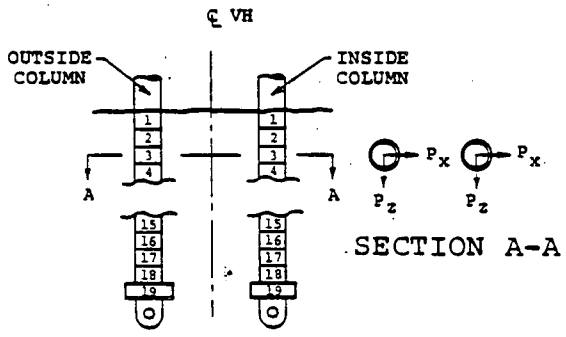

ELEVATION VIEW - MITER JOINT

SEGMENT NUMBER	PRESSURE MAGNITUDE (psi)			
	INSIDE COLUMN		OUTSIDE COLUMN	
	P_x	P_z	P_x	P_z
1	0.30	-1.53	-0.07	-1.22
2	0.98	-4.73	-0.21	-3.69
3	1.87	-8.33	-0.36	-6.24
4	3.15	-12.51	-0.53	-8.84
5	4.87	-17.25	-0.70	-11.35
6	6.83	-22.01	-0.86	-13.53
7	8.37	-25.52	-0.96	-14.99
8	8.65	-26.30	-0.99	-15.45
9	5.93	-19.08	-0.84	-13.53
10	4.43	-15.93	-0.73	-12.28
11	0.24	-1.21	-0.06	-1.11
12	0.77	-3.75	-0.19	-3.36
13	1.48	-6.60	-0.33	-5.67
14	2.49	-9.91	-0.48	-8.03
15	3.86	-13.66	-0.64	-10.32
16	9.92	-31.96	-4.82	-75.96
17	12.16	-37.05	-5.42	-84.18
18	12.55	-38.18	-5.55	-86.79
19	10.92	-35.11	-5.21	-83.51

1. LOADS SHOWN INCLUDE DLF'S, BUT DO NOT INCLUDE FSI EFFECTS.

Table 3-2.2-24

DOWNCOMER LONGITUDINAL BRACING AND TIE RODS

POST-CHUG SUBMERGED STRUCTURE LOAD DISTRIBUTION

BRACING MEMBER (1)	SEGMENT NUMBER (2)	PRESSURE MAGNITUDE (psi)		
		P_x	P_y	P_z
1	8	-4.18	-3.44	0.00
	10	-6.17	-4.43	0.00
	12	-11.87	-7.26	0.00
	14	-20.89	-11.27	0.00
2	6	-3.42	-2.98	0.00
	8	-2.51	-2.48	0.00
	12	-2.82	-2.68	0.00
	19	-20.86	-11.17	0.00
3	6	0.88	-1.48	0.00
	10	0.64	-1.35	0.00
	20	3.63	-2.64	0.00
	30	14.19	-7.20	0.00
4	6	-0.36	-4.96	0.00
	8	-0.33	-4.83	0.00
	12	-0.34	-4.89	0.00
	19	-0.49	-5.33	0.00
5	8	-0.93	-2.66	-2.01
	10	-0.72	-2.83	-2.13
	12	-0.54	-2.89	-2.18
	14	-0.36	-2.87	-2.16
6 TIE ROD	1	0.00	-8.05	13.79
	2	0.00	-1.60	1.08

(1) REFER TO FIGURE 3-2.2-9 FOR BRACING MEMBER DESIGNATION AND AXIS ORIENTATION.

(2) THE SEGMENTS SELECTED GIVE A REPRESENTATIVE DISTRIBUTION OF PRESSURE MAGNITUDE.

(3) LOADS SHOWN INCLUDE DLF'S, BUT DO NOT INCLUDE FSI EFFECTS.

Table 3-2.2-25

SUPPORT COLUMN SRV DISCHARGE SUBMERGED STRUCTURE

LOAD DISTRIBUTION

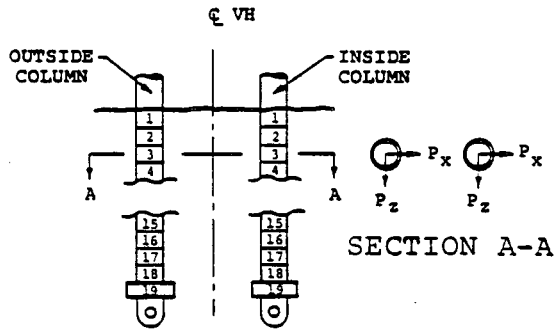

ELEVATION VIEW - MITER JOINT

SEGMENT NUMBER	PRESSURE MAGNITUDE (psi)			
	INSIDE COLUMN		OUTSIDE COLUMN	
	P_x	P_z	P_x	P_z
1	2.13	-13.36	2.13	-13.36
2	2.13	-13.36	2.13	-13.36
3	4.62	-24.38	4.62	-24.38
4	4.62	-24.38	4.62	-24.38
5	6.84	27.93	6.84	27.93
6	6.84	27.93	6.84	27.93
7	9.41	33.61	9.41	33.61
8	9.41	33.61	9.41	33.61
9	3.30	10.60	3.30	10.60
10	3.30	10.60	3.30	10.60
11	3.90	13.33	3.90	13.33
12	19.54	28.97	19.54	28.97
13	19.79	30.47	19.79	30.47
14	19.79	30.47	19.79	30.47
15	23.00	33.56	23.00	33.56
16	23.67	35.20	23.67	35.20
17	22.85	25.81	22.85	25.81
18	22.85	25.81	22.85	25.81
19	22.55	24.11	22.55	24.11

1. LOADS IN X AND Z DIRECTIONS INCLUDE DLF'S OF 2.30 AND 1.26, RESPECTIVELY.

Table 3-2.2-26

DOWNCOMER SRV DISCHARGE SUBMERGED STRUCTURE LOAD DISTRIBUTION

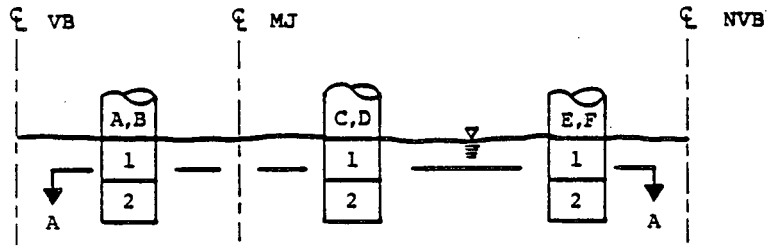

ELEVATION VIEW-DOWNCOMERS

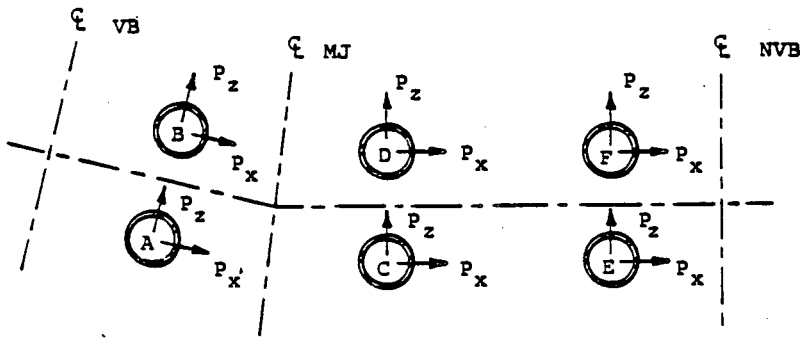

SECTION A-A

ITEM		SEGMENT NUMBER	PRESSURE MAGNITUDE (psi) (1)	
			P_x	P_z
DOWNCOMER	A	1	-1.98	0.39
		2	-4.16	1.19
	B	1	-2.35	0.53
		2	-4.92	1.48
	C	1	-0.69	0.79
		2	-1.95	2.45
	D	1	-1.88	3.88
		2	-4.1	7.36
	E	1	-0.36	0.20
		2	-1.05	0.63
	F	1	-0.41	0.17
		2	-1.23	0.47

(1) LOADS IN X AND Z DIRECTIONS INCLUDE DLF'S OF 1.1 AND 3.0, RESPECTIVELY.

Table 3-2.2-27

DOWNCOMER LONGITUDINAL BRACING AND TIE RODS

SRV DISCHARGE SUBMERGED STRUCTURE

LOAD DISTRIBUTION

BRACING MEMBER (1)	SEGMENT NUMBER (2)	PRESSURE MAGNITUDE (psi) (3)		
		P_x	P_y	P_z
1	5 9 14	-1.16 -0.98 -0.97	0.50 0.42 0.45	0.00 0.00 0.00
2	9	-1.88	0.54	0.00
3	5 17	7.52 30.67	1.21 -1.63	0.55 -2.23
4	5 9	0.23 -0.34	0.46 0.44	0.00 0.00
5	5 10	1.03 -0.69	0.32 0.34	-1.38 -1.44
6 TIE ROD	1 2	0.00 0.00	-1.61 -1.04	-2.02 -1.01

(1) REFER TO FIGURE 3-2.2-9 FOR BRACING MEMBER DESIGNATION AND AXIS ORIENTATION.

(2) THE SEGMENTS SELECTED GIVE A REPRESENTATIVE DISTRIBUTION OF PRESSURE MAGNITUDE.

(3) LOADS SHOWN INCLUDE DLF'S.

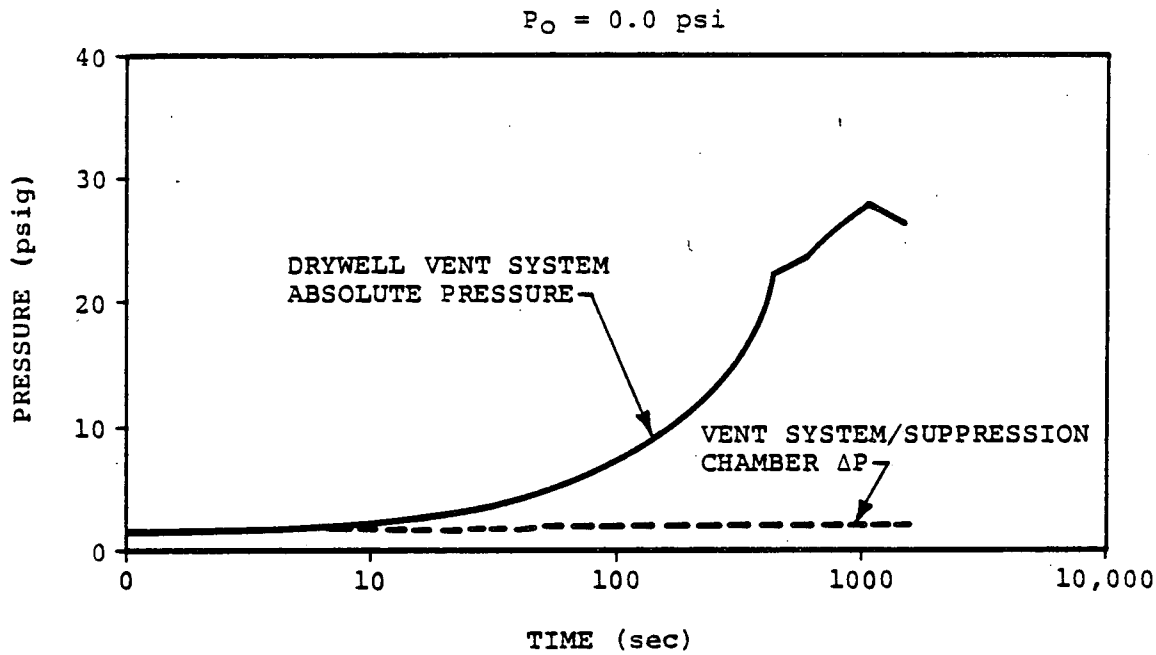

EVENT DESCRIPTION	PRESSURE DESIGNATION	TIME (sec)		PRESSURE (psig)			
		t_{min}	t_{max}	P_{min}	ΔP_{min}	P_{max}	ΔP_{max}
INSTANT OF BREAK TO ONSET OF CHUGGING	P_1	0.0	300.0	0.750	0.175	14.8	2.0
ONSET OF CHUGGING TO INITIATION OF ADS	P_2	300.0	600.0	14.8	2.0	23.2	2.0
INITIATION OF ADS TO RPV DEPRESSURIZATION	P_3	600.0	1200.0	23.2	2.0	28.0	2.0

Figure 3-2.2-1

VENT SYSTEM INTERNAL PRESSURES FOR SBA EVENT

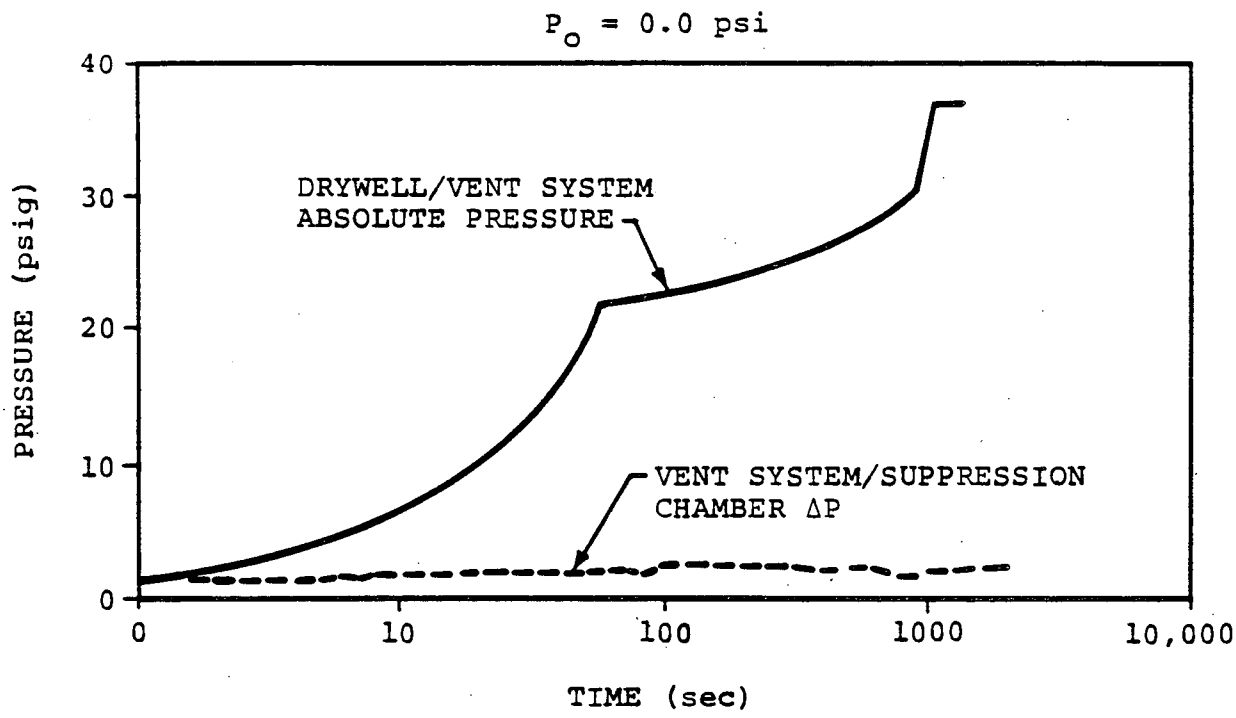

EVENT DESCRIPTION	PRESSURE DESIGNATION	TIME (sec)		PRESSURE (psig)			
		t_{min}	t_{max}	P_{min}	ΔP_{min}	P_{max}	ΔP_{max}
INSTANT OF BREAK TO ONSET OF CO AND CHUGGING	P_1	0.0	5.0	0.750	0.175	4.3	1.5
ONSET OF CO AND CHUGGING TO INITIATION OF ADS	P_2	5.0	900.0	4.3	1.5	30.1	1.8
INITIATION OF ADS TO RPV DEPRESSURIZATION	P_3	900.0	1100.0	30.1	1.8	36.8	2.4

Figure 3-2.2-2

VENT SYSTEM INTERNAL PRESSURES FOR IBA EVENT

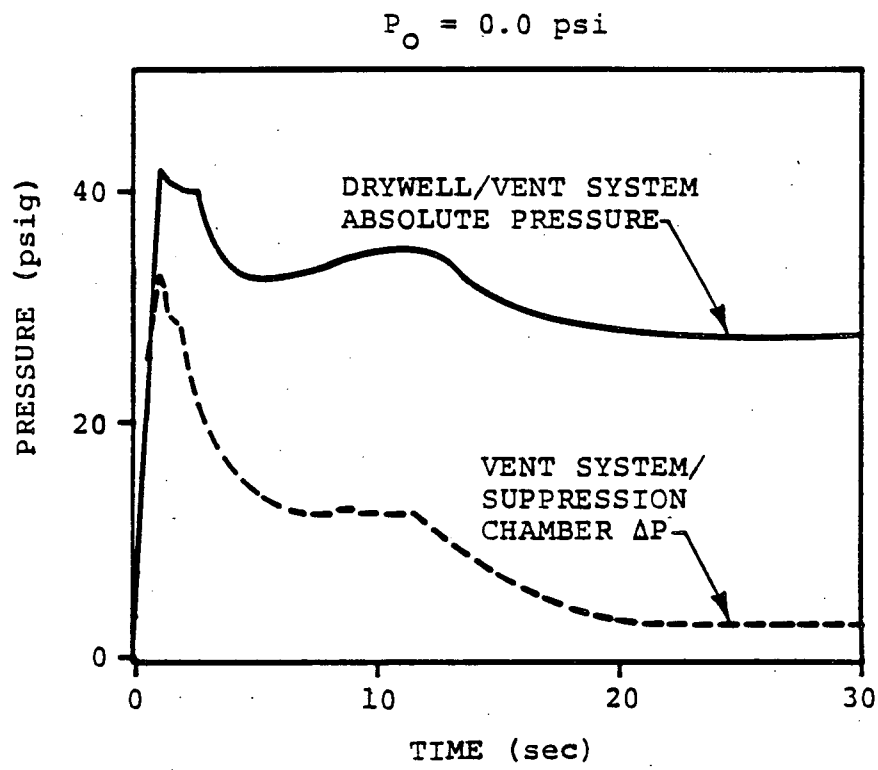

EVENT DESCRIPTION	PRESSURE DESIGNATION	TIME (sec)		PRESSURE (psig)			
		t_{min}	t_{max}	P_{min}	ΔP_{min}	P_{max}	ΔP_{max}
INSTANT OF BREAK TO TERMINATION OF POOL SWELL	P_1	0.0	1.5	0.750	0.175	41.4	32.9
TERMINATION OF POOL SWELL TO ONSET OF CO	P_2	1.5	5.0	32.3	13.8	40.2	29.2
ONSET OF CO TO ONSET OF CHUGGING	P_3	5.0	35.0	28.2	3.0	35.2	12.8
ONSET OF CHUGGING TO RPV DEPRESSURIZATION	P_4	35.0	65.0	28.2	3.0	28.2	3.0

1. DBA VENT SYSTEM INTERNAL PRESSURE LOADS ARE INCLUDED IN VENT SYSTEM PRESSURIZATION AND THRUST LOADS SHOWN IN TABLE 3-2.2-3.

Figure 3-2.2-3

VENT SYSTEM INTERNAL PRESSURES FOR DBA EVENT

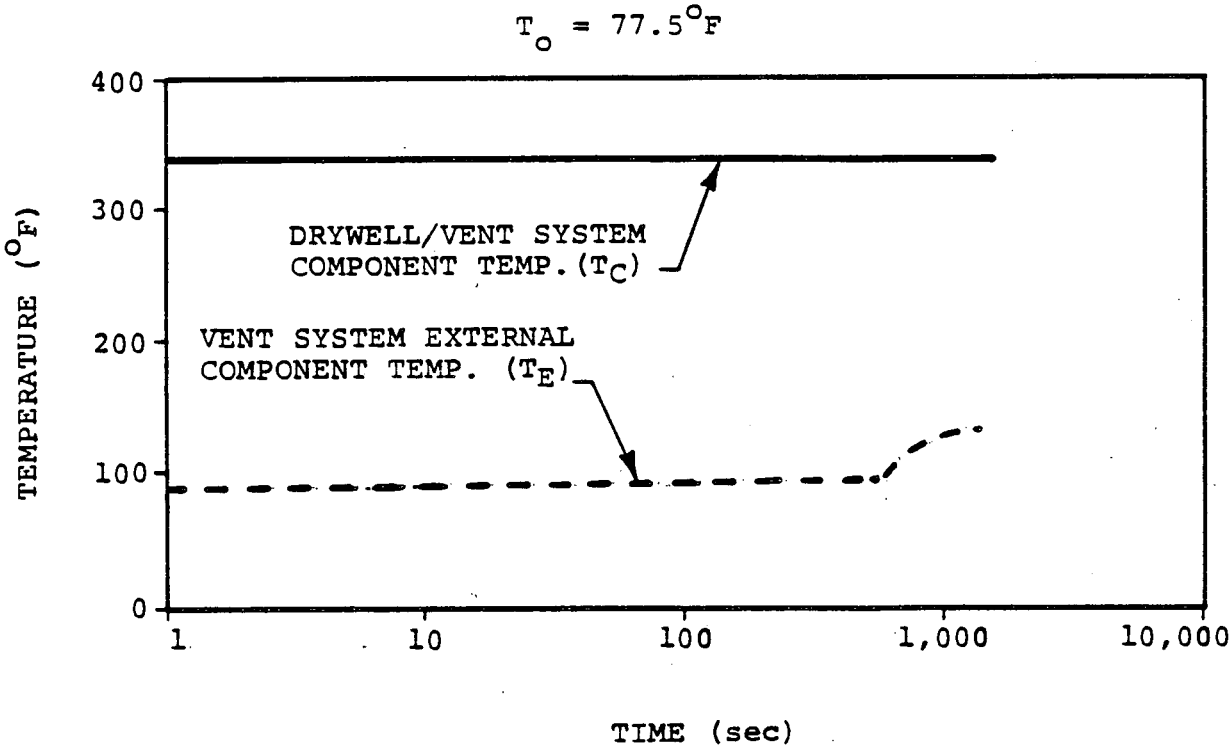

EVENT DESCRIPTION	TEMPERATURE DESIGNATION	TIME (sec)		TEMPERATURE (°F)			
		t_{min}	t_{max}	$T_{C_{min}}$	$T_{E_{min}}$	$T_{C_{max}}$	$T_{E_{max}}$
INSTANT OF BREAK TO ONSET OF CHUGGING	T_1	0.0	300.0	150.0	90.0	340.0	97.0
ONSET OF CHUGGING TO INITIATION OF ADS	T_2	300.0	600.0	340.0	97.0	340.0	98.6
INITIATION OF ADS TO RPV DEPRESSURIZATION	T_3	600.0	1200.0	340.0	102.0	340.0	136.0

1. SEE TABLE 3-2.2-2 FOR ADDITIONAL SBA EVENT TEMPERATURES.

Figure 3-2.2-4

VENT SYSTEM TEMPERATURES FOR SBA EVENT

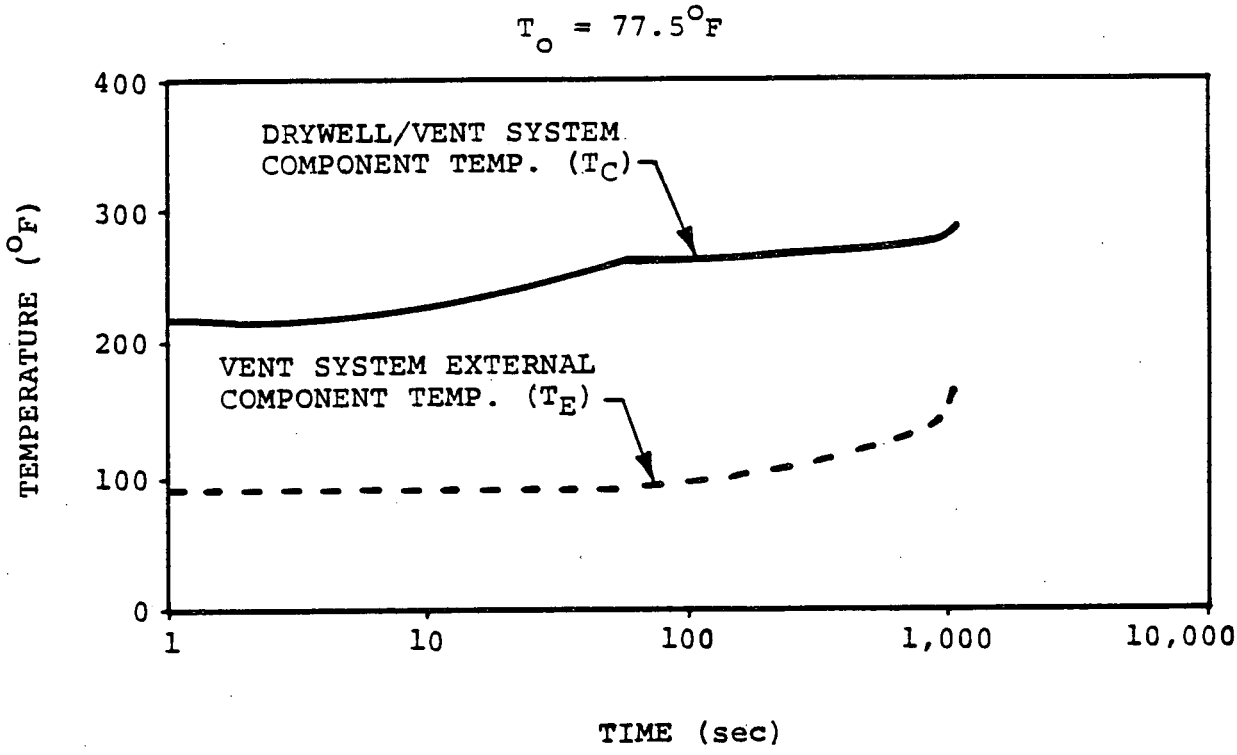

EVENT DESCRIPTION	TEMPERATURE DESIGNATION	TIME (sec)		TEMPERATURE (°F)			
		t_{min}	t_{max}	$T_{C_{min}}$	$T_{E_{min}}$	$T_{C_{max}}$	$T_{E_{max}}$
INSTANT OF BREAK TO ONSET OF CO AND CHUGGING	T_1	0.0	5.0	135.0	95.0	220.0	90.0
ONSET OF CO AND CHUGGUNG TO INITIATION OF ADS	T_2	5.0	900.0	220.0	90.0	270.0	142.0
INITIATION OF ADS TO RPV DEPRESSURIZATION	T_3	900.0	1100.0	270.0	112.0	283.0	167.0

Figure 3-2.2-5

VENT SYSTEM TEMPERATURES FOR IBA EVENT

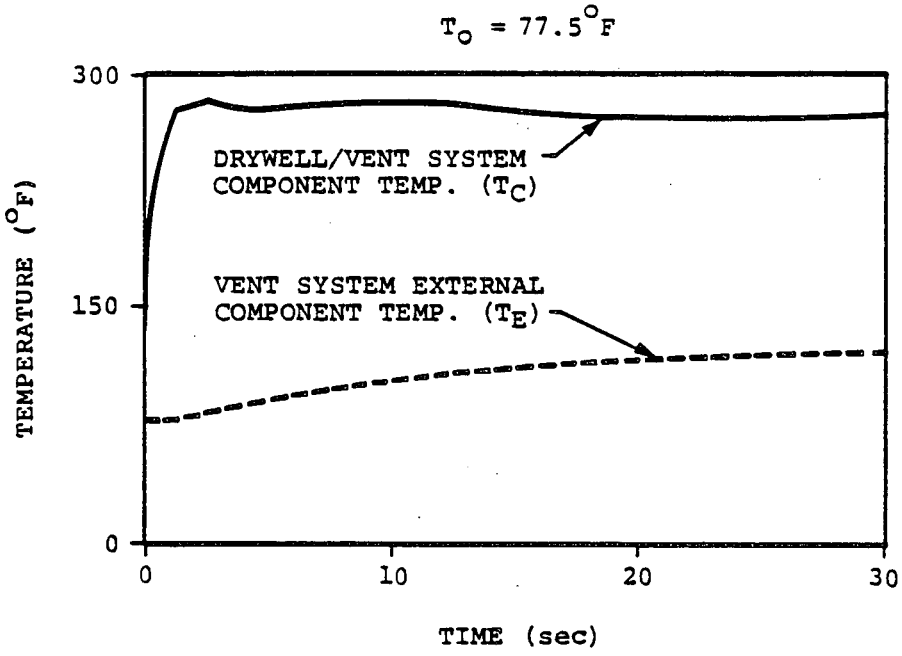

EVENT DESCRIPTION	TEMPERATURE DESIGNATION	TIME (sec)		TEMPERATURE (°F)			
		t_{min}	t_{max}	$T_{C_{min}}$	$T_{E_{min}}$	$T_{C_{max}}$	$T_{E_{max}}$
INSTANT OF BREAK TO TERMINATION OF POOL SWELL	T_1	0.0	1.5	150.0	77.5	277.2	80.6
TERMINATION OF POOL SWELL TO ONSET OF CO	T_2	1.5	5.0	273.4	80.6	281.0	89.8
ONSET OF CO TO ONSET OF CHUGGING	T_3	5.0	35.0	269.6	89.8	281.0	120.9
ONSET OF CHUGGING TO RPV DEPRESSURIZATION	T_4	35.0	65.0	269.6	120.9	269.6	120.9

Figure 3-2.2-6

VENT SYSTEM TEMPERATURES FOR DBA EVENT

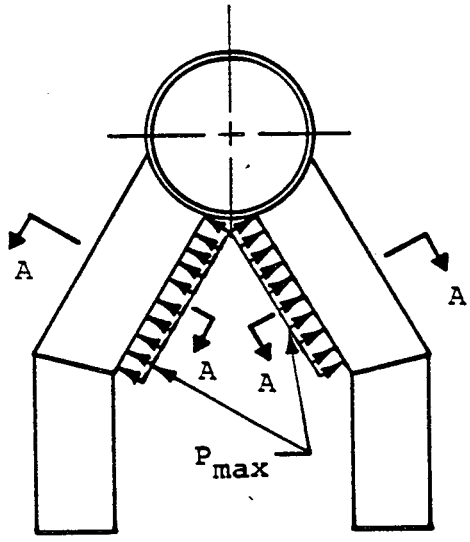

ELEVATION VIEW

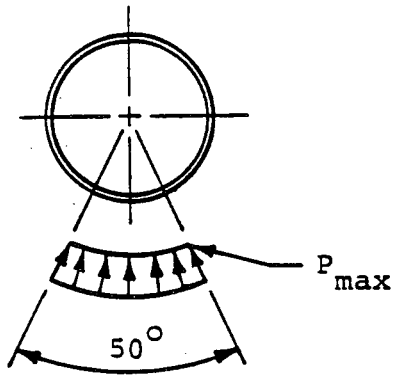

SECTION A-A

PRESSURE DISTRIBUTION

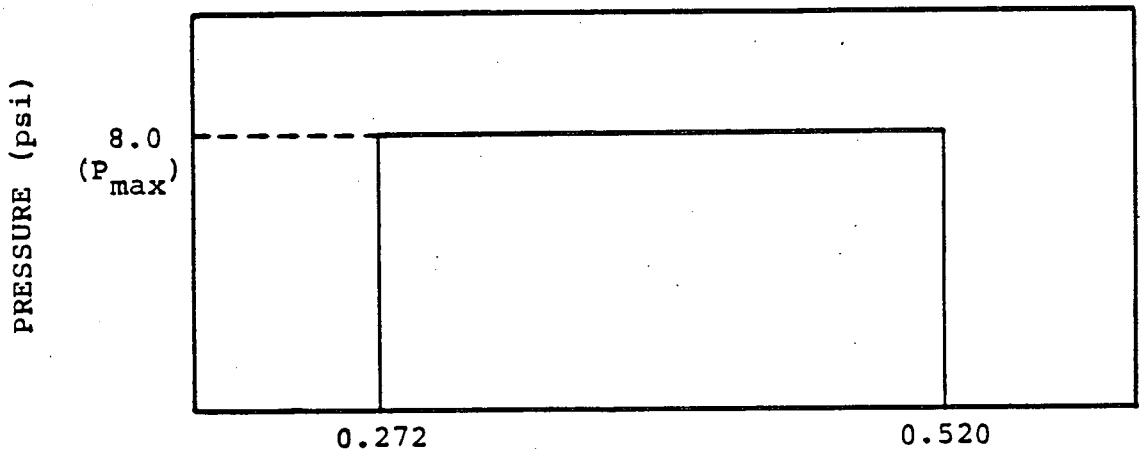

PRESSURE TRANSIENT

1. PRESSURES SHOWN ARE APPLIED IN A DIRECTION NORMAL TO DOWNCOMER'S SURFACE.

Figure 3-2.2-7

DOWNCOMER POOL SWELL IMPACT LOADS

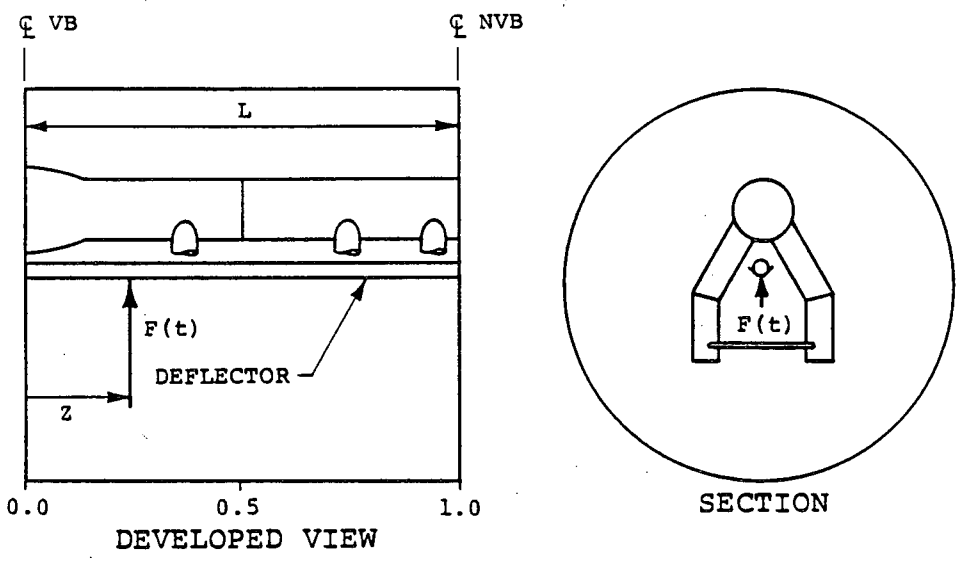

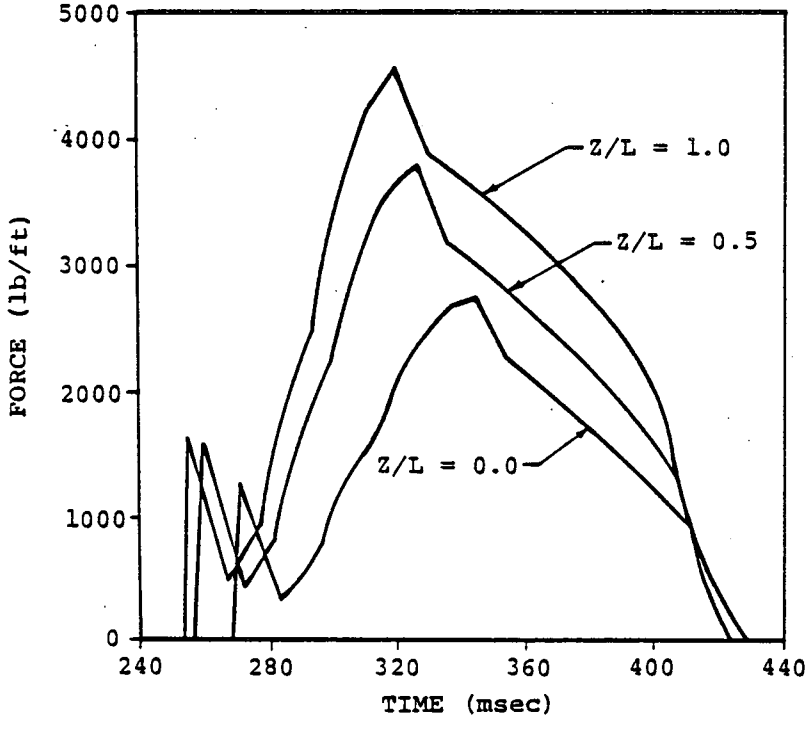

1. LOADS AT DISCRETE LOCATIONS ALONG DEFLECTOR OBTAINED BY LINEAR INTERPOLATION.

Figure 3-2.2-8

POOL SWELL IMPACT LOADS FOR VENT HEADER DEFLECTORS AT SELECTED LOCATIONS

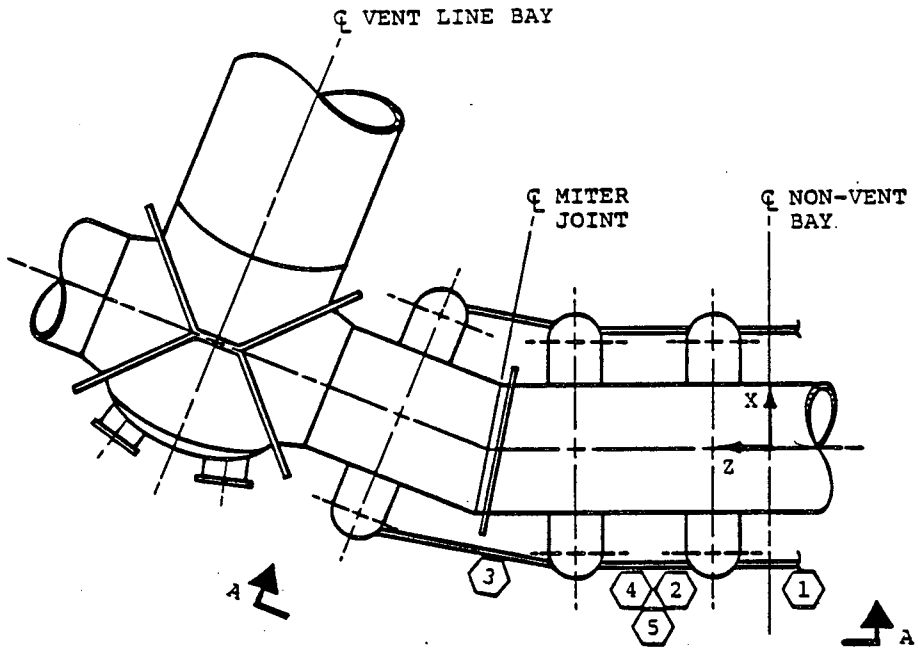

PLAN VIEW

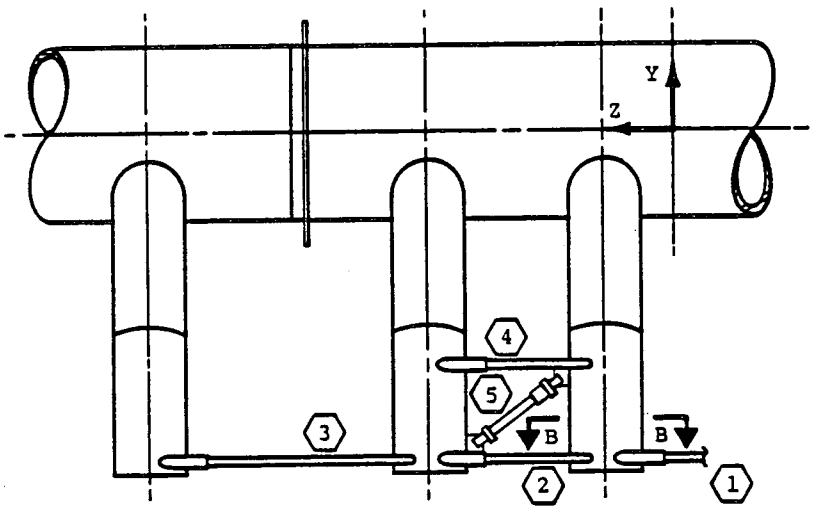

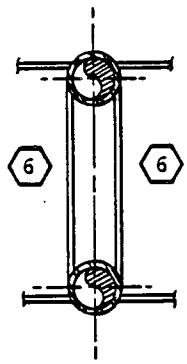

SECTION B-B
(TYPICAL AT
ALL DOWNCOMERS)

⬡ DESIGNATES BRACING MEMBER NUMBER

VIEW A-A

Figure 3-2.2-9

DOWNCOMER LONGITUDINAL BRACING AND TIE RODS

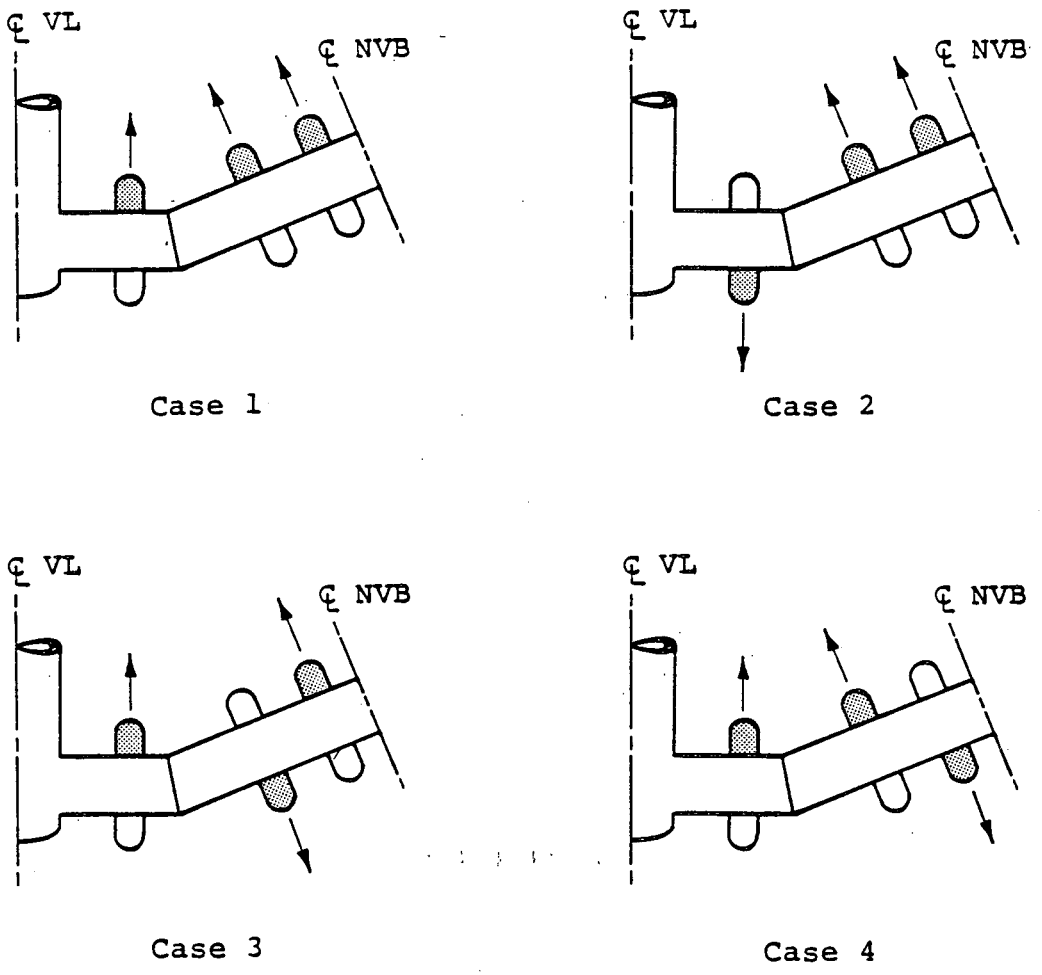

1. SEE TABLE 3-2.2-10 FOR IBA PRESSURE AMPLITUDES AND FREQUENCIES.
2. SEE TABLE 3-2.2-11 FOR DBA PRESSURE AMPLITUDES AND FREQUENCIES.
3. FOUR ADDITIONAL CASES WITH PRESSURES IN DOWNCOMERS OPPOSITE THOSE SHOWN ARE ALSO CONSIDERED.

Figure 3-2.2-10

IBA AND DBA CONDENSATION OSCILLATION DOWNCOMER DIFFERENTIAL PRESSURE LOAD DISTRIBUTION

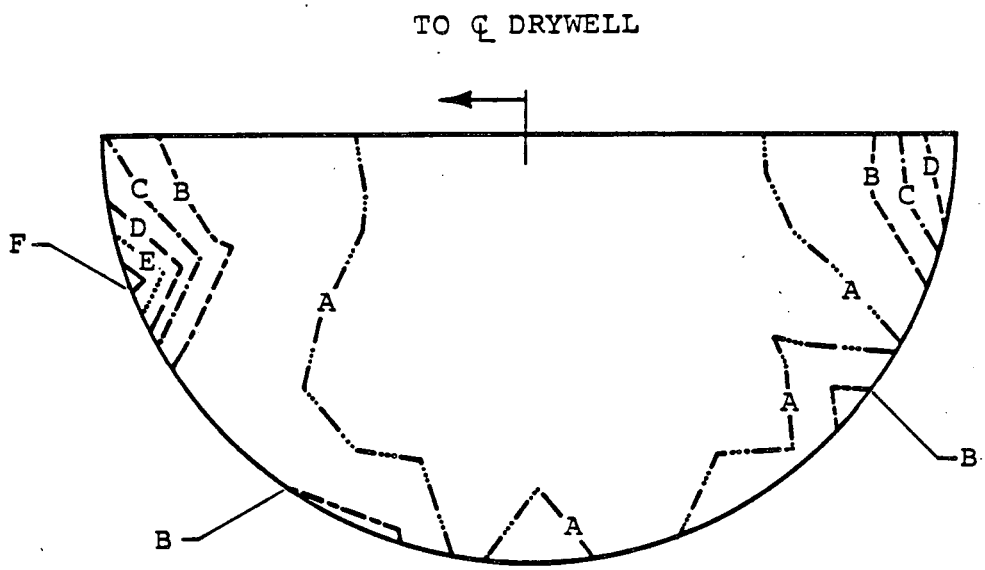

KEY DIAGRAM

NORMALIZED POOL ACCELERATIONS	
PROFILE	POOL ACCELERATION (ft/sec^2)
A	50.0
B	100.0
C	150.0
D	200.0
E	250.0
F	300.0

1. POOL ACCELERATIONS DUE TO HARMONIC APPLICATION OF TORUS SHELL PRESSURES SHOWN IN FIGURE 2-2.2-10 AT A SUPPRESSION CHAMBER FREQUENCY OF 24.14 HERTZ.

Figure 3-2.2-11

POOL ACCELERATION PROFILE
FOR DOMINANT SUPPRESSION CHAMBER FREQUENCY
AT MIDBAY LOCATION

3-2.2.2 Load Combinations

The load categories and associated load cases for which the vent system is evaluated are presented in Section 3-2.2.1. The general NUREG-0661 criteria for grouping the respective loads and load categories into event combinations are discussed in Section 1-3.2 (Table 3-2.2-28).

The 27 general event combinations shown are expanded to form a total of 69 specific vent system load combinations for the Normal Operating, SBA, IBA, and DBA events. The specific load combinations reflect a greater level of detail than is contained in the general event combinations, including distinction between SBA and IBA, distinction between pre-chug and post-chug, and consideration of multiple cases of particular loadings. The total number of vent system load combinations consists of 3 for the Normal Operating event, 18 for the SBA event, 24 for the IBA event, and 24 for the DBA event. Several different service level limits and corresponding sets of allowable stresses are associated with these load combinations.

Not all of the possible vent system load combinations are evaluated since many are enveloped by others and do not lead to controlling vent system stresses. The enveloping load combinations are determined by examining the possible vent system load combinations and comparing the respective load cases and allowable stresses. Table 3-2.2-29 shows the results of this examination. Here each enveloping load combination is assigned a number for ease of identification.

The enveloping load combinations are further reduced by examining relative load magnitudes and individual load characteristics to determine which load combinations lead to controlling vent system stresses. The load combinations which have been found to produce controlling vent system stresses are separated into two groups. The SBA II, IBA I, DBA I, DBA II, and DBA III combinations are used to evaluate stresses in all vent system components except those associated with the vent line-SRV piping penetrations. The NOC I, SBA II, IBA I, and DBA III combinations are use to evaluate stresses in the vent line-SRV piping penetrations. An explanation of the logic behind these controlling vent system load combinations is presented in the following paragraphs. Table 3-2.2-30 summarizes the controlling load combina-

tions and identifies which load combinations are enveloped by each of the controlling combinations.

Many of the general event combinations (Table 3-2.2-28) have the same allowable stresses and are enveloped by others which contain the same or additional load cases. There is no distinction between Service Level A and B conditions for the vent system since the Service Level A and B allowable stress values are the same.

Except for seismic loads, many pairs of load combinations contain identical load cases. One of the load combinations in the pair contains OBE loads and has Service Level A or B allowables, while the other contains SSE loads with Service Level C allowables. Examining the load magnitudes presented in Section 3-2.2.1 shows that both the OBE and SSE vertical accelerations are small compared to gravity. As a result, vent system stresses and support column reactions due to vertical seismic loads are small compared to those caused by other loads in the load combination. The horizontal loads for OBE and SSE are less than 50% of gravity and also result in small vent system stresses compared to those caused by other loads in the load combinations, except at the vent line-drywell penetra-

tions which provide horizontal support for the vent system. The Service Level C primary stress allowables for the load combinations containing SSE loads are 40% to 80% higher than the Service Level B allowables for the corresponding load combination containing OBE loads. Therefore the controlling load combinations for evaluation of all vent system components, except the vent line-drywell penetration, are those containing OBE loads and Service Level B allowables.

For the vent line-drywell penetration, evaluation of both OBE and SSE combinations is necessary since seismic loads are a large contributor to the total lateral load acting on the vent system for which the penetrations provide support.

Application of the above reasoning to the total number of vent system load combinations yields a reduced number of enveloping load combinations for each event. Table 3-2.2-29 shows the resulting vent system load combinations for the Normal Operating, SBA, IBA and DBA events, along with the associated service level assignments. For ease of identification, each load combination in each event is assigned a number. The reduced number of enveloping load combinations (Table 3-2.2-29) consists

of one for the Normal Operating event, four for the SBA event, five for the the IBA event, and six for the DBA event. The load case designations for the loads which make up the combinations are the same as those presented in Section 3-2.2.1.

An examination of Table 3-2.2-29 shows that further reductions are possible in the number of vent system load combinations requiring evaluation. Any of the SBA or IBA combinations envelop the NOC I combination since they contain the same loadings as the NOC I combination and, in addition, contain condensation oscillation or chugging loads. The NOC I combination does, however, result in local thermal effects in the vent line-SRV piping penetration when the penetration assembly is cold and the corresponding SRV piping is hot (during an SRV discharge). The SBA and IBA combinations, therefore, envelop the NOC I combination for all vent system components except the vent line-SRV piping penetration. The NOC I combination is evaluated for the vent line-SRV piping penetration since it may result in controlling penetration stresses. The effects of the NOC I combination are also considered in the vent system fatigue evaluation.

The SBA II combination is the same as the IBA III combination except for negligible differences in internal pressure loads. Thus IBA III can be eliminated from consideration. The SBA II combination envelops the SBA I and IBA II combinations since the submerged structure loads due to post-chug are more severe than those due to pre-chug. It also follows, from the reasoning presented earlier for OBE and SSE loads, that the SBA II combination envelops the SBA III, SBA IV, IBA IV, and IBA V combinations except when the effects of lateral loads on the vent line-drywell penetration are evaluated. Similarly, the SBA II combination envelops the DBA V and DBA VI combinations; these combinations, however, contain vent system discharge loads which are somewhat larger than the pressure loads for the SBA II combination. This effect is accounted for by substituting the vent system discharge loads which occur during the chugging phase of a DBA event for the SBA II pressure loads when this load combination is evaluated.

Examination of Table 3-2.2-29 shows that the load combinations which result in maximum lateral loads on the vent line-drywell penetration are SBA IV, IBA V, and DBA VI. All of these contain SSE loads and chugging downcomer lateral loads which, when combined, result in the maximum possible lateral load on the vent system.

As previously discussed, the SBA II combination envelops the above combinations except for seismic loads. The effects of seismic loads are accounted for by substituting SSE loads for OBE loads when evaluating the SBA II combination.

The DBA II combination envelops the DBA IV combination since the SRV discharge loads which occur late in the DBA event have a negligible effect on the vent system. The DBA II combination also has more restrictive allowables than the DBA IV combination.

The controlling vent system load combinations evaluated in the remaining report sections can now be summarized. The SBA II, IBA I, DBA I, DBA II, and DBA III combinations are evaluated for all vent system components except those associated with the vent line-SRV piping penetration. The DBA I and DBA II combinations do not need to be examined when evaluating the vent line-SRV piping penetration. This is because they do not contain SRV discharge loads, which are a large contributor to loads on the penetration. Thus, the NOC I, SBA II, IBA I and DBA III combinations are evaluated for the vent line-SRV piping penetration. As previously noted, SSE loads and the vent system discharge loads which occur during the chugging phase of the DBA event are conser-

vatively substituted for OBE loads and the SBA pressure loads when evaluating the SBA II load combination.

To ensure that fatigue is not a concern for the vent system over the life of the plant, the combined effects of fatigue due to Normal Operating plus SBA events and Normal Operating plus IBA events are evaluated. Figures 3-2.2-12, 3-2.2-13 and 3-2.2-14 show the relative sequencing and timing of each loading in the SBA, IBA, and DBA events used in this evaluation. The fatigue effects for Normal Operating plus DBA events are enveloped by the Normal Operating plus SBA or IBA events since the combined effects of SRV discharge loads and other loads for the SBA and IBA events are more severe than those for DBA. Table 3-2.2-29 summarizes additional information used in the vent system fatigue evaluation.

The load combinations and event sequencing described in the preceding paragraphs envelop those which could actually occur during a LOCA or SRV discharge event. An evaluation of these load combinations results in a conservative estimate of the vent system response and leads to bounding values of vent system stresses and fatigue effects.

Table 3-2.2-28

MARK I CONTAINMENT EVENT COMBINATIONS

EVENT COMBINATIONS			SRV	SRV + EQ		SBA IBA		SBA + EQ IBA + EQ				SBA+SRV IBA+SRV		SBA + SRV + EQ IBA + SRV + EQ				DBA		DBA + EQ				DBA+SRV		DBA + SRV + EQ			
							CO, CH			CO, CH			CO, CH			CO, CH		PS	CO, CH	PS		CO,CH		PS	CO, CH	PS		CO, CH	
TYPE OF EARTHQUAKE				0	S			0	S	0	S			0	S	0	S			0	S	0	S			0	S	0	S
COMBINATION NUMBER			1	2	3	4	5	6	7	8	9	10	11	12	13	14	15	16	17	18	19	20	21	22	23	24	25	26	27
LOADS	NORMAL	N	X	X	X	X	X	X	X	X	X	X	X	X	X	X	X	X	X	X	X	X	X	X	X	X	X	X	X
	EARTHQUAKE	EQ		X	X			X	X	X	X			X	X	X	X			X	X	X	X			X	X	X	X
	SRV DISCHARGE	SRV	X	X	X							X	X	X	X	X	X							X	X	X	X	X	X
	LOCA THERMAL	T_A				X	X	X	X	X	X	X	X	X	X	X	X	X	X	X	X	X	X	X	X	X	X	X	X
	LOCA REACTIONS	R_A				X	X	X	X	X	X	X	X	X	X	X	X	X	X	X	X	X	X	X	X	X	X	X	X
	LOCA QUASI-STATIC PRESSURE	P_A				X	X	X	X	X	X	X	X	X	X	X	X	X	X	X	X	X	X	X	X	X	X	X	X
	LOCA POOL SWELL	P_{PS}																X		X	X			X		X	X		
	LOCA CONDENSATION OSCILLATION	P_{CO}					X			X	X		X			X	X		X			X	X		X			X	X
	LOCA CHUGGING	P_{CH}					X			X	X		X			X	X		X			X	X		X			X	X

1. SEE SECTION 1-3.2 FOR ADDITIONAL EVENT COMBINATION INFORMATION.

nutech ENGINEERS

Table 3-2.2-29

CONTROLLING VENT SYSTEM LOAD COMBINATIONS

SECTION 3-2.2.1 LOAD DESIGNATION	CONDITION/EVENT	NOC	SBA				IBA					DBA					
	VOLUME 3 LOAD COMBINATION NUMBER	I	I	II	III	IV	I	II	III	IV	V	I	II	III	IV	V	VI
	TABLE 3-2.2-24 LOAD COMBINATION NUMBER	2	14	14	15	15	14	14	14	15	15	19	20	25	27	27	27
DEAD WEIGHT		1a →															← 1a
SEISMIC	OBE	2a →		← 2a			2a →		← 2a			2a	2a				
	SSE				2b	2b				2b	2b			2b →			← 2b
PRESSURE (1)		P(2)	P_2, P_3	P_2, P_3	P_2, P_3	P_2, P_3	P_2, P_3	P_2, P_3	P_2, P_3	P_2, P_3	P_2, P_3	P_1	P_3	P_1	P_3	P_4	P_4
TEMPERATURE (3)		T(4)	T_2, T_3	T_2, T_3	T_2, T_3	T_2, T_3	T_2, T_3	T_2, T_3	T_2, T_3	T_2, T_3	T_2, T_3	T_1	T_3	T_1	T_3	T_4	T_4
VENT SYSTEM DISCHARGE												4a →					← 4a
POOL SWELL												5a-5f		5a-5f			
CONDENSATION OSCILLATION							6b,6c 6e						6b,6d 6f		6b,6d 6f		
CHUGGING	PRE-CHUG		7a-7c		7a-7c			7a-7c		7a-7c						7a,7c	
	POST-CHUG			7a,7b 7d		7a,7b 7d			7a,7b 7d		7a,7b 7d						7a,7b 7d
SRV DISCHARGE		8a,8b →									← 8a,8b			8a,8b	8a,8b	8a,8b	8a,8b
PIPING REACTIONS		9a →															← 9a
CONTAINMENT INTERACTION		10a →															← 10a
SERVICE LEVEL		B	B	B	C	C	B	B	B	C	C	B(6,7)	B(7)	C	C	C	C
NUMBER OF EVENT OCCURRENCES (8)		150	1 →														← 1
NUMBER OF SRV ACTUATIONS (9)		934	50 →			← 50	25 →				← 25	0	0	1 →			← 1

nutech ENGINEERS

NOTES TO TABLE 3-2.2-29

1. SEE FIGURES 3-2.2-1 THROUGH 3-2.2-3 FOR SBA, IBA, AND DBA INTERNAL PRESSURE VALUES.
2. THE RANGE OF NORMAL OPERATING INTERNAL PRESSURES IS -0.1 TO 1.0 psi AS SPECIFIED BY THE FSAR.
3. SEE FIGURES 3-2.2-4 THROUGH 3-2.2-6 FOR SBA, IBA, AND DBA TEMPERATURE VALUES.
4. THE RANGE OF NORMAL OPERATING TEMPERATURES IS 65° TO 150°F AS SPECIFIED BY THE FSAR. SEE TABLE 3-2.2-2 FOR ADDITIONAL NORMAL OPERATING TEMPERATURES.
5. THE SRV DISCHARGE LOADS WHICH OCCUR DURING THIS PHASE OF THE DBA EVENT HAVE A NEGLIGIBLE EFFECT ON THE VENT SYSTEM.
6. EVALUATION OF PRIMARY-PLUS-SECONDARY STRESS RANGE OR FATIGUE IS NOT REQUIRED.
7. THE ALLOWABLE STRESS VALUE FOR LOCAL PRIMARY MEMBRANE STRESS AT PENETRATIONS MAY BE INCREASED BY 1.3.
8. THE NUMBER OF SEISMIC LOAD CYCLES USED FOR FATIGUE IS 1000.
9. THE VALUES SHOWN ARE CONSERVATIVE ESTIMATES OF THE NUMBER OF ACTUATIONS EXPECTED FOR A BWR 3 PLANT WITH A REACTOR SIZE OF 205.

Table 3-2.2-30

ENVELOPING LOGIC FOR CONTROLLING
VENT SYSTEM LOAD COMBINATIONS

CONDITION/EVENT			NOC	SBA				IBA					DBA					
TABLE 3-2.2-29 ENVELOPING LOAD COMBINATIONS			2	14	14	15	15	14	14	14	15	15	18	20	25	27	27	27
TABLE 3-2.2-29 LOAD COMBINATIONS ENVELOPED			1	4-6, 8, 10-12	4-6, 8, 10-12	3, 7, 9, 13	3, 7, 9, 13	4-6, 8, 10-12	4-6, 8, 10-12	4-6, 8, 10-12	3, 7, 9, 13	3, 7, 9, 13	16	17	19, 22, 24	21, 23, 26	21, 23, 26	21, 23, 26
VOLUME 3 LOAD COMBINATION DESIGNATION			I	I	II	III	IV	I	II	III	IV	V	I	II	III	IV	V	VI
CONTROLLING LOAD COMBINATIONS EVALUATED	VENT SYSTEM COMPONENTS AND SUPPORTS	SBA II (1)	X	X		X	X		X	X	X	X					X	X
		IBA I	X															
		DBA I																
		DBA II														X		
		DBA III																
	VENT LINE-SRV PIPING PENETRATION	NOC I																
		SBA II (1)		X		X	X		X	X	X	X					X	X
		IBA I																
		DBA III											X	X		X		

(1) SSE LOADS AND DBA PRESSURIZATION AND THRUST LOADS ARE SUBSTITUTED FOR OBE LOADS AND SBA II INTERNAL PRESSURE LOADS WHEN EVALUATING THE SBA II LOAD COMBINATION.

nutech ENGINEERS

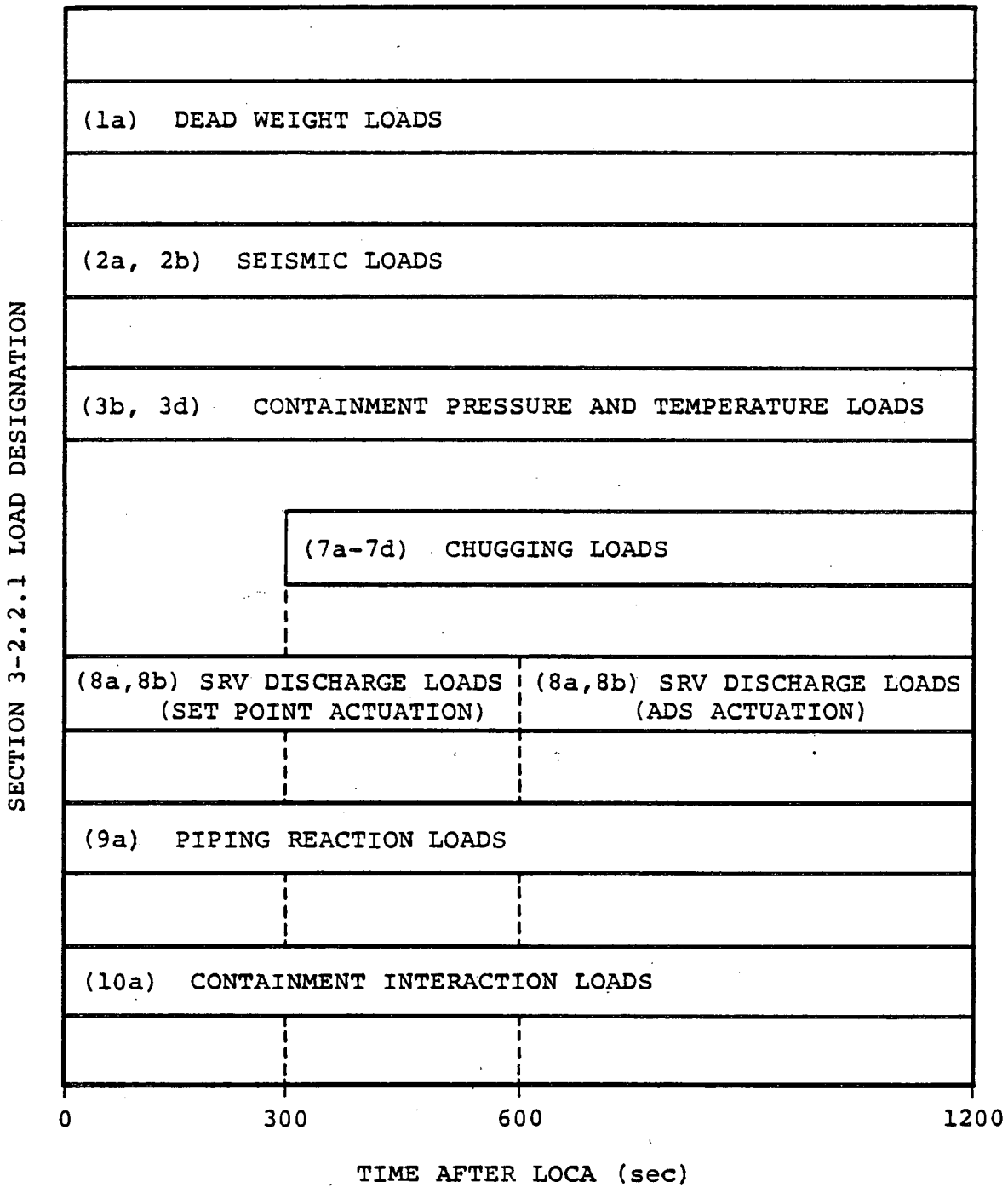

Figure 3-2.2-12

VENT SYSTEM SBA EVENT SEQUENCE

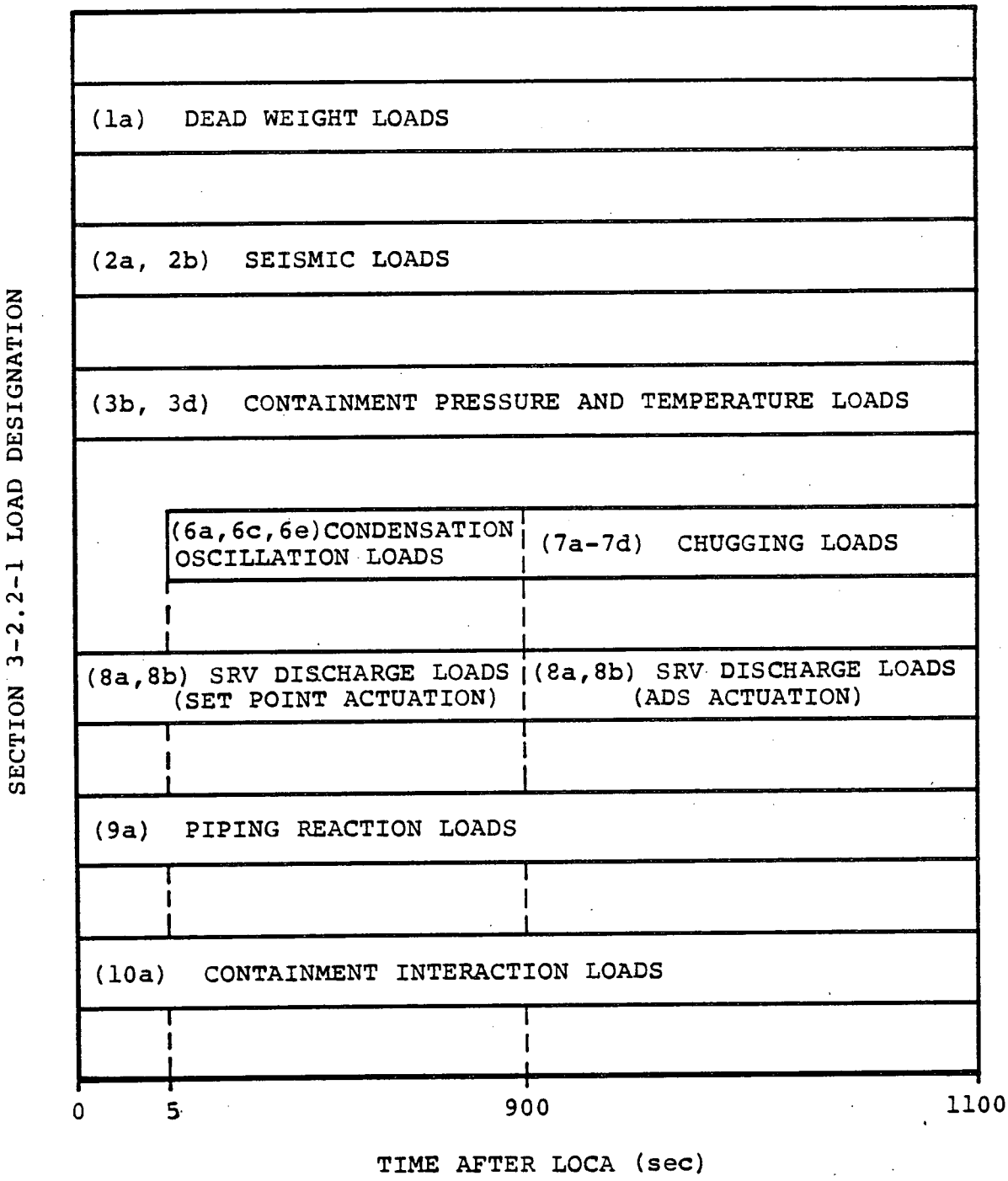

Figure 3-2.2-13

VENT SYSTEM IBA EVENT SEQUENCE

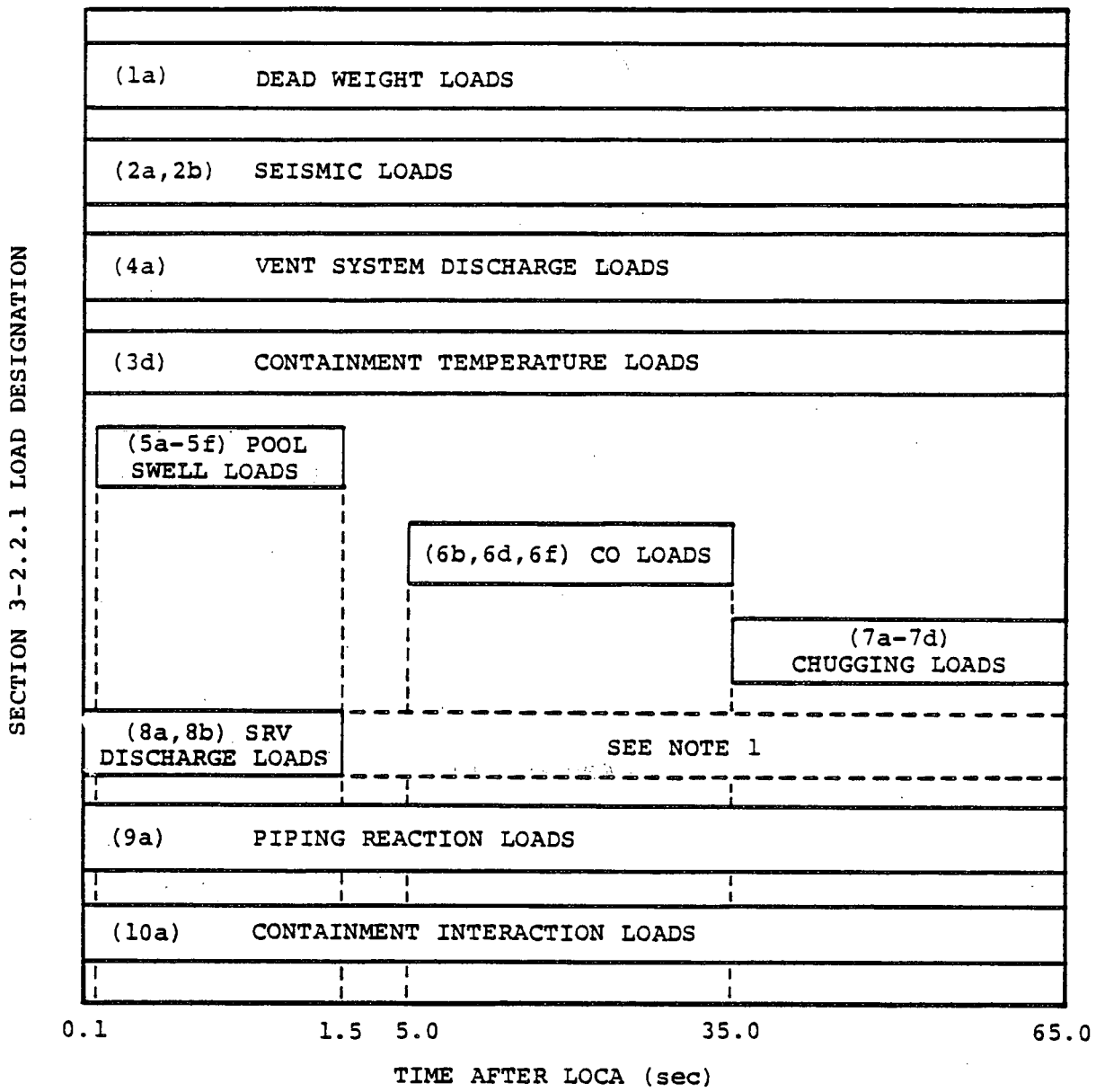

1. THE SRV DISCHARGE LOADS WHICH OCCUR DURING THIS PHASE OF THE DBA EVENT ARE NEGLIGIBLE.

Figure 3-2.2-14

VENT SYSTEM DBA EVENT SEQUENCE

3-2.3 Analysis Acceptance Criteria

The NUREG-0661 acceptance criteria on which the Monticello vent system analysis is based are discussed in Section 1-3.2. In general, the acceptance criteria follow the rules contained in the ASME Code, Section III, Division 1, including the Summer 1977 Addenda for Class MC components and component supports (Reference 4). The corresponding service limit assignments, jurisdictional boundaries, allowable stresses, and fatigue requirements are consistent with those contained in the applicable subsections of the ASME Code and the "Mark I Containment Program Plant Unique Analysis Application Guide" (PUAAG) (Reference 5). The following paragraphs summarize the acceptance criteria used in the analysis of the vent system.

The items evaluated in the analysis of the vent system are the vent lines, the vent header, the downcomers, the support columns and associated support elements, the drywell shell near the vent line penetrations, the vent header deflectors, the downcomer-vent header intersection stiffener plates and bracing system, the vacuum breaker penetration, the vent line-SRV piping penetration assembly, the vent header support collar-miter

assembly, and the vent line bellows assembly. Figures 3-2.1-1 through 3-2.1-14 identify the specific components associated with each of these items.

The vent lines, the vent header, the downcomers, the support column ring plate away from the pin locations, the drywell shell, the downcomer-vent header intersection stiffener plates, the stiffener plates attached to the vent line-vent header intersection, the vacuum breaker nozzle, the vent header support collar-miter assembly, and the vent line-SRV piping penetration assembly are evaluated in accordance with the requirements for Class MC components contained in Subsection NE of the ASME Code. Fillet welds and partial penetration welds joining these components or attaching other structures to them are also examined in accordance with the requirements for Class MC welds contained in Subsection NE of the ASME Code.

The support columns, the downcomer bracing members, and the associated connecting elements and welds are evaluated in accordance with the requirements contained in Subsection NF of the ASME Code for Class MC component supports. The vent header deflectors and associated components and welds are also evaluated in accordance

with the requirements for Class MC component supports with allowable stresses corresponding to Service Level D.

The NOC I, SBA II, IBA I, DBA I, and DBA II combinations all have Service Level B limits while the DBA III combination has Service Level C limits (Table 3-2.2-29). Since these load combinations have somewhat different maximum temperatures, the allowable stresses for the two load combination groups with Service Level B and C limits are conservatively determined at the highest temperature for each load combination group.

The allowable stresses for all the major components of the vent system, such as the vent line, the vent header and the downcomers, are determined at the maximum DBA temperature of 281°F. The allowable stresses for the vent line-SRV piping nozzle and adjoining components are determined at 375°F. Table 3-2.3-1 shows the allowable stresses for the load combinations with Service Level B and C limits.

Table 3-2.3-2 shows the allowable displacements and associated number of cycles for the vent line bellows. These values are taken from the FSAR, as permitted by

NUREG-0661 in cases where the analysis technique used in the evaluation is the same as that contained in the plant's FSAR.

The acceptance criteria described in the preceding paragraphs result in conservative estimates of the existing margins of safety and ensure that the original vent system design margins are restored.

Table 3-2.3-1

ALLOWABLE STRESSES FOR VENT SYSTEM COMPONENTS AND COMPONENT SUPPORTS

ITEM		MATERIAL	MATERIAL PROPERTIES (ksi)[1]	STRESS TYPE	ALLOWABLE STRESS (ksi) SERVICE LEVEL B[2]	ALLOWABLE STRESS (ksi) SERVICE LEVEL C[3]
COMPONENTS	DRYWELL SHELL	SA-516 GRADE 70	S_{mc} = 19.30 S_{ml} = 22.68 S_y = 33.97	LOCAL PRIMARY MEMBRANE	28.95	50.96
				PRIMARY + (4) SECONDARY STRESS RANGE	68.04	N/A
	VENT LINE	SA-516 GRADE 70	S_{mc} = 19.30 S_{ml} = 22.68 S_y = 33.97	PRIMARY MEMBRANE	19.30	33.97
				LOCAL PRIMARY MEMBRANE	28.95	50.96
				PRIMARY + (4) SECONDARY STRESS RANGE	68.04	N/A
	VENT HEADER	SA-516 GRADE 70	S_{mc} = 19.30 S_{ml} = 22.68 S_y = 33.97	PRIMARY MEMBRANE	19.30	33.97
				LOCAL PRIMARY MEMBRANE	28.95	50.96
				PRIMARY + (4) SECONDARY STRESS RANGE	68.04	N/A
	DOWNCOMER	SA-516 GRADE 70	S_{mc} = 19.30 S_{ml} = 22.68 S_y = 33.97	PRIMARY MEMBRANE	19.30	33.97
				LOCAL PRIMARY MEMBRANE	28.95	50.96
				PRIMARY + (4) SECONDARY STRESS RANGE	68.04	N/A
	SUPPORT COLUMN RING PLATE	SA-516 GRADE 70	S_{mc} = 19.30 S_{ml} = 22.68 S_y = 33.97	PRIMARY MEMBRANE	19.30	N/A
				LOCAL PRIMARY MEMBRANE	28.95	50.96
				PRIMARY + (4) SECONDARY STRESS RANGE	68.04	N/A
	SRV PIPING PENETRATION INSERT PLATE	SA-516 GRADE 70	S_{mc} = 19.30 S_{ml} = 22.30 S_y = 33.43	PRIMARY MEMBRANE	19.30	33.43
				LOCAL PRIMARY MEMBRANE	28.95	50.15
				PRIMARY + (4) SECONDARY STRESS RANGE	66.90	N/A
COMPONENT SUPPORTS	COLUMNS[7]	SA-333 GRADE 1	S_y = 28.19	BENDING	18.61	24.81
				TENSILE	16.91	22.55
				COMBINED	1.00	1.00
				COMPRESSIVE	13.49	17.99
				INTERACTION	1.00	1.00
WELDS	COLUMN RING PLATE TO VENT HEADER	SA-516 GRADE 70	S_{mc} = 19.30 S_y = 33.97	PRIMARY	15.01	26.42
				SECONDARY	45.03	N/A

NOTES TO TABLE 3-2.3-1

(1) MATERIAL PROPERTIES TAKEN AT MAXIMUM EVENT TEMPERATURES.

(2) SERVICE LEVEL B ALLOWABLES ARE USED WHEN EVALUATING NOC I, SBA II, IBA I, DBA I, AND DBA II LOAD COMBINATION RESULTS.

(3) SERVICE LEVEL C ALLOWABLES ARE USED WHEN EVALUATING THE DBA III LOAD COMBINATION RESULTS.

(4) THERMAL BENDING STRESSES ARE EXCLUDED WHEN EVALUATING PRIMARY-PLUS-SECONDARY STRESS RANGES.

(5) EVALUATION OF PRIMARY-PLUS-SECONDARY STRESS INTENSITY RANGE AND FATIGUE ARE NOT REQUIRED FOR LOAD COMBINATION DBA I.

(6) THE ALLOWABLE STRESSES FOR LOCAL PRIMARY MEMBRANE STRESSES AT PENETRATIONS ARE INCREASED BY 1.3 WHEN EVALUATING LOAD COMBINATIONS DBA I AND DBA II.

(7) STRESS DUE TO THERMAL LOADS MAY BE EXCLUDED WHEN EVALUATING COMPONENT SUPPORTS.

Table 3-2.3-2

ALLOWABLE DISPLACEMENTS AND CYCLES FOR VENT LINE BELLOWS

TYPE		ALLOWABLE VALUE
AXIAL	COMPRESSION	0.875 in
	EXTENSION	0.375 in
LATERAL	MERIDIONAL	±0.625 in
	LONGITUDINAL	±0.625 in
NUMBER OF CYCLES OF MAXIMUM DISPLACEMENTS		1000

3-2.4 Methods of Analysis

Section 3-2.2.1 presents the governing loads for which the Monticello vent system is evaluated. Section 3-2.4.1 discusses the methodology used to evaluate the vent system for the overall effects of all loads except for those loads which exhibit asymmetric characteristics. The effects of asymmetric loads on the vent system are evaluated using the methodology discussed in Section 3-2.4-2. The methodology used to examine the local effects at the penetrations and intersections of the vent system major components is discussed in Section 3-2.4.3.

Section 3-2.4.4 discusses the methodology used to formulate results for the controlling load combinations, examine fatigue effects, and evaluate the analysis results for comparison with the applicable acceptance limits.

3-2.4.1 Analysis for Major Loads

The repetitive nature of the vent system geometry is such that the vent system can be divided into 16 identical segments which extend from midbay of the vent line bay to midbay of the non-vent line bay (Figure 3-2.1-6). The governing loads which act on the vent system, except for seismic loads and a few chugging load cases, exhibit symmetric or anti-symmetric characteristics (or both) with respect to a 1/16 segment of the vent system. The analysis of the vent system for the majority of the governing loads is therefore performed for a typical 1/16 segment.

A beam model of a 1/16 segment of the vent system (Figure 3-2.4-1) is used to obtain the response of the vent system to all loads except those resulting in asymmetric effects on the vent system. The model includes the vent line, the vent header, the downcomers, and the support columns. The model also includes the vent header deflectors, the downcomer bracing system, and the vacuum breaker.

The local stiffness effects at the penetrations and intersections of the major vent system components

(Figures 3-2.1-7 through 3-2.1-12) are included by using stiffness matrix elements of these penetrations and intersections. A matrix element for the vent line-drywell penetration, which connects the upper end of the vent line to the transition segment, is developed using the finite difference model of the penetration (Figure 3-2.4-2). A matrix element which connects the lower end of the vent line to the beams on the centerline of the vent header is developed using the finite element model of the vent line-vent header intersection (Figure 3-2.4-3). Figure 3-2.4-4 shows a finite element model used to develop a matrix element for the vacuum breaker penetration at the end cap of the vent line.

Finite element models of each downcomer-vent header intersection, similar to the one shown in Figure 3-2.4-5, are used to develop matrix elements which connect the beams on the centerline of the vent header to the upper ends of the downcomers at the downcomer miters. The length of the vent header segment in the analytical models used for downcomer-vent header intersection stiffness determination is increased to ensure that vent header ovaling effects are properly accounted for. Use of this modeling approach has been verified using results from FSTF tests. Additional

information on the analytical models used to evaluate the penetrations and intersections of major vent system components is contained in Section 3-2.4.3.

The 1/16 beam model contains 158 nodes, 153 beam elements, and 7 matrix elements. The node spacing used in the analytical model is refined to ensure adequate distribution of mass and determination of component frequencies and mode shapes and to facilitate accurate application of loadings. The stiffness and mass properties used in the model are based on the nominal dimensions and densities of the materials used to construct the vent system. Small displacement linear-elastic behavior is assumed throughout.

The boundary conditions used in the 1/16 beam model are both physical and mathematical in nature. The physical boundary conditions consist of the elastic restraints provided at the attachments of the support columns. The associated stiffnesses are developed using the analytical model of the ring girder described in Volume 2 of this report. Additional physical boundary conditions include the elastic restraints provided at the attachment of the vent line to the drywell. The associated vent line-drywell penetration stiffnesses are

included as a stiffness matrix element, the development of which is discussed in the preceding paragraphs. The mathematical boundary conditions consist of either symmetry, anti-symmetry, or a combination of both at the midbay planes, depending on the characteristics of the load being evaluated.

Additional mass is lumped along the length of the submerged portions of the downcomers, support columns, and bracings to account for the effective mass of water which acts with these components during dynamic loadings. The total mass of water added is equal to the mass of water displaced by each of these components. For all but the pool swell and condensation oscillation dynamic loadings, the mass of water inside the submerged portion of the downcomers is included. The downcomers are assumed to contain air or steam (or both) during pool swell and condensation oscillation. The mass of this mixture is considered negligible. An additional mass of 937 pounds to account for the weight of the drywell/wetwell vacuum breaker is lumped at the center of gravity of the vacuum breaker.

A frequency analysis is performed using the 1/16 beam model of the vent system for the case with water inside

the downcomers and for the case with no water inside the downcomers. All structural modes in the range of 0 to 80 hertz and 0 to 90 hertz, respectively, are extracted for these cases. Tables 3-2.4-1 and 3-2.4-2 show the resulting frequencies and mass participation factors.

A dynamic analysis using the 1/16 beam model of the vent system is performed for the pool swell loads and condensation oscillation loads specified in Section 3-2.2-1. The analysis consists of a transient analysis for pool swell loads and a harmonic analysis for condensation oscillation loads. The modal superposition technique with 2% damping is utilized in both the transient and harmonic analyses. The pool swell and condensation oscillation load frequencies are enveloped by including vent system frequencies to 90 hertz and 60 hertz, respectively.

The remaining vent system load cases specified in Section 3-2.2.1 involve either static loads or dynamic loads, which are evaluated using an equivalent static approach. For the latter, conservative dynamic amplification factors are developed and applied to the maximum spatial distributions of the individual dynamic loadings.

The effects of asymmetric loads are evaluated by applying loads generated using the 180° beam model discussed in Section 3-2.4.2 to the 1/16 beam model. Displacements taken from the 180° beam model results are imposed at the midcylinder boundary planes of the 1/16 beam model. Inertia forces due to horizontal seismic loads and concentrated forces due to asymmetric chugging loads, both of which are taken from the 180° beam model results, are applied to the portion of the 1/16 beam model which lies between the midcylinder boundary planes. Additional information related to the vent system analysis for asymmetric loads is provided in Section 3-2.4.2.

The 1/16 beam model is also used to generate loads for the evaluation of stresses in the major vent system component penetrations and intersections. Beam end loads, distributed loads, reaction loads, and inertia loads are developed and applied to the analytical models of the vent system penetrations and intersections (Figures 3-2.4-2 through 3-2.4-4). Additional information related to the vent system penetrations and intersection stress evaluation is provided in Section 3-2.4.3.

The specific treatment of each load in the load categories identified in Section 3-2.2.1 is discussed in the following paragraphs.

1. Dead Weight Loads

   a. Dead Weight of Steel: A static analysis is performed for a unit vertical acceleration applied to the weight of vent system steel.

2. Seismic Loads

   a. OBE Loads: A static analysis is performed for a 0.153g vertical seismic acceleration applied to the weight of steel included in the 1/16 beam model. An additional static analysis is performed for the boundary displacements and associated inertia loads generated for a 0.23g seismic acceleration applied in each horizontal direction using the 180° beam model. The results of the three earthquake directions are combined using SRSS.

   b. SSE Loads: The procedure used to evaluate the 0.307g vertical and 0.46g horizontal SSE seismic accelerations is the same as that discussed for OBE seismic loads in Load Case 2a.

3. Containment Pressure and Temperature Loads

a. Normal Operating Internal Pressure Loads: A static analysis is performed for a 1.0 psi internal pressure applied as concentrated forces to the unreacted areas of the vent system.

b. LOCA Internal Pressure Loads: A static analysis is performed for the SBA and IBA net internal pressures applied as concentrated forces to the unreacted areas of the major components of the vent system. Figures 3-2.2-1 through 3-2.2-3 show these pressures. The effects of DBA internal pressure loads are included in the pressurization and thrust loads discussed in Load Case 4a.

Concentrated forces are also applied at the vent line-drywell penetration location using the SBA, IBA, and DBA drywell internal pressures. These forces account for the pressures acting on the vent line-drywell penetration unreacted area and for the movement of the drywell due to internal pressure. The movement of the suppression

chamber due to internal pressure, although small in magnitude, is also applied.

c. Normal Operating Temperature Loads: A static analysis is performed for the case with the containment at an ambient temperature of 77.5°F and with a temperature of 375°F uniformly applied to the wetwell SRV piping. The methodology used to evaluate local thermal effects in the vent line-SRV piping penetration is discussed in Section 3-2.4.3.

An additional static analysis is performed for the maximum normal operating temperature (Table 3-2.2-2). This temperature is uniformly applied to the portion of the vent system inside the suppression chamber. Corresponding temperatures of 77.5°F for the drywell and vent system components outside the suppression chamber, 168°F for the suppression chamber, and 375°F for the SRV piping are also applied in this analysis.

d. LOCA Temperature Loads: A static analysis is performed for the SBA, IBA, and DBA temperatures, which are uniformly applied to the major components and external components of the vent system. Figures 3-2.2-4 through 3-2.2-6 show these temperatures. A temperature of 375°F is also uniformly applied to the SRV piping for those controlling load combinations which include SRV discharge loads. Reaction loads applied to the vent line-SRV piping penetration are calculated on the basis of the methods described in Volume 5.

Concentrated forces are applied at the vent line-drywell penetration and at the support column attachment points to the suppression chamber to account for the thermal expansion of the drywell and suppression chamber during the SBA, IBA, and DBA events. The greater of the temperatures specified in Figure 3-2.2-4 and Table 3-2.2-2 is used in the analysis for SBA temperatures.

4. Vent System Discharge Loads

   a. DBA Pressurization and Thrust Loads: A dynamic analysis is performed for the DBA pressurization and thrust loads (Table 3-2.2-3).

5. Pool Swell Loads

   a. Vent System Impact and Drag Loads: A dynamic analysis is performed for the vent line, downcomer, and vent header deflector pool swell impact loads (Table 3-2.2-4, Figures 3-2.2-7 and 3-2.2-8).

   b. Impact and Drag Loads on Other Structures: A dynamic analysis is performed for pool swell impact loads on the vacuum breaker and on pool swell drag loads on the downcomer tie rods and the downcomer longitudinal members. Tables 3-2.2-5 and 3-2.2-6 show these loads. Response spectra are developed at the vent line-SRV piping penetration node for input into analysis performed in Volume 5.

   c. Froth Impingement and Fallback Loads: A dynamic analysis is performed for froth impinge-

ment and fallback loads on the vacuum breaker. These loads are shown in Table 3-2.2-5.

d. Pool Fallback Loads: A dynamic analysis is performed for pool fallback loads on the downcomer longitudinal bracing members. Table 3-2.2-6 shows these loads. Response spectra are developed at the vent line-SRV piping penetration node for input into analysis performed in Volume 5.

e. LOCA Water Clearing Submerged Structure Loads: An equivalent static analysis is performed for LOCA water clearing submerged structure loads on the vent system support columns. Table 3-2.2-7 shows these loads. The values of the loads include dynamic amplification factors which are computed on the basis of methods described in Reference 7 and through use of the dominant frequency of the support columns. The dominant frequencies are derived from harmonic analyses of these components. Figure 3-2.4-6 shows the results of these harmonic analyses.

f. LOCA Air Clearing Submerged Structure Loads: An equivalent static analysis is performed for LOCA air clearing submerged structure loads on the downcomers, the downcomer tie rods, the downcomer longitudinal bracing members, and the support columns. Tables 3-2.2-7, 3-2.2-8, and 3-2.2-9 show these loads. The values of the loads include dynamic amplification factors computed using the dominant frequencies of the affected structures. The dominant frequencies are derived from harmonic analyses of these components (Figures 3-2.4-6 through 3-2.4-9). The LOCA air clearing submerged structure loads acting on the submerged portion of the SRV piping are also applied using the procedures described in Volume 5.

6. Condensation Oscillation Loads

a. IBA Condensation Oscillation Downcomer Loads: A dynamic analysis is performed for the IBA condensation oscillation downcomer loads (Table 3-2.2-10). The dominant downcomer frequency is determined from the harmonic results (Figure 3-2.4-10). Figure 3-2.4-6 indicates that the dominant downcomer frequency occurs in the frequency range of the

second condensation oscillation downcomer load harmonic. The first and third condensation oscillation downcomer load harmonics are therefore applied at frequencies equal to 0.5 and 1.5 times the value of the dominant downcomer frequency.

b. DBA Condensation Oscillation Loads: The procedure used to evaluate the DBA condensation oscillation downcomer loads (Table 3-2.2-11) is the same as that discussed for IBA condensation oscillation downcomer loads in Load Case 6a.

c. IBA Condensation Oscillation Vent System Pressures: A dynamic analysis is performed for IBA condensation oscillation vent system pressures on the vent line and vent header. Table 3-2.2-12 shows these loads. The dominant vent line and vent header frequencies are determined from the harmonic analysis results (Figure 3-2.4-11). An additional static analysis is performed for a 1.55 psi

internal pressure applied as concentrated forces to the unreacted areas of the vent system.

d. DBA Condensation Oscillation Vent System Pressure Loads: The procedure used to evaluate the DBA condensation oscillation vent system pressure loads (Table 3-2.2-12) is the same as that discussed for IBA condensation oscillation vent system pressure loads in Load Case 6c.

e. IBA Condensation Oscillation Submerged Structure Loads: As previously discussed, pre-chug loads described in Load Case 7c are specified in lieu of IBA condensaton oscillation loads.

f. DBA Condensation Oscillation Submerged Structure Loads: An equivalent static analysis is performed for the DBA condensation oscillation submerged structure loads on the downcomer tie rods, the downcomer longitudinal bracing members, and the support columns. Tables 3-2.2-13 and 3-2.2-14 show these loads, which include dynamic amplification factors computed

using the methodology described for LOCA water and air clearing submerged structure loads in Load Cases 5e and 5f. The DBA condensation oscillation submerged structure loads acting on the submerged portion of the SRV piping are also applied, following the procedures described in Volume 5.

7. Chugging Loads

a. Chugging Downcomer Lateral Loads: A harmonic analysis of the downcomers is performed to determine the dominant downcomer frequency for use in calculating the maximum chugging load magnitude. Figure 3-2.4-12 shows the harmonic analysis results. Table 3-2.2-15 shows the resulting chugging load magnitudes. A static analysis using the 1/16 beam model is performed for chugging downcomer lateral Load Cases 8 through 22. Tables 3-2.2-17 and 3-2.2-18 show these load cases. An additional static analysis using the 180° beam model is performed for boundary displacements and associated concentrated forces generated for Load Cases 1 through 7.

A static analysis is also performed for the maximum chugging load (Table 3-2.2-19) applied to a single downcomer in the in-plane and out-of-plane directions. The results of this analysis are used in evaluating fatigue.

b. Chugging Vent System Pressures: An equivalent static analysis is performed for the chugging vent system pressures applied to the unreacted areas of the vent system. Table 3-2.2-20 shows these loads. The dominant vent line and vent header frequencies are determined from the harmonic analysis results (Figure 3-2.4-13).

c. Pre-Chug Submerged Structure Loads: An equivalent static analysis is performed for the pre-chug submerged structure loads on the downcomer tie rods, the downcomer longitudinal bracing members, and the support columns. Tables 3-2.2-21 and 3-2.2-22 show these loads. The loads include dynamic amplification factors which are computed using the methodology described for submerged structure LOCA air clearing loads in Load Case 5f. The pre-

chug submerged structure loads acting on the submerged portion of the SRV piping are also applied using the procedures described in Volume 5.

d. Post-Chug Submerged Structure Loads: The procedure used to evaluate the post-chug submerged structure loads on the downcomer tie rods, the downcomer longitudinal bracing members, and the support columns is the same as that discussed for pre-chug submerged structure loads in Load Case 6c. Tables 3-2.2-23 and 3-2.2-24 show these loads.

8. Safety Relief Valve Discharge Loads

a. SRV Discharge Water Clearing Submerged Structure Loads: An equivalent static analysis is performed for SRV discharge water clearing submerged structure loads on the vent system support columns. Table 3-2.2-25 shows these loads. The values of the loads include dynamic amplification factors which are calculated on the basis of methods described in Reference 7 and use of the dominant frequency of the support columns.

b. SRV Discharge Air Clearing Submerged Structure Loads: An equivalent static analysis is performed for SRV discharge drag loads on the downcomers, the downcomer tie rods, the downcomer longitudinal bracing members, and the support columns. Tables 3-2.2-25, 3-2.2-26, and 3-2.2-27 show these loads. The loads include a dynamic load factor of 3.0, as discussed in Section 1-4.2.4. A dynamic load factor of 1.1 is used for the downcomer loads applied in the out-of-plane direction, since the out-of-plane downcomer frequency is well above the maximum SRV discharge load frequency (Figure 3-2.4-7). The SRV discharge submerged structure loads acting on the submerged portion of the SRV piping are also applied using the procedures described in Volume 5.

9. Piping Reaction Loads

a. At the vent line-SRV piping penetration, the reaction loads are developed using the procedures described in Volume 5. These reaction

loads are applied to the local vent line-SRV piping finite element model described in Section 3-2.4.3.

10. Containment Interaction Loads

a. Containment Structure Motions: The motions of the drywell and the suppression chamber due to internal pressure and thermal expansion are applied to the 1/16 beam model. The motions caused by loads in other load categories acting on the drywell and suppression chamber have been evaluated and found to have a negligible effect on the vent system.

The methodology described in the preceding paragraphs results in a conservative evaluation of the vent system response and associated stresses for the governing loads.

Table 3-2.4-1

VENT SYSTEM FREQUENCY ANALYSIS RESULTS
WITH WATER INSIDE DOWNCOMERS

MODE NUMBER	FREQUENCY (Hz)	MODAL WEIGHT (lb) (1)		
		X	Y	Z
1	11.11	599.55	1.08	11076.98
2	16.52	80.31	9.60	1260.05
3	21.95	0.26	13.28	1149.95
4	22.01	0.00	0.01	0.22
5	22.40	0.02	809.29	0.08
6	25.45	162.27	56.58	64.45
7	26.54	0.25	9830.53	100.19
8	30.51	23.94	760.87	561.29
9	34.57	144.44	2.68	122.36
10	36.58	1091.34	91.57	3.22
11	36.83	1.21	0.01	13.04
12	41.42	1.27	61.56	33.50
13	41.53	8.76	76.52	923.97
14	42.63	49.81	3232.26	0.01
15	43.45	3.05	113.90	7347.27
16	49.51	1385.42	0.18	42.10
17	54.50	1765.92	207.68	73.70
18	54.66	1167.13	97.80	515.52
19	56.15	1370.89	80.06	22.66
20	57.77	16.39	1.45	0.53
21	57.98	28.15	1.52	38.39
22	58.10	94.67	0.47	15.09
23	58.31	57.35	6.14	181.29
24	60.47	10.88	136.57	17.47
25	61.06	304.08	1.00	21.19
26	62.07	893.82	86.42	194.13
27	63.16	3277.43	173.99	322.36
28	66.91	1257.80	11.44	315.69
29	73.21	230.10	1093.13	721.64
30	81.98	142.70	5.06	1.88

(1) SEE FIGURE 3-2.4-1 FOR COORDINATE SYSTEM DIRECTIONS.

Table 3-2.4-2

VENT SYSTEM FREQUENCY ANALYSIS RESULTS

WITHOUT WATER INSIDE DOWNCOMER

MODE NUMBER	FREQUENCY (Hz)	MODAL WEIGHT (lb) (1)		
		X	Y	Z
1	13.08	415.46	1.87	7833.58
2	19.79	56.40	28.42	996.58
3	21.95	0.09	12.20	1104.73
4	22.01	0.00	0.01	0.22
5	22.40	0.38	804.51	0.29
6	26.54	1.93	9864.80	107.16
7	30.25	97.50	266.48	556.58
8	30.81	15.29	520.98	86.17
9	34.57	142.86	2.43	116.78
10	36.59	1025.70	87.80	4.10
11	36.83	1.15	0.05	9.10
12	41.43	0.01	36.80	5.18
13	41.66	3.15	92.74	887.51
14	42.76	0.96	3233.97	23.02
15	43.94	3.37	172.66	7486.08
16	49.62	1258.92	0.03	128.62
17	55.46	195.96	318.69	10.89
18	56.22	379.36	3.36	103.93
19	57.02	541.79	3.35	4.17
20	57.83	11.07	1.77	0.81
21	58.06	3.01	0.01	0.00
22	58.11	121.93	0.15	4.86
23	60.43	1.40	133.03	0.57
24	61.38	30.90	0.02	60.90
25	62.03	1.76	177.19	98.21
26	63.66	3.75	7.43	966.65
27	69.19	1336.30	346.03	15.20
28	73.76	312.48	609.98	403.68
29	74.77	4816.39	269.88	388.62
30	89.70	45.41	1.49	0.10

(1) SEE FIGURE 3-2.4-1 FOR COORDINATE DIRECTIONS.

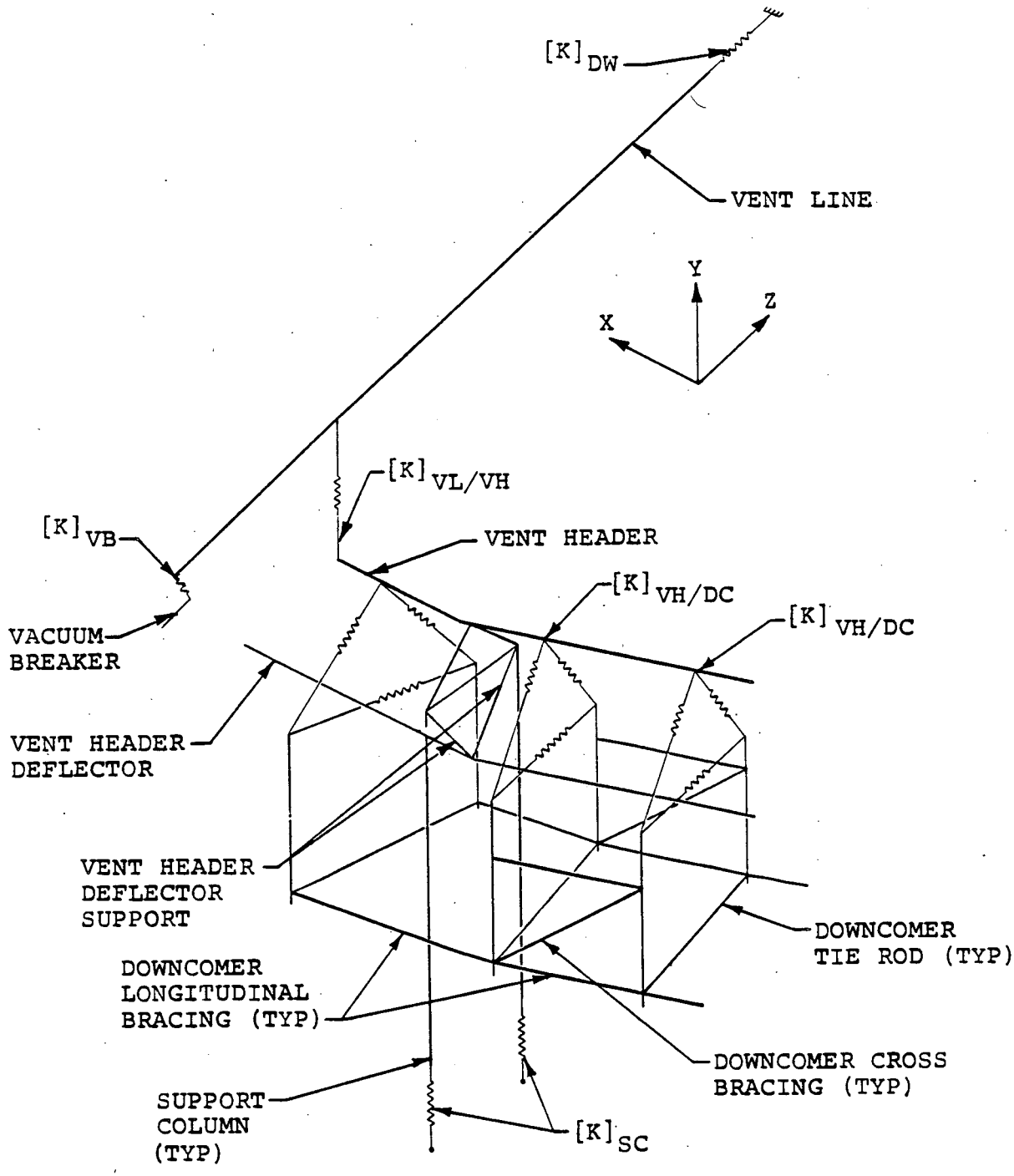

Figure 3-2.4-1

VENT SYSTEM 1/16 SEGMENT BEAM MODEL - ISOMETRIC VIEW

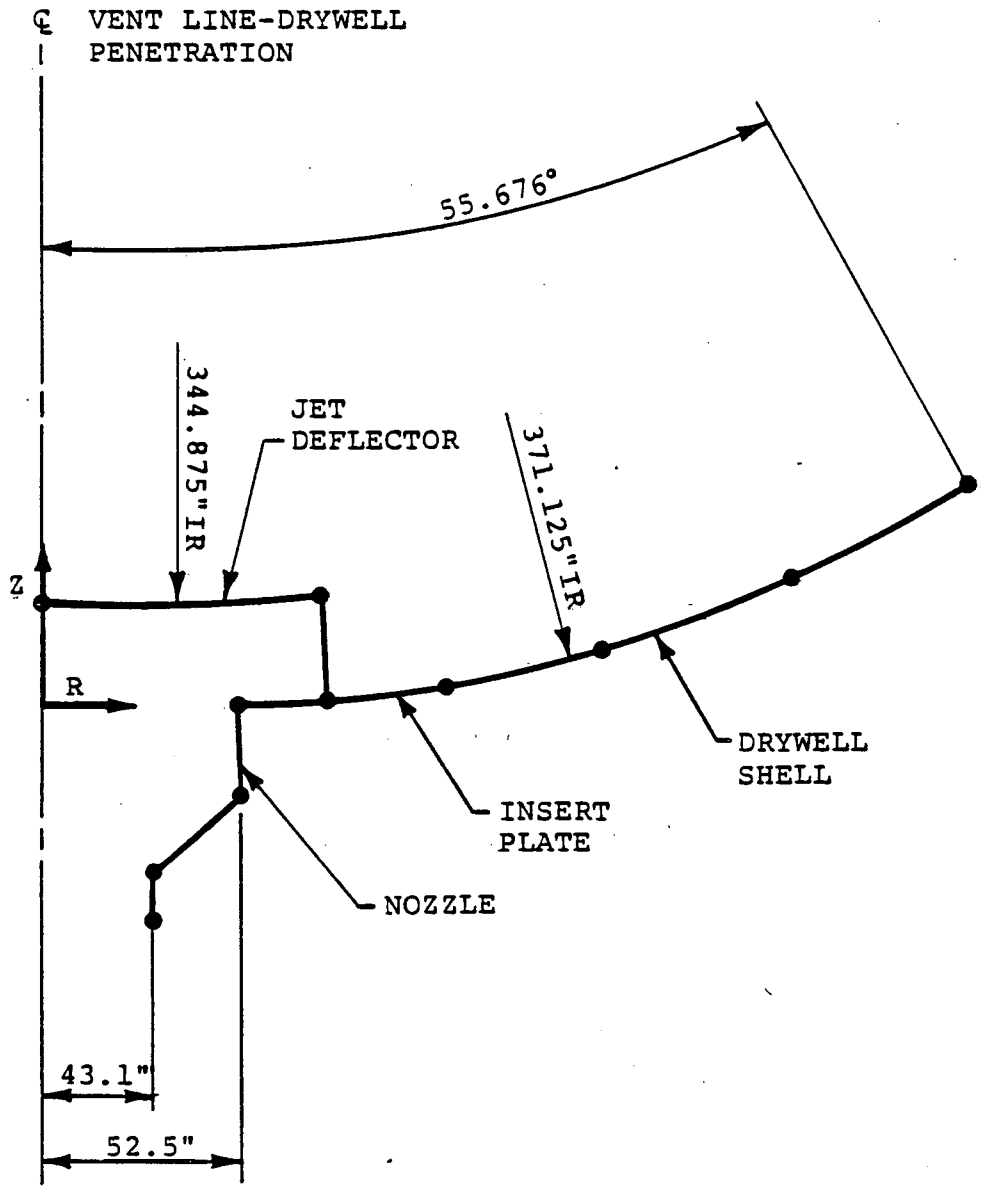

Figure 3-2.4-2

VENT LINE-DRYWELL PENETRATION AXISYMMETRIC FINITE DIFFERENCE MODEL - VIEW OF TYPICAL MERIDIAN

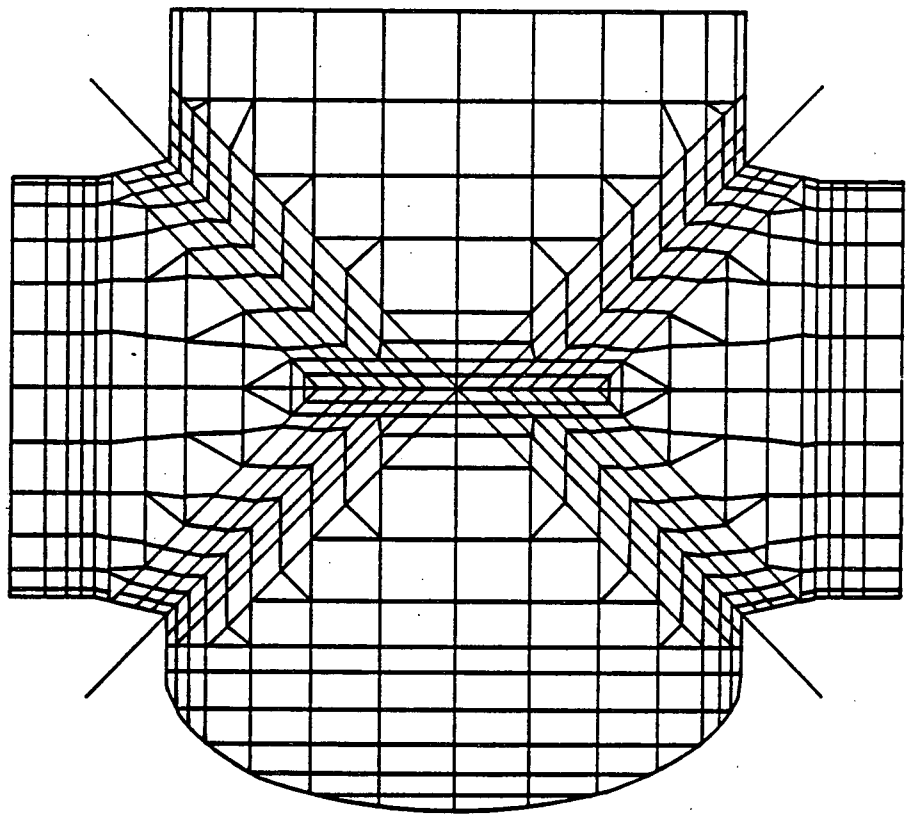

Figure 3-2.4-3

VENT LINE-VENT HEADER INTERSECTION

FINITE ELEMENT MODEL

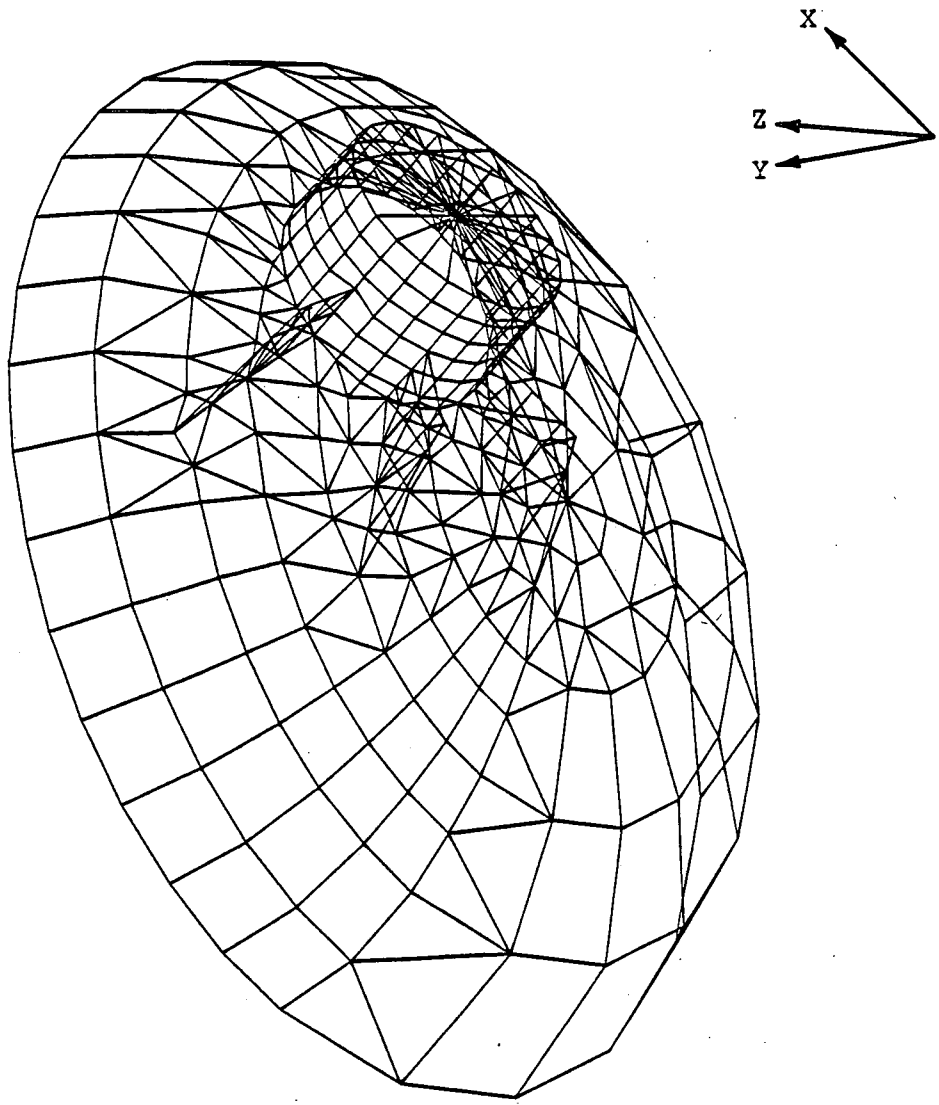

Figure 3-2.4-4

VACUUM BREAKER PENETRATION

FINITE ELEMENT MODEL

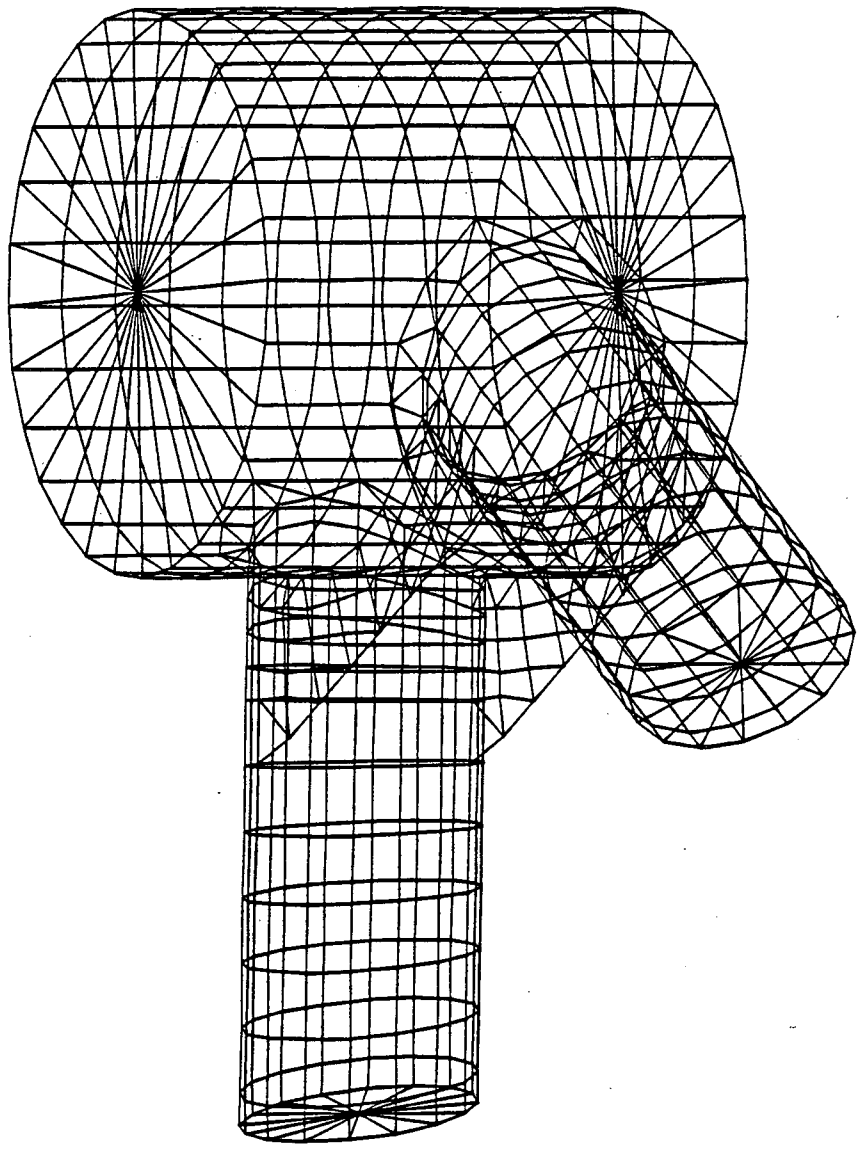

Figure 3-2.4-5

DOWNCOMER-VENT HEADER INTERSECTION

FINITE ELEMENT MODEL - ISOMETRIC VIEW

IN-PLANE, f_{cr} = 21.97 Hz
OUT-OF-PLANE, f_{cr} = 36.62 Hz

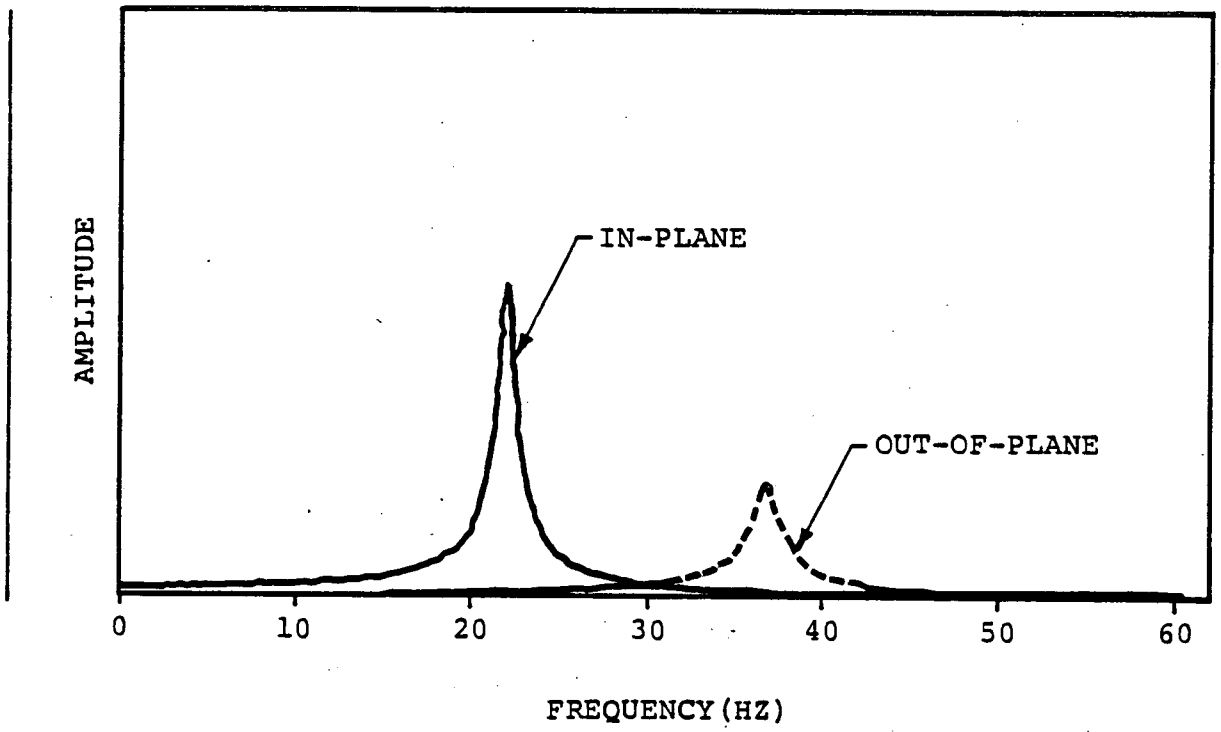

1. RESULTS SHOWN ARE OBTAINED BY APPLYING UNIT DRAG PRESSURES TO SUBMERGED PORTION OF COLUMNS IN THE IN-PLANE AND OUT-OF-PLANE DIRECTIONS RELATIVE TO THE MITER JOINT.

2. RESULTS SHOWN ARE TYPICAL FOR INSIDE AND OUTSIDE COLUMNS.

Figure 3-2.4-6

HARMONIC ANALYSIS RESULTS FOR SUPPORT COLUMN SUBMERGED STRUCTURE LOAD FREQUENCY DETERMINATION

IN-PLANE, f_{cr} = 11.11 Hz

OUT-OF-PLANE, f_{cr} = 54.69 Hz

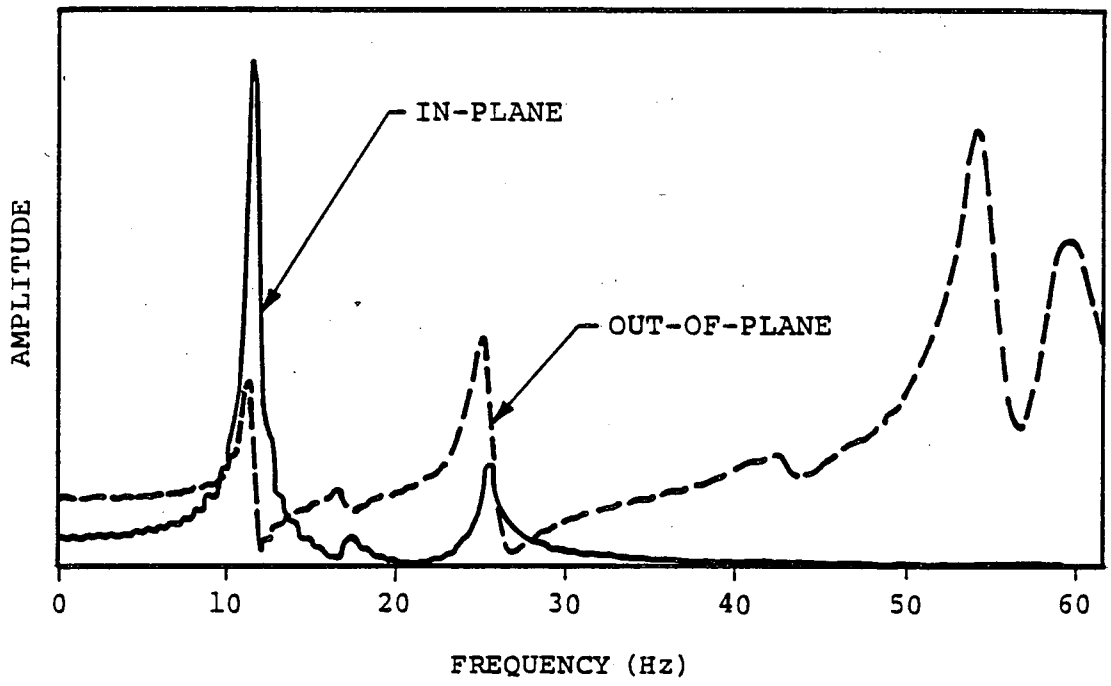

1. RESULTS SHOWN ARE OBTAINED BY APPLYING UNIT DRAG PRESSURES TO SUBMERGED PORTION OF DOWNCOMERS IN THE IN-PLANE AND OUT-OF-PLANE DIRECTIONS.

2. FREQUENCIES ARE DETERMINED WITH WATER INSIDE SUBMERGED PORTION OF DOWNCOMERS.

3. RESULTS SHOWN ARE TYPICAL FOR ALL DOWNCOMERS.

4. THE AMPLITUDE SCALE SHOWN APPLIES TO THE IN-PLANE PLOT. FOR PRESENTATION PURPOSES, THE OUT-OF-PLANE AMPLITUDES HAVE BEEN MULTIPLIED BY 250.

Figure 3-2.4-7

HARMONIC ANALYSIS RESULTS FOR DOWNCOMER SUBMERGED STRUCTURE LOAD FREQUENCY DETERMINATION

LONGITUDINAL, f_{cr} = 58.11 Hz
VERTICAL, f_{cr} = 57.86 Hz

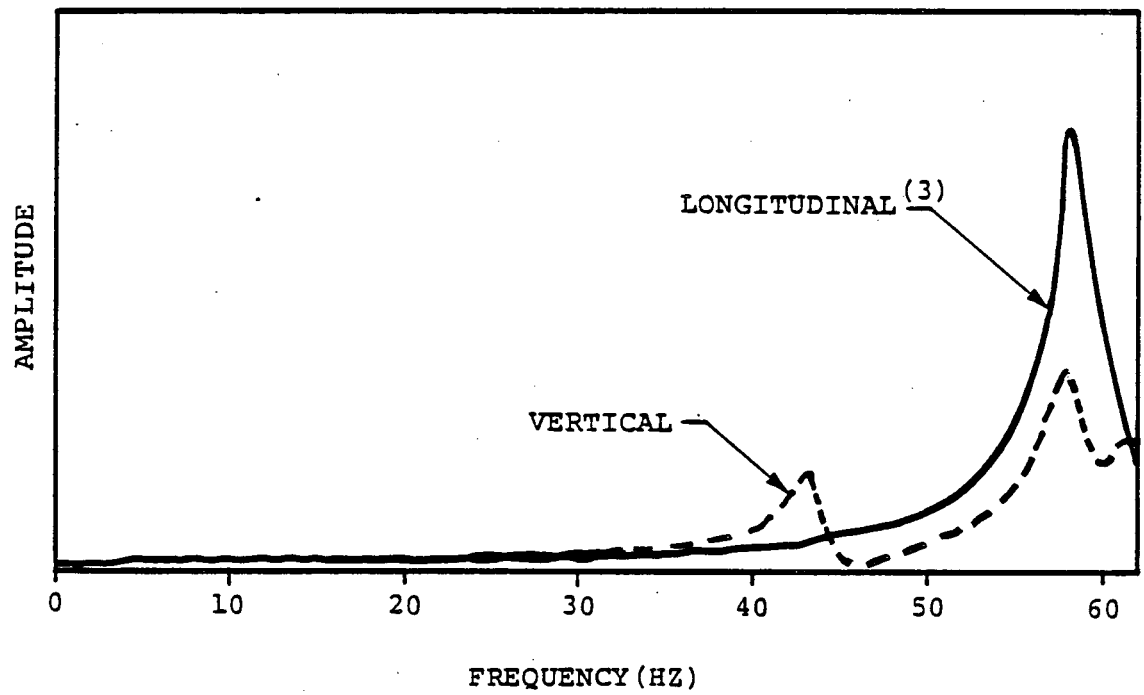

1. RESULTS SHOWN ARE OBTAINED BY APPLYING UNIT DRAG PRESSURES TO SUBMERGED TIE RODS.
2. RESULTS SHOWN ARE TYPICAL FOR ALL TIE RODS.
3. LONGITUDINAL DIRECTION IS PARALLEL TO THE VENT HEADER AXIS.

Figure 3-2.4-8

HARMONIC ANALYSIS RESULTS FOR TIE RODS

SUBMERGED STRUCTURE LOAD FREQUENCY DETERMINATION

VERTICAL, f_{cr} = 59.81 Hz
TRANSVERSE, f_{cr} = 61.04 Hz

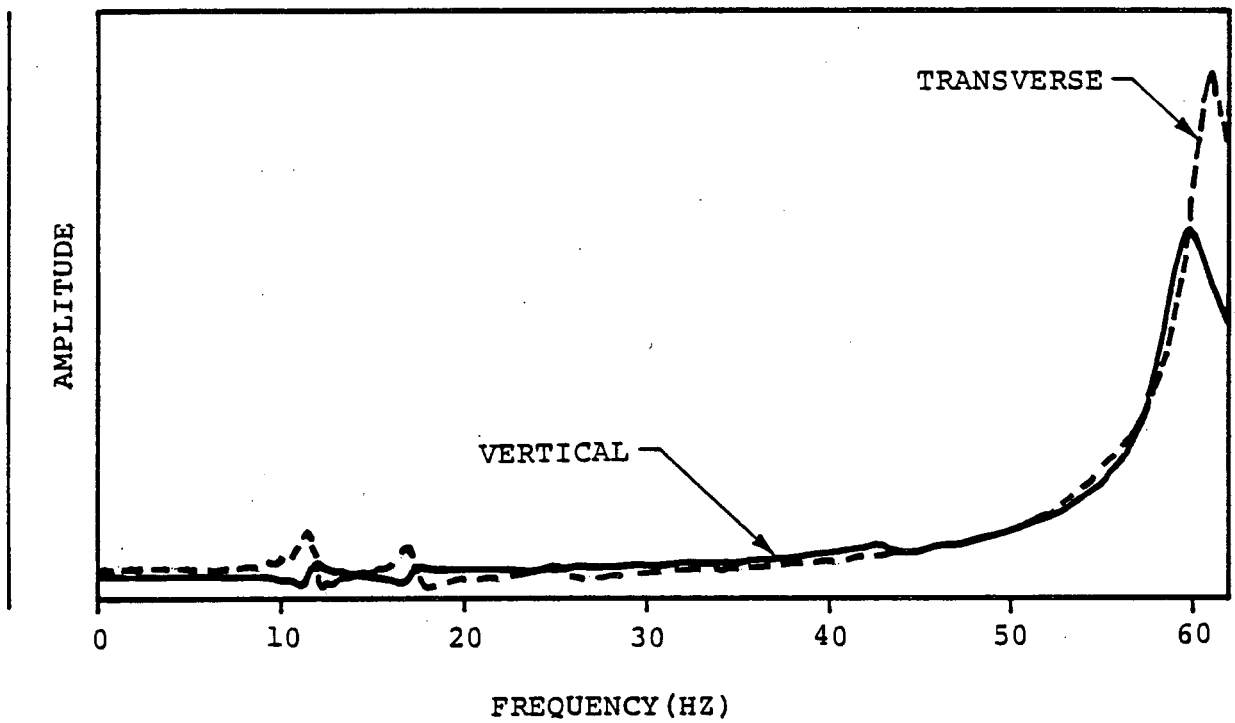

1. RESULTS SHOWN ARE OBTAINED BY APPLYING UNIT DRAG PRESSURES TO SUBMERGED LONGITUDINAL BRACING.

2. RESULTS SHOWN ARE FOR THE LONGEST LONGITUDINAL BRACING.

Figure 3-2.4-9

HARMONIC ANALYSIS RESULTS FOR LONGITUDINAL BRACING
SUBMERGED STRUCTURE LOAD FREQUENCY DETERMINATION

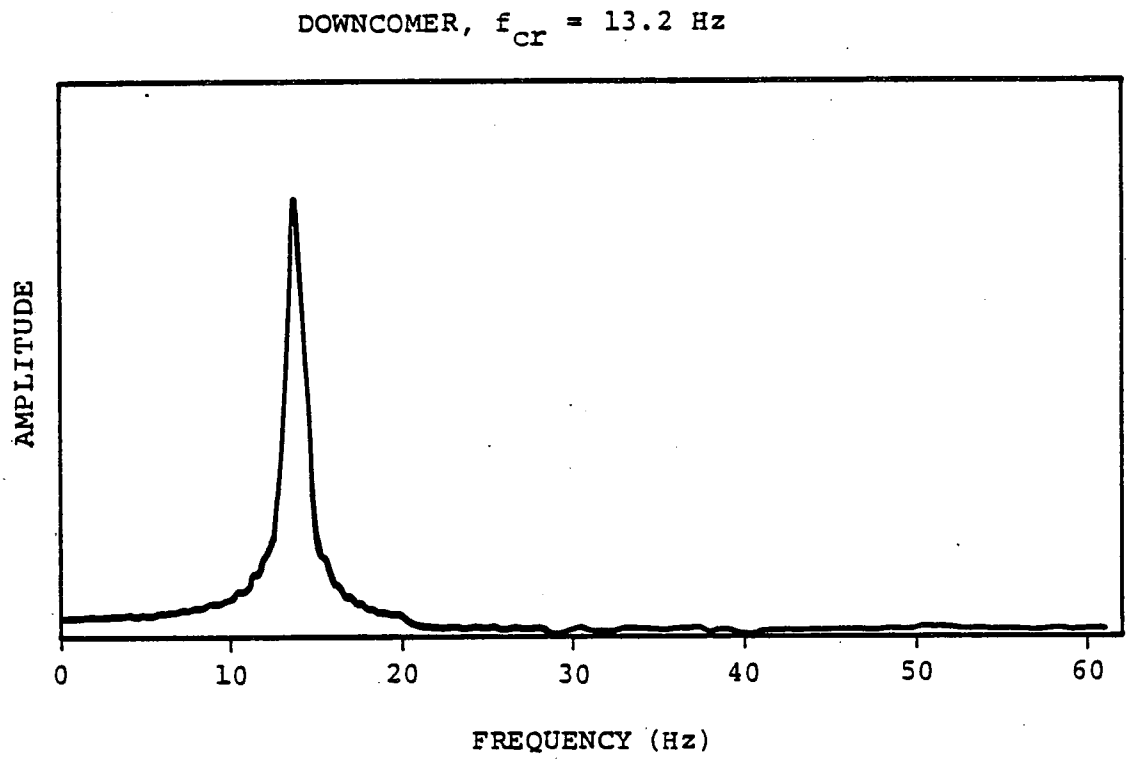

1. RESULTS SHOWN ARE OBTAINED BY APPLYING UNIT INTERNAL PRESSURES TO ONE DOWNCOMER IN A DOWNCOMER PAIR.

2. FREQUENCIES ARE DETERMINED WITHOUT WATER INSIDE SUBMERGED PORTION OF THE DOWNCOMERS.

3. RESULTS SHOWN ARE TYPICAL FOR ALL DOWNCOMERS.

FIGURE 3-2.4-10

HARMONIC ANALYSIS RESULTS FOR CONDENSATION OSCILLATION DOWNCOMER LOAD FREQUENCY DETERMINATION

VENT LINE, f_{cr} = 43.7 Hz
VENT HEADER, f_{cr} = 42.7 Hz

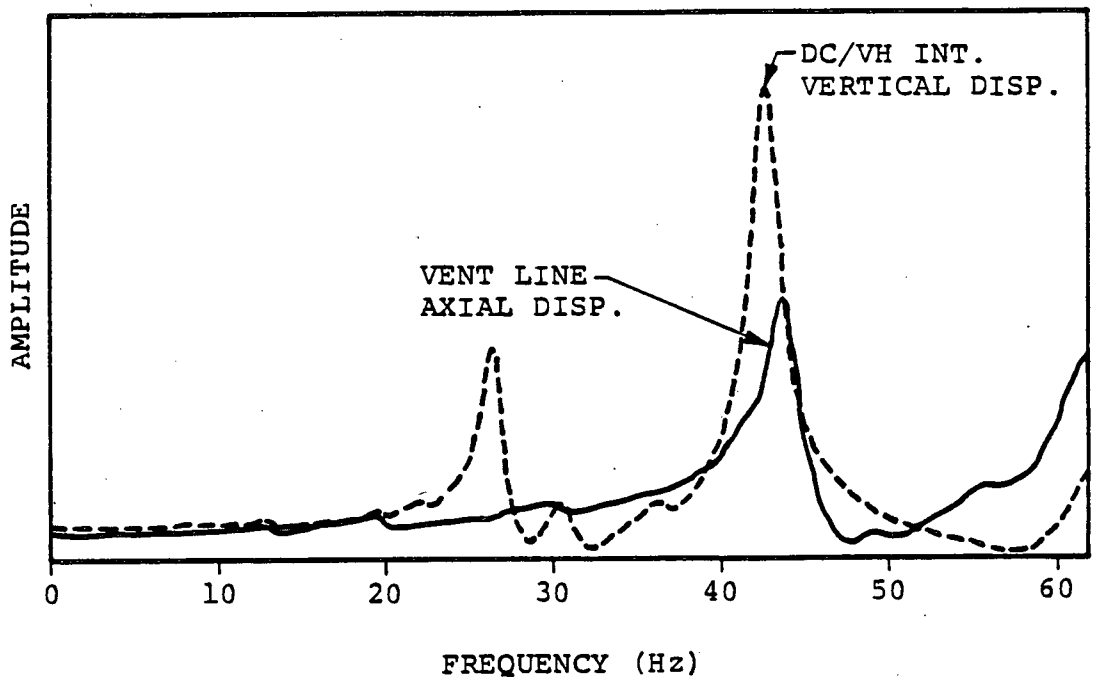

1. RESULTS SHOWN ARE OBTAINED BY APPLYING 2.5 psi INTERNAL PRESSURES TO UNREACTED AREAS OF VENT SYSTEM.

Figure 3-2.4-11

HARMONIC ANALYSIS RESULTS FOR CONDENSATION OSCILLATION VENT SYSTEM PRESSURE LOAD FREQUENCY DETERMINATION

DOWNCOMER, f_{cr} = 11.1 Hz

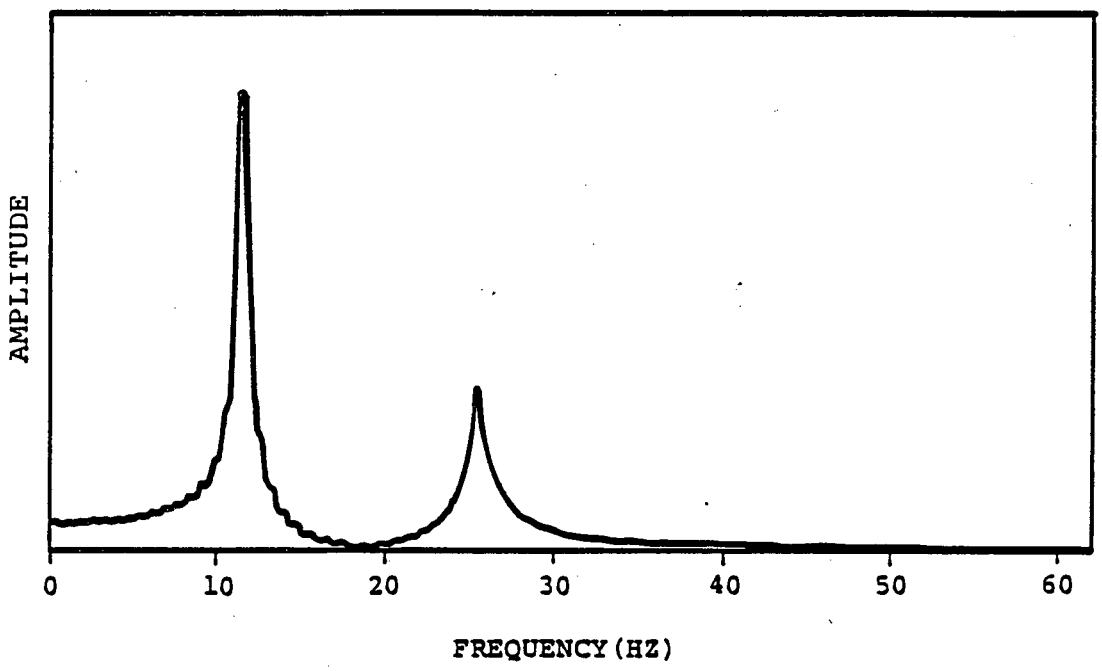

1. RESULTS SHOWN ARE OBTAINED BY APPLYING UNIT FORCES TO DOWNCOMER ENDS IN THE PLANE OF THE DOWNCOMERS IN THE SAME DIRECTION.

2. FREQUENCIES ARE DETERMINED WITH WATER INSIDE SUBMERGED PORTION OF THE DOWNCOMER.

3. RESULTS SHOWN ARE TYPICAL FOR ALL DOWNCOMERS.

Figure 3-2.4-12

HARMONIC ANALYSIS RESULTS FOR CHUGGING DOWNCOMER LATERAL LOAD FREQUENCY DETERMINATION

VENT LINE, f_{cr} = 43.21 Hz

VENT HEADER, f_{cr} = 42.73 Hz

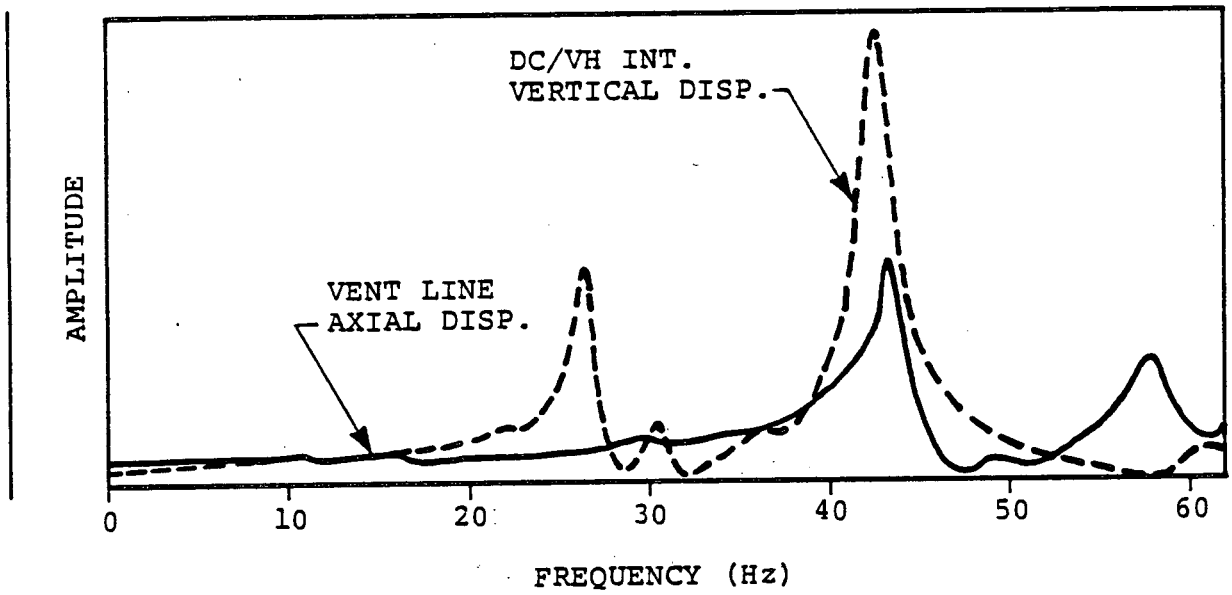

1. RESULTS SHOWN ARE OBTAINED BY APPLYING 2.5 AND 3.0 psi INTERNAL PRESSURES TO UNREACTED AREAS OF VENT LINE AND VENT HEADER, RESPECTIVELY.

Figure 3-2.4-13

HARMONIC ANALYSIS RESULTS FOR CHUGGING VENT SYSTEM PRESSURE LOAD FREQUENCY DETERMINATION

3-2.4.2 Analysis for Asymmetric Loads

The asymmetric loads acting on the vent system are evaluated by decomposing each of the asymmetric loadings into symmetric or asymmetric components, or both, with respect to a 180° segment of the vent system. The analysis of the vent system for asymmetric loads is performed for a typical 180° segment of the vent system cut along the plane of a principal azimuth.

A beam model of a 180° segment of the vent system (Figure 3-2.4-14) is used to obtain the response of the vent system to asymmetric loads. The model includes the vent line, vent header, downcomers, downcomer tie rods, downcomer longitudinal bracing members, and support columns.

Many of the modeling techniques used in the 180° beam model, such as those used for local mass and stiffness determination, are the same as those utilized in the 1/16 beam model of the vent system discussed in Section 3-2.4.1. The local stiffness effects at the vent line-drywell penetrations and vent line-vent header intersections are included using stiffness matrix elements for these penetrations and intersections. The

local stiffness effects at the attachments of the support columns to the support ring girder are included in the model.

The 180° beam model contains 286 nodes, 382 beams, and 16 matrix elements. The model is less refined than the 1/16 beam model of the vent system and is used to characterize the overall response of the vent system to asymmetric loadings. It includes those components and local stiffnesses which have an effect on the overall response of the vent system. The stiffness and mass properties used in the model are based on the nominal dimensions and densities of the materials used to construct the vent system. Small displacement linear-elastic behavior is assumed throughout.

The boundary conditions used in the 180° beam model are both physical and mathematical in nature. The physical boundary conditions used in the model are similar to those used in the 1/16 beam model of the vent system. The mathematical boundary conditions used in the model consist of either symmetry, anti-symmetry, or a combination of both at the 0° and 180° planes. The specific boundary condition used depends on the characteristics of the load being evaluated.

Additional mass is lumped along the length of the submerged portion of the downcomers and support columns in a manner similar to that used in the 1/16 beam model. The mass of water inside the submerged portion of the downcomers is also included. An additional mass of 937 lbs is lumped at the center of gravity of the drywell/wetwell vacuum breaker to account for its weight. The masses of other vent system components are also lumped at the appropriate locations in the model.

The asymmetric loads which act on the vent system are horizontal seismic loads and asymmetric chugging loads, as specified in Section 3-2.2.1. An equivalent static analysis is performed for each of the loads using the 180° beam model.

The 180° beam model analysis results are used to generate loads for use in the 1/16 beam model analysis. This allows evaluation of the effects of asymmetric loads on the component parts of the vent system not included in the 180° beam model. Beam stresses in the vent line and vent header are examined for each asymmetric loading to determine which 1/16 segment or segments of the 180° beam model produce the maximum response. The forces at the midcylinder planes of the controlling 1/16 segments

are imposed on the corresponding midcylinder boundary planes of the 1/16 beam model. The inertia forces and concentrated forces acting on the 180° beam model between the midcylinder boundary planes are also applied to the 1/16 beam model at the appropriate node locations.

The magnitudes and characteristics of governing asymmetric loads on the vent system are presented and discussed in Section 3-2.2.1. The overall effects of asymmetric loads on the vent system are evaluated using the 180° beam model and the general analysis techniques discussed in the preceding paragraphs. The specific treatment of each load which results in asymmetric loads on the vent system is discussed in the following paragraphs.

2. Seismic Loads

   a. OBE Loads: A static analysis is performed for a 0.23g horizontal seismic acceleration applied to the weight of steel and water included in the 180° beam model. Seismic loads are applied in the direction of both principal azimuths.

b. SSE Loads: The procedure used to evaluate 0.46g horizontal SSE accelerations is the same as that discussed for OBE loads in Load Case 2a.

7. Chugging Loads

a. Chugging Downcomer Lateral Loads: A static analysis is performed for chugging downcomer lateral Load Cases 1 through 7 (Table 3-2.2-17).

Use of the methodology described in the preceding paragraphs results in a conservative evaluation of vent system response to the asymmetric loads defined in NUREG-0661.

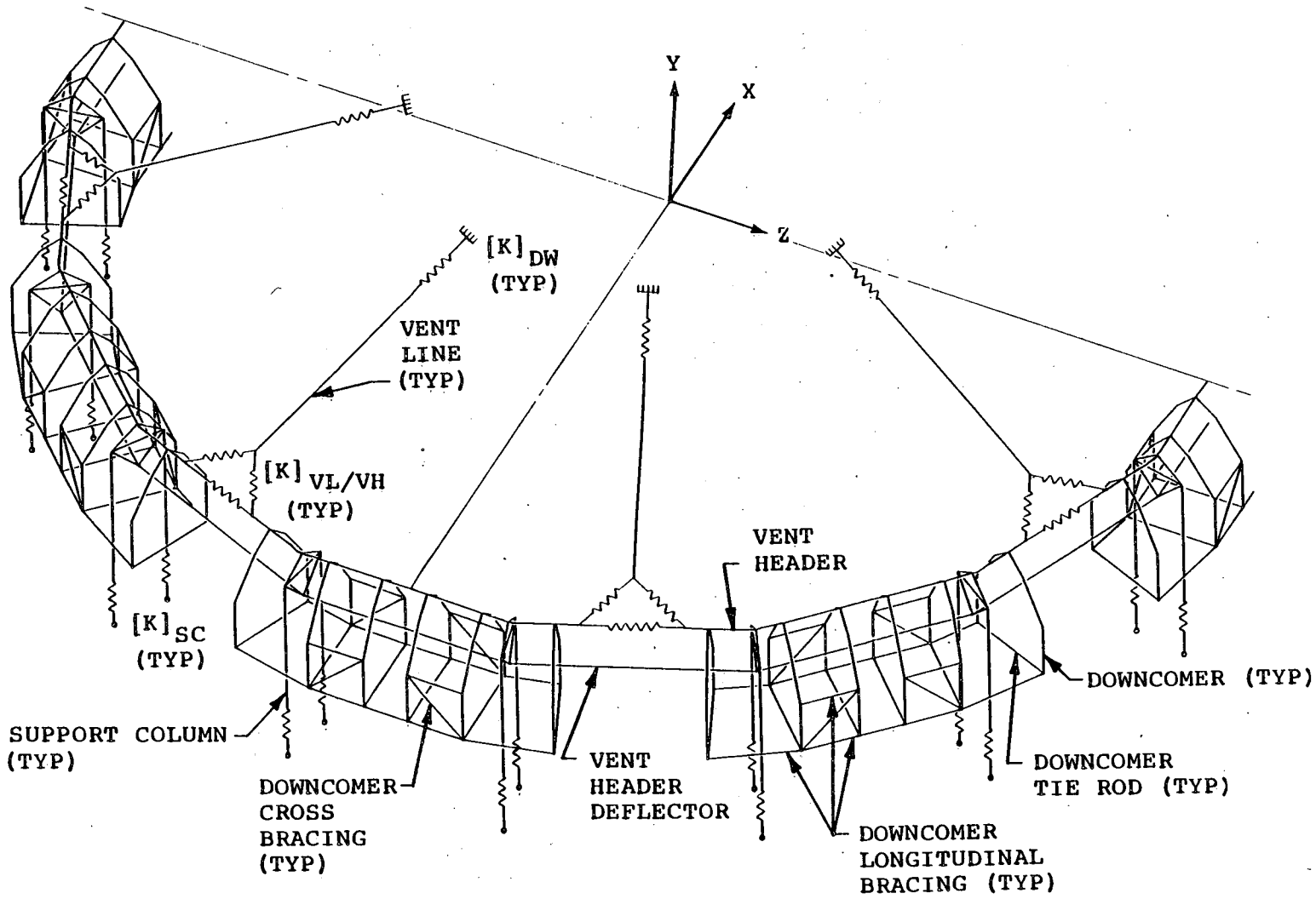

Figure 3-2.4-14

VENT SYSTEM 180° BEAM MODEL - ISOMETRIC VIEW

nutech ENGINEERS

3-2.4.3 Analysis for Local Effects

The penetrations and intersections of the major components of the vent system are evaluated using refined analytical models of each penetration and intersection. These include the vent line-drywell penetration, the vent line-SRV piping penetration, the vent line-vent header intersection, the downcomer-vent header intersections, and the vacuum breaker penetration. Figures 3-2.4-2 through 3-2.4-5 and Figure 3-2.4-15 show analytical models used to evaluate these penetrations and intersections.

Each of the penetration and intersection analytical models includes mesh refinement near discontinuities to facilitate evaluation of local stresses. The stiffness properties used in the model are based on the nominal dimensions of the materials used to construct the penetrations and intersections. Small displacement linear-elastic theory is assumed throughout.

The analytical models are used to generate local stiffnesses of the penetrations and intersections for use in the 1/16 beam model and the 180° beam model, as discussed in Sections 3-2.4.1 and 3-2.4.2. Local stiff-

nesses are developed which represent the stiffness of the entire penetration or intersection in terms of a few local degrees of freedom on the penetration or intersection. This is accomplished either by applying unit forces or displacements to the selected local degrees of freedom or by performing a matrix condensation to reduce the total stiffness of the penetration or intersection to those of the selected local degrees of freedom. The results are used to formulate stiffness matrix elements which are added to the 1/16 beam model and the 180° beam model at the corresponding penetration or intersection locations.

In order to account for the ovaling behavior of the shell segment of the vent header, the shell segment of the vent header at the downcomer intersection is extended at least to the location of the first circumferential collar for the intersection stiffness calculation.

The analytical models are also used to evaluate stresses in the penetrations and intersections. Stresses are computed by idealizing the penetrations and intersections as free bodies in equilibrium under a set of statically applied loads. The applied loads, which are

extracted from the 1/16 beam model results or the SRV piping analysis described in Volume 5, consist of loads acting on the penetration and intersection model boundaries and of loads acting on the interior of penetration and intersection models. The loads acting on the penetration and intersection model boundaries are the beam end loads taken from the vent system and SRV piping models at nodes coincident with the penetration or intersection model boundary locations.

The loads which act on the interior of the penetration or intersection models consist of reaction loads and distributed loads taken from the 1/16 beam model results. The reaction loads include the forces and moments applied to the appropriate penetration or intersection at the attachment points of the SRV piping, the downcomer miter joint, the vent header, the vent line, and the support columns. The distributed loads include the pressures and acceleration loads applied to penetration and intersection models to account for internal pressure loads, thrust loads, pool swell loads, and inertia loads. By the application of boundary loads, reaction loads, and distributed loads to the penetration and intersection models, equilibrium of the penetrations and intersections is achieved for each of the governing

vent system loadings. The inertia loads are found to be insignificant for most of the load cases.

Loads which act on the shell segment boundaries are applied to the penetration and intersection models through a system of radial beams. The radial beams extend from the middle surface of each of the shell segments to a node located on the centerline of the corresponding shell segment. The beams have large bending stiffnesses, zero axial stiffness, and are pinned in all directions at the shell segment middle surface. Boundary loads applied to the centerline nodes cause only shear loads to be transferred to the shell segment middle surface with no local bending effects. Use of this boundary condition minimizes end effects on penetration and intersection stresses in the local areas of interest. The system of radial beams constrains the boundary planes to remain plane during loading, which is consistent with the assumption made in small deflection beam theory.

Section 3-2.4.1 discusses the methodology used to evaluate the overall effects of the governing loads acting on the vent system using the 1/16 beam model. The general methodology used to evaluate local vent system

penetration and intersection stresses is discussed in the preceding paragraphs. Descriptions of each vent system penetration and intersection analytical model and its use are provided in the following paragraphs.

- Vent Line-Drywell Penetration Axisymmetric Finite Difference Model: The vent line-drywell penetration model (Figure 3-2.4-2) includes a segment of the drywell shell, the jet deflector, the cylindrical penetration nozzle, the annular pad plate, and the conical transition piece. The analytical model contains 10 segments with 145 mesh points. The reaction loads applied to the model include those computed at the upper end of the vent line. The distributed loads applied to the model are internal pressure loads.

- Vent Line-SRV Piping Penetration Finite Element Model: The vent line-SRV piping penetration model (Figure 3-2.4-15) includes a segment of the vent line, the penetration insert plate and the penetration nozzle. The model contains 1,381 nodes, 82 beam elements, and 1,719 plate bending and stretching elements. Boundary loads are applied at each end of the vent line shell segment. The reaction

loads applied to the analytical model include the drywell and wetwell SRV piping reaction loads. The distributed loads applied to the analytical model are internal pressure loads.

- Vent Line-Vent Header Intersection Finite Element Model: The vent line-vent header intersection finite element model (Figure 3-2.4-3) includes a segment of the vent line, a segment of the vent header with conical transitions, and the intersection stiffener plates. The model contains 1512 nodes and 1544 plate bending and stretching elements. Boundary loads are applied at the end of the vent line shell segment and at each end of the vent header shell segment. The distributed loads applied to the analytical model are internal pressure loads and thrust loads.

- Downcomer-Vent Header Intersection Finite Element Model: The downcomer vent header intersection finite element model (Figure 3-2.4-5) includes a segment of the vent header, a segment of each downcomer, and two gusset plates. The analytical model contains 796 nodes, 154 beam elements, and 740 plate bending and stretching elements.

Boundary loads are applied at the ends of the vent header segment and at the ends of the downcomer segment. The distributed loads applied to the model are internal pressure loads, pool swell loads on the downcomers, and pool swell inertia loads.

- Vacuum Breaker Penetration Finite Element Model: The vacuum breaker penetration model (Figure 3-2.4-4) includes a vent line cap, a segment of a nozzle, and three stiffener plates. The analytical model contains 564 nodes, 24 beam elements, and 458 plate bending and stretching elements. Boundary loads are applied at the end of the nozzle segment. The distributed loads applied to the model are pool swell loads and pool swell inertia loads.

Use of the methodology described in the preceding paragraphs results in a conservative evaluation of vent system local stresses due to the loads defined in NUREG-0661.

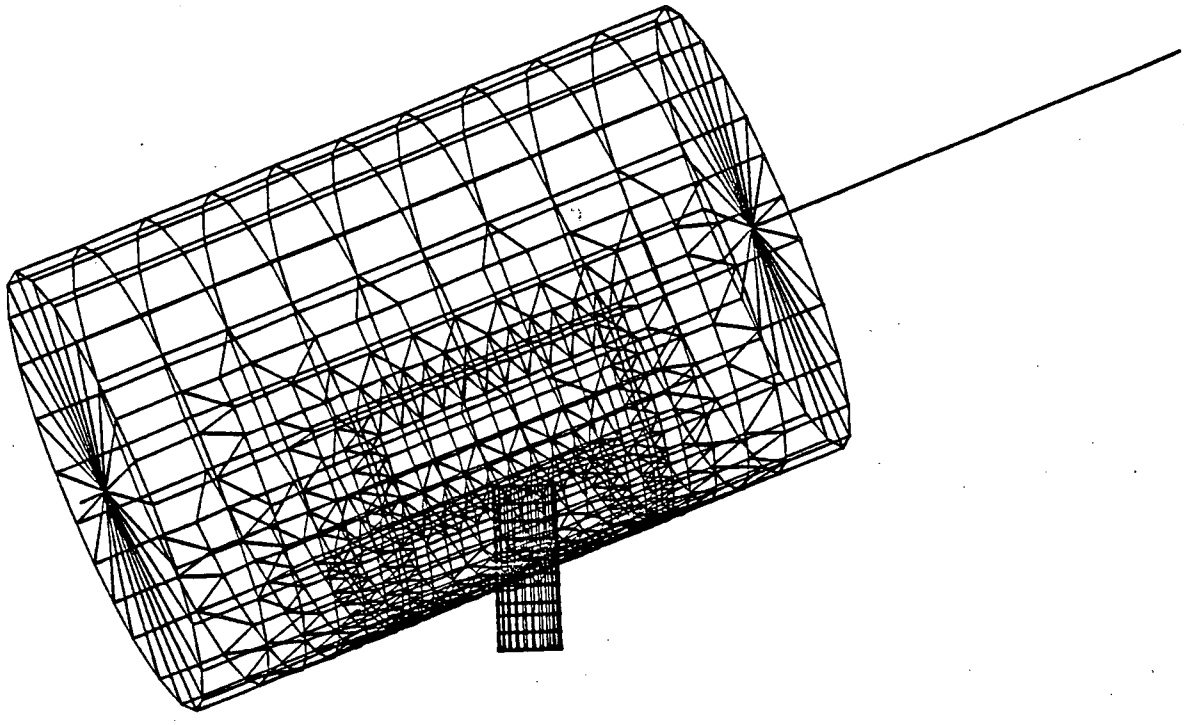

Figure 3-2.4-15

SRV PIPING-VENT LINE PENETRATION
FINITE ELEMENT MODEL - ISOMETRIC VIEW

3-2.4.4 Methods for Evaluating Analysis Results

The methodology discussed in Sections 3-2.4.1 and 3-2.4.2 is used to determine element forces and component stresses in the vent system component parts. The following paragraphs discuss the methodology used to evaluate the analysis results, determine the controlling stresses in the vent system components parts, and examine fatigue effects.

To evaluate analysis results for the vent system Class MC components, membrane and extreme fiber stress intensities are computed. The values of the membrane stress intensities away from discontinuities are computed using 1/16 beam model results. These stresses are compared with the primary membrane stress allowables (Table 3-2.3-1). The values of membrane stress intensities near discontinuities are computed using results from the penetration and intersection analytical models. These stresses are compared with local primary membrane stress allowables (Table 3-2.3-1). Primary stresses in vent system Class MC component welds are computed using maximum principal stresses or the resultant forces acting on the weld throat. The results are compared to primary weld stress allowables (Table 3-2.3-1).

Many of the loads contained in each of the controlling load combinations are dynamic loads which result in stresses which cycle with time and are partially or fully reversible. The maximum stress intensity ranges for all vent system Class MC components are calculated using the maximum values of the extreme fiber stress differences which occur near discontinuities in the penetration and intersection analytical models. These stresses are compared to the secondary stress range allowables (Table 3-2.3-1). A similar procedure is used to compute the stress range for the vent system Class MC component welds. The results are compared to the secondary weld stress allowables (Table 3-2.3-1).

To evaluate the vent system Class MC component supports, beam end loads obtained from the 1/16 beam model results are used to compute stresses. The results are compared with the corresponding allowable stresses (Table 3-2.3-1). Stresses in vent system Class MC component support welds are obtained using the 1/16 beam model results to compute the maximum resultant force acting on the associated weld throat. The results are compared to weld stress limits discussed in Section 3-2.3.

Section 3-2.2.2 defines the controlling vent system load combinations. During load combination formulation, the maximum stress components in a particular vent system part at a given location are combined for the individual loads contained in each combination. The stress components for dynamic loadings are combined to obtain the maximum stress intensity.

The maximum differential displacements of the vent line bellows are determined using results from the 1/16 beam model of the vent system and the analytical model of the suppression chamber discussed in Volume 2 of this report. The displacements of the attachment points of the bellows to the suppression chamber and to the vent line are determined for each load case. The differential displacement is computed from these values. The results for each load are combined to determine the total differential displacements for the controlling load combinations. These results are compared to the allowable bellows displacements (Table 3-2.3-2).

d.

To evaluate fatigue effects in the vent system Class MC components and associated welds, extreme fiber alternating stress intensity histograms are determined for each load in each event or combination of events. Fatigue

effects for chugging downcomer lateral loads are evaluated using the stress reversal histrograms (Table 3-2.2-19). Stress intensity histograms are developed for the most highly stressed area in the vent system, which is the downcomer-vent header intersection. For each combination of events, a load combination stress intensity histogram is formulated and the corresponding fatigue usage factors are determined using the curve shown in Figure 3-2.4-16. The usage factors for each event are then summed to obtain the total fatigue usage.

Use of the methodology described above results in a conservative evaluation of the vent system design margins.

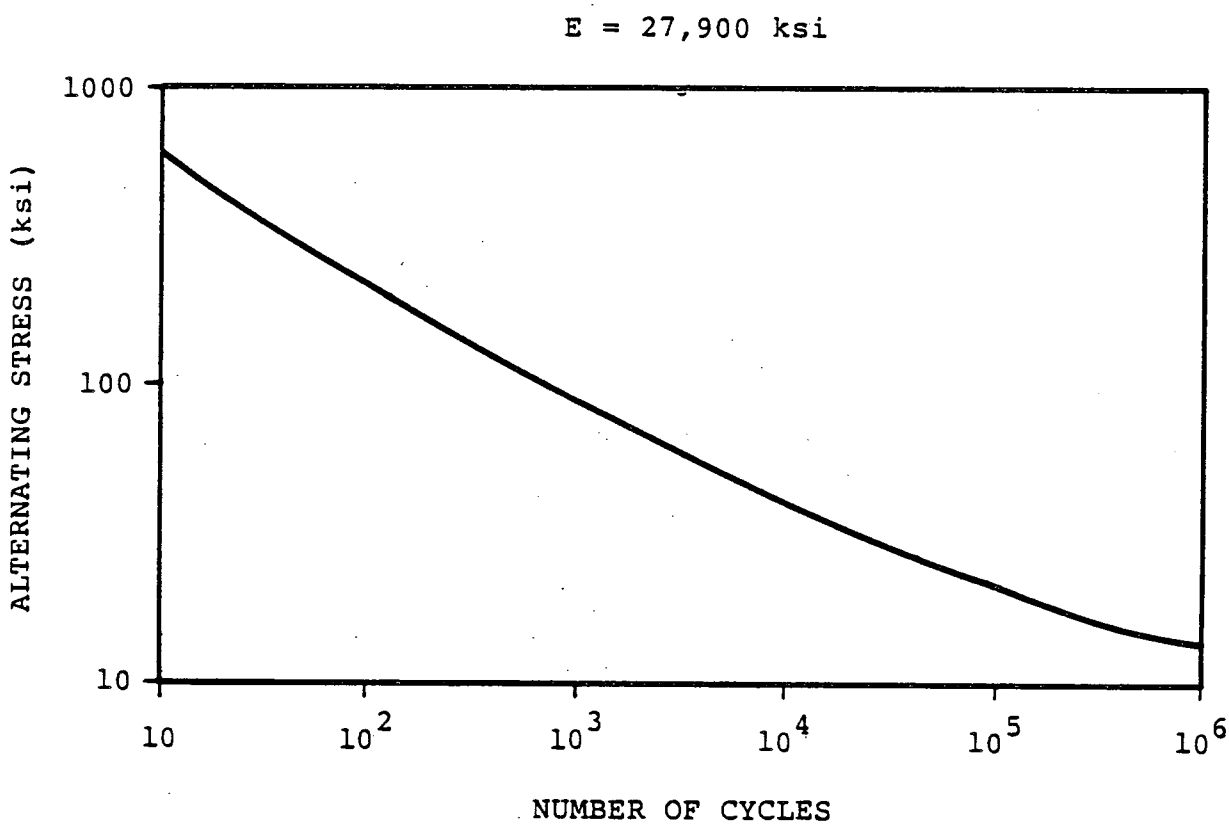

Figure 3-2.4-16

ALLOWABLE NUMBER OF STRESS CYCLES FOR VENT SYSTEM

FATIGUE EVALUATION

3-2.5 Analysis Results

The geometry, loads and load combinations, acceptance criteria, and analysis methods used in the evaluation of the Monticello vent system are presented and discussed in the preceding sections. The results and conclusions derived from the evaluation of the vent system are presented in the following paragraphs and sections.

Table 3-2.5-1 shows the maximum primary membrame stresses for the major components of the vent system for each of the governing loads. Tables 3-2.5-2 and 3-2.5-3 show the corresponding reaction loads for the vent system support columns and vent line-drywell penetration. Table 3-2.5-4 shows the maximum differential displacements of the vent line bellows for the governing load cases. Figures 3-2.5-1 and 3-2.5-2 show the transient response of the vent system support columns for pool swell loads.

Table 3-2.5-5 shows the maximum stresses and associated design margins for the major vent system components, component supports, and welds for the SBA II, IBA I, DBA I, DBA II, and DBA III load combinations. Table 3-2.5-6 shows the maximum stresses and associated design margins

for the components and welds of the vent line-SRV piping penetration for the NOC I, SBA II, IBA I, and DBA III load combinations. Table 3-2.5-7 shows the maximum differential displacements and design margins for the vent line bellows for the SBA II, IBA I, DBA II, and DBA III load combinations. Table 3-2.5-8 shows the fatigue usage factors for the controlling vent system component and weld for the Normal Operating plus SBA events, and the Normal Operating plus IBA events.

Stresses at the vacuum breaker penetration are evaluated for pool swell impact and drag loads. The maximum local primary membrane stress is 0.43 of the allowable at the gusset plate location.

Stresses in the downcomer bracings are evaluated for chugging lateral loads and SRV submerged structure loads. The maximum stress is 0.62 of the allowable.

Section 3-2.5.1 discusses the vent system evaluation results presented in the preceding paragraphs.

Table 3-2.5-1

MAJOR VENT SYSTEM COMPONENT MAXIMUM MEMBRANE STRESSES FOR GOVERNING LOADS

SECTION 3-2.2.1 LOAD DESIGNATION		PRIMARY MEMBRANE STRESS (ksi) (1)		
LOAD TYPE	LOAD CASE NUMBER	VENT LINE	VENT HEADER	DOWNCOMER
DEAD WEIGHT	1a	0.30	0.62	0.22
SEISMIC	2a	0.75	2.08	0.34
	2b	1.51	4.16	0.68
PRESSURE AND TEMPERATURE	3b	6.46	5.36	0.98
	3d	N/A	N/A	N/A
VENT SYSTEM DISCHARGE AND POOL SWELL	4a, 5a-5d	4.39	8.96	4.05
	5e+5f	0.32	1.87	1.20
CONDENSATION OSCILLATION	6a+6c	0.26	0.88	0.44
	6b+6d	1.85	5.82	2.17
	6f	0.15	0.69	0.47
CHUGGING	7a	4.40	6.29	4.68
	7b	0.24	0.50	0.31
	7c(6e)	0.03	0.13	0.08
	7d	0.33	1.38	0.86
SRV DISCHARGE	8a+8b	2.25	6.32	4.80

(1) VALUES SHOWN ARE MAXIMUMS REGARDLESS OF TIME AND LOCATION FOR INDIVIDUAL LOAD TYPES AND MAY NOT BE ADDED TO OBTAIN LOAD COMBINATION RESULTS.

Table 3-2.5-2

MAXIMUM COLUMN REACTIONS FOR GOVERNING VENT SYSTEM LOADS

SECTION 3-2.2.1 LOAD DESIGNATION				COLUMN REACTION LOAD (kips)		
LOAD TYPE		LOAD CASE NUMBER	DIRECTION	INSIDE	OUTSIDE	TOTAL (1)
DEAD WEIGHT		1a	COMPRESSION	8.61	7.11	15.72
SEISMIC	OBE	2a	TENSION	2.11	6.19	8.30
			COMPRESSION	2.11	6.19	8.30
	SSE	2b	TENSION	4.22	12.38	16.60
			COMPRESSION	4.22	12.38	16.60
INTERNAL PRESSURE		3b	TENSION	22.23	9.72	31.95
TEMPERATURE		3d	COMPRESSION	22.32	-9.37	12.95
VENT SYSTEM DISCHARGE AND POOL SWELL		4a, 5a-5d	TENSION	78.92	69.93	148.85
			COMPRESSION	26.63	15.88	42.51
CONDENSATION OSCILLATION	IBA	6a+6c	TENSION	4.36	3.45	7.81
			COMPRESSION	4.36	3.45	7.81
	DBA	6b+6d	TENSION	8.73	13.86	22.59
			COMPRESSION	8.73	13.86	22.59
CHUGGING		7a+7b	TENSION	12.33	17.55	29.88
			COMPRESSION	12.33	17.55	29.88
SRV DISCHARGE		8b	TENSION	4.26	4.52	8.78
			COMPRESSION	4.26	4.52	8.78

(1) FOR DYNAMIC LOADS, REACTIONS ARE ADDED IN TIME.

Table 3-2.5-3

MAXIMUM VENT LINE-DRYWELL PENETRATION REACTIONS FOR GOVERNING VENT SYSTEM LOADS

SECTION 3-2.2.1 LOAD DESIGNATION			PENETRATION REACTION LOAD					
LOAD TYPE		LOAD CASE NUMBER	FORCE (kips)			MOMENTS (in-kips)		
			RADIAL	MERIDIONAL	CIRCUMFERENTIAL	RADIAL	MERIDIONAL	CIRCUMFERENTIAL
DEAD WEIGHT		1a	-3.30	-2.64	0.00	0.00	0.00	257.28
SEISMIC	OBE	2a	21.74	0.80	2.27	74.78	516.36	98.50
	SSE	2b	43.48	1.60	4.54	149.56	1032.72	197.00
INTERNAL PRESSURE		3b	-58.13	4.35	0.00	0.00	0.00	-363.02
TEMPERATURE		3d	-160.47	11.89	0.00	0.00	0.00	-1726.42
VENT SYSTEM DISCHARGE AND POOL SWELL		4a, 5a-5d	30.11	37.39	0.00	0.00	0.00	3669.16
CONDENSATION OSCILLATION	IBA	6a+6c	5.66	2.36	0.00	0.00	0.00	133.92
	DBA	6b+6d	18.33	13.57	0.00	0.00	0.00	573.42
CHUGGING		7a+7b	25.99	-0.97	5.08	-474.93	-1291.40	137.29
SRV DISCHARGE		8a+8b	10.42	7.13	0.00	0.00	0.00	-319.97

nutech ENGINEERS

Table 3-2.5-4

MAXIMUM VENT LINE BELLOWS DISPLACEMENTS FOR GOVERNING VENT SYSTEM LOADS

SECTION 3-2.2.1 LOAD DESIGNATION			DIFFERENTIAL BELLOWS DISPLACEMENTS (in)			
LOAD TYPE		LOAD CASE NUMBER	AXIAL		LATERAL	
			COMPRESSION	EXTENSION	MERIDIONAL	LONGITUDINAL
DEAD WEIGHT		1a	.006	.001	.002	0
SEISMIC	OBE	2a	.021	.021	.003	.020
	SSE	2b	.042	.042	.005	.041
INTERNAL PRESSURE		3b	.031	.002	.057	0
TEMPERATURE		3d	.762	.141	.211	0
VENT SYSTEM DISCHARGE AND POOL SWELL		4a, 5a-5d	.044	.044	.063	0
CONDENSATION OSCILLATION	IBA	6a+6c	.002	.020	.004	0
	DBA	6b+6d	.034	.034	.045	0
CHUGGING		7a+7b	.035	.035	.016	.047
SRV DISCHARGE		8a+8b	.039	.039	.048	0

1. THE VALUES SHOWN ARE MAXIMUMS REGARDLESS OF TIME FOR INDIVIDUAL LOAD TYPES AND MAY NOT BE ADDED TO OBTAIN LOAD COMBINATION RESULTS.

Table 3-2.5-5

MAXIMUM VENT SYSTEM STRESSES FOR CONTROLLING LOAD COMBINATIONS

ITEM		STRESS TYPE	LOAD COMBINATION STRESS (ksi)									
			SBA II (1)		IBA I (1)		DBA I (1)		DBA II (1)		DBA III (1)	
			CALCULATED STRESS	CALCULATED / ALLOWABLE (2)	CALCULATED STRESS	CALCULATED / ALLOWABLE (2)	CALCULATED STRESS	CALCULATED / ALLOWABLE (2)	CALCULATED STRESS	CALCULATED / ALLOWABLE (2)	CALCULATED STRESS	CALCULATED / ALLOWABLE (2)
COMPONENTS	DRYWELL SHELL	LOCAL PRIMARY MEMBRANE	11.56	0.40	14.44	0.50	17.04	0.59	16.72	0.58	17.51	0.34
		PRIMARY AND SECONDARY STRESS RANGE	24.02	0.35	22.86	0.34	N/A	N/A	26.95	0.40	N/A	N/A
	VENT LINE	PRIMARY MEMBRANE	8.28	0.43	3.53	0.18	12.24	0.63	10.14	0.53	14.12	0.42
		LOCAL PRIMARY MEMBRANE	23.48	0.81	11.06	0.38	34.90	0.90	21.83	0.75	41.56	0.82
		PRIMARY AND SECONDARY STRESS RANGE	63.73	0.94	38.83	0.57	N/A	N/A	55.23	0.81	N/A	N/A
	VENT HEADER	PRIMARY MEMBRANE	15.10	0.78	8.04	0.42	18.89	0.98	15.35	0.80	24.12	0.71
		LOCAL PRIMARY MEMBRANE	28.73	0.99	16.86	0.58	28.06	0.97	27.86	0.96	35.42	0.70
		PRIMARY AND SECONDARY STRESS RANGE	65.54	0.96	40.63	0.60	N/A	N/A	60.05	0.88	N/A	N/A
	DOWNCOMER	PRIMARY MEMBRANE	9.25	0.48	3.85	0.20	7.82	0.41	6.58	0.34	10.57	0.31
		LOCAL PRIMARY MEMBRANE	22.33	0.77	10.95	0.38	17.82	0.62	18.92	0.65	23.84	0.47
		PRIMARY AND SECONDARY STRESS RANGE	38.97	0.57	21.88	0.32	N/A	N/A	36.39	0.53	N/A	N/A
	SUPPORT COLUMN RING PLATE	PRIMARY MEMBRANE	5.03	0.26	2.32	0.12	9.86	0.39	2.90	0.15	10.66	0.31
		LOCAL PRIMARY MEMBRANE	19.66	0.68	9.01	0.31	37.62	0.99	11.10	0.38	40.50	0.79
		PRIMARY AND SECONDARY STRESS RANGE	23.65	0.35	15.64	0.23	N/A	N/A	6.79	0.10	N/A	N/A

nutech ENGINEERS

Table 3-2.5-5

MAXIMUM VENT SYSTEM STRESSES FOR CONTROLLING LOAD COMBINATIONS

(Concluded)

ITEM		STRESS TYPE	LOAD COMBINATION STRESS (ksi)									
			SBA II[1]		IBA I[1]		DBA I[1]		DBA II[1]		DBA III[1]	
			CALCULATED STRESS	CALCULATED / ALLOWABLE[2]	CALCULATED STRESS	CALCULATED / ALLOWABLE[2]	CALCULATED STRESS	CALCULATED / ALLOWABLE[2]	CALCULATED STRESS	CALCULATED / ALLOWABLE[2]	CALCULATED STRESS	CALCULATED / ALLOWABLE[2]
SUPPORTS	SUPPORT COLUMNS	BENDING[4]	13.10	0.68	3.82	0.21	9.05	0.47	1.27	0.07	11.71	0.45
		TENSILE	2.67	0.15	1.86	0.11	8.20	0.46	3.57	0.21	9.49	0.40
		COMBINED[3]	N/A	0.83	N/A	0.32	N/A	0.93	N/A	0.28	N/A	0.85
		BENDING[5]	16.25	0.85	4.01	0.22	2.67	0.14	1.41	0.08	5.75	0.22
		COMPRESSION	1.86	0.13	3.88	0.29	6.63	0.47	1.76	0.13	7.38	0.39
		COMBINED[3]	N/A	0.98	N/A	0.53	N/A	0.64	N/A	0.21	N/A	0.68
WELDS	COLUMN RING PLATE TO VENT HEADER	PRIMARY	2.27	0.21	1.06	0.10	4.38	0.36	1.28	0.12	4.74	0.17
		SECONDARY	2.75	0.09	1.82	0.06	N/A	N/A	0.83	0.03	N/A	N/A

(1) SEE TABLE 3-2.2-29 FOR LOAD COMBINATION DESIGNATIONS.

(2) SEE TABLE 3-2.3-1 FOR ALLOWABLE STRESSES.

(3) THE COMBINED STRESS RATIO IS DETERMINED BY INTERACTION FORMULA. THEREFORE, CALCULATED STRESSES ARE NOT DIRECTLY ADDITIVE.

(4) BENDING STRESS CORRESPONDS TO AXIAL TENSILE STRESS.

(5) BENDING STRESS CORRESPONDS TO AXIAL COMPRESSIVE STRESS.

nutech ENGINEERS

Table 3-2.5-6

MAXIMUM VENT LINE-SRV PIPING PENETRATION STRESSES FOR CONTROLLING LOAD COMBINATIONS

ITEM		STRESS TYPE	LOAD COMBINATION STRESSES (ksi)							
			NOC I (1)		SBA II (1)		IBA I (1)		DBA III (1)	
			CALCULATED (ksi)	CALCULATED / ALLOWABLE (2)	CALCULATED (ksi)	CALCULATED / ALLOWABLE (2)	CALCULATED (ksi)	CALCULATED / ALLOWABLE (2)	CALCULATED (ksi)	CALCULATED / ALLOWABLE (2)
COMPONENT	INSERT PLATE	LOCAL PRIMARY MEMBRANE	2.21	0.11	4.14	0.22	3.49	0.18	3.80	0.08
		PRIMARY + SECONDARY STRESS RANGE	25.69	0.38	45.46	0.68	41.50	0.62	N/A	N/A
	VENT LINE SHELL	LOCAL PRIMARY MEMBRANE	7.45	0.39	12.97	0.67	11.45	0.59	12.00	0.24
		PRIMARY + SECONDARY STRESS RANGE	21.77	0.33	38.01	0.57	33.57	0.50	N/A	N/A

(1) SEE TABLE 3-2.2-29 FOR LOAD COMBINATION DESIGNATIONS.

(2) SEE TABLE 3-2.3-1 FOR ALLOWABLE STRESSES.

nutech ENGINEERS

Table 3-2.5-7

MAXIMUM VENT LINE BELLOWS DIFFERENTIAL DISPLACEMENTS
FOR CONTROLLING LOAD COMBINATIONS

DISPLACEMENT COMPONENT		SBA II		IBA I		DBA II		DBA III	
		CALCULATED (in)	CALCULATED / ALLOWABLE	CALCULATED (in)	CALCULATED / ALLOWABLE	CALCULATED (in)	CALCULATED / ALLOWABLE	CALCULATED (in)	CALCULATED / ALLOWABLE
AXIAL	COMPRESSION	.850	.972	.629	.718	.686	.784	.756	.865
	TENSION	.208	.555	.209	.556	.153	.409	.115	.307
LATERAL	MERIDIONAL	.280	.448	.284	.455	.249	.398	.174	.278
	LONGITUDINAL	.067	.107	.020	.033	.020	.033	.041	.065

1. THE DBA III BELLOWS DISPLACEMENTS ENVELOP THOSE OF DBA I SINCE DBA III CONTAINS SRV DISCHARGE LOADS IN ADDITION TO THE OTHER LOADS IN DBA I (TABLE 3-2.2-29)

nutech ENGINEERS

Table 3-2.5-8

MAXIMUM FATIGUE USAGE FACTORS FOR VENT SYSTEM COMPONENTS AND WELDS

EVENT[1] SEQUENCE	LOAD CASE CYCLES[1]		CONDENSATION OSCILLATION (sec)	CHUGGING (sec)	EVENT USAGE FACTOR	
	SEISMIC	SRV[2] DISCHARGE			VENT[3] HEADER	WELD[4]
NOC	0	934	N/A	N/A	.522	.350
SBA 0.0 TO 900 SEC	1000	50	N/A	900	.162	.040
IBA/CO 0.0 TO 300 SEC	0	0	300	N/A	.016	.000
IBA/CHUGGING 300 TO 500 SEC	1000	25	N/A	200	.074	.000
MAXIMUM CUMULATIVE USAGE FACTORS			NOC + SBA		.684	.390
			NOC + IBA		.613	.350

(1) SEE TABLE 3-2.2-29 AND FIGURES 2-2.2-12 AND 3-2.2-13 FOR LOAD CYCLES AND EVENT SEQUENCING INFORMATION.

(2) TOTAL NUMBER OF SRV ACTUATIONS ARE CONSERVATIVELY ASSUMED TO OCCUR IN THE SAME SUPPRESSION CHAMBER BAY. THE DURATION OF SIGNIFICANT RESPONSE FOR A SINGLE ACTUATION IS 1.5 SECOND.

(3) THE MAXIMUM CUMULATIVE USAGE FOR A VENT SYSTEM COMPONENT OCCURS IN THE VENT HEADER AT THE DOWNCOMER-VENT HEADER INTERSECTION.

(4) THE MAXIMUM CUMULATIVE USAGE FOR A VENT SYSTEM COMPONENT WELD OCCURS IN THE SRV PIPING-VENT LINE PENETRATION.

nutech ENGINEERS

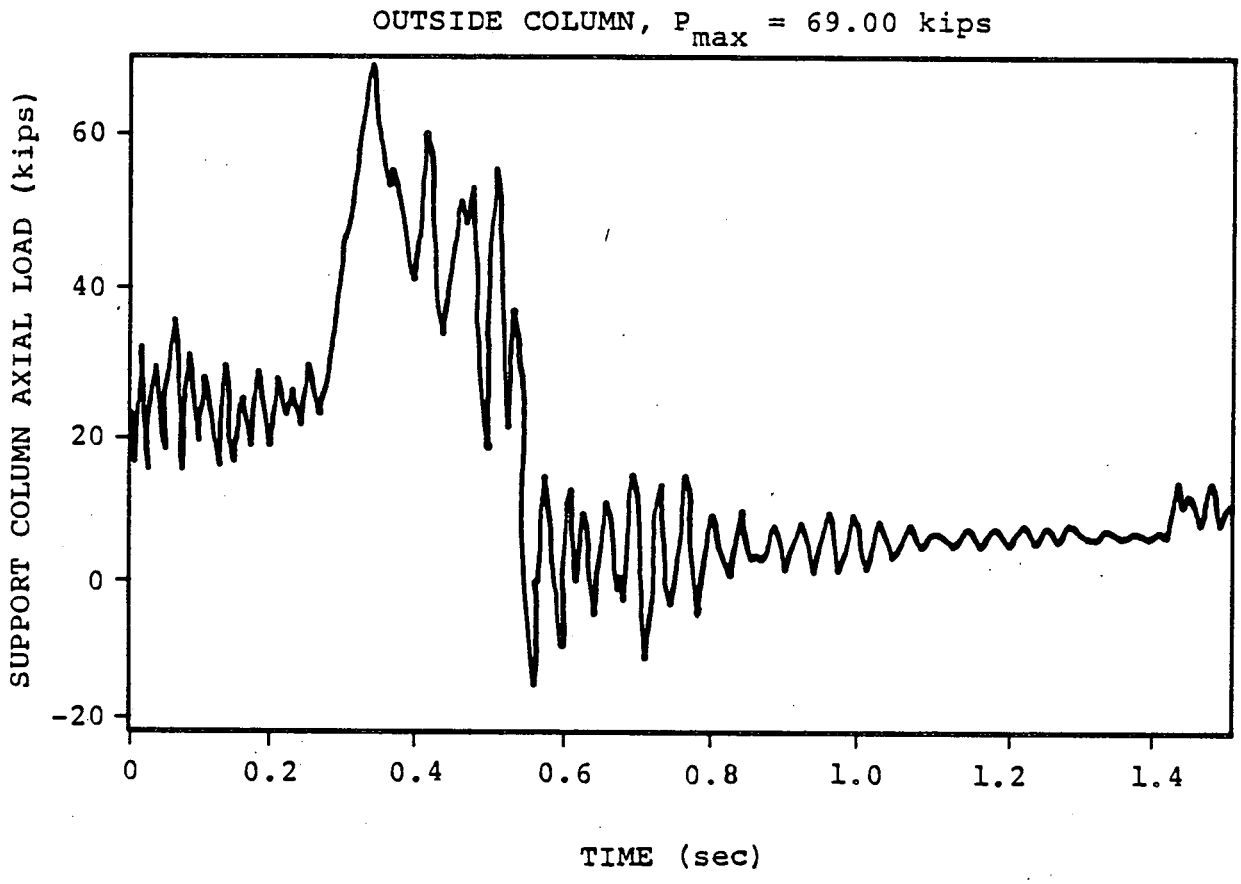

FIGURE 3-2.5-1

VENT SYSTEM SUPPORT COLUMN RESPONSE DUE TO POOL SWELL IMPACT LOADS – OUTSIDE COLUMN

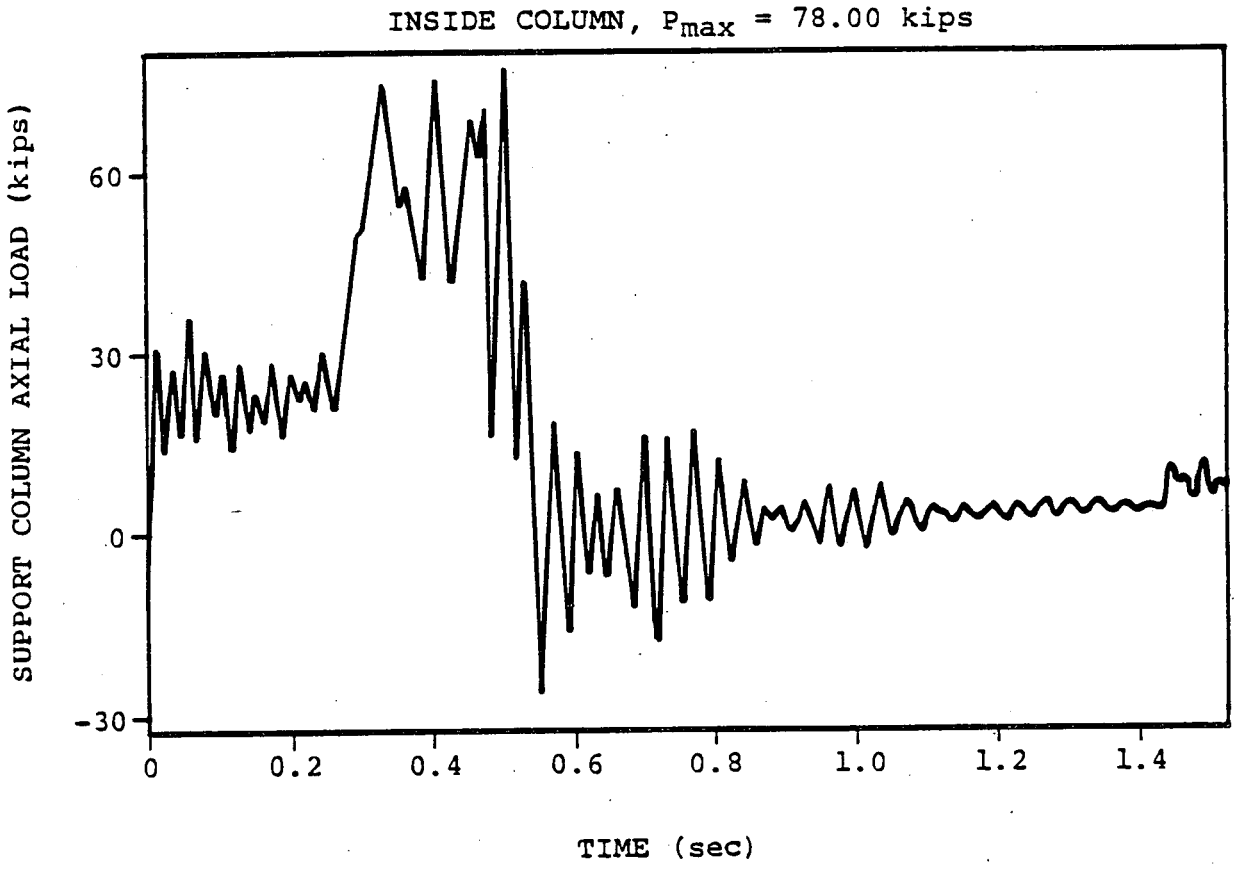

Figure 3-2.5-2

VENT SYSTEM SUPPORT COLUMN RESPONSE DUE TO POOL SWELL IMPACT LOADS - INSIDE COLUMN

3-2.5.1 Discussion of Analysis Results

The results (Table 3-2.5-1) indicate that the largest vent system primary membrane stresses occur for internal pressure loads, vent system discharge loads, pool swell impact loads, DBA condensation oscillation downcomer loads, chugging downcomer lateral loads, and SRV discharge loads. The remaining loadings result in small primary stresses in the vent system major components.

Table 3-2.5-2 shows that the largest vent system support column reactions occur for internal pressure loads, vent system discharge loads, pool swell impact loads, and DBA condensation oscillation loads. The distribution of loads between the inner and outer support columns varies from load case to load case. The magnitude and distribution of reaction loads on the drywell penetrations also vary from load case to load case (Table 3-2.5-3). Table 3-2.5-4 shows that the differential displacements of the vent line bellows are small for all loadings, except for thermal loadings.

The results (Table 3-2.5-5) indicate that the highest stresses in the vent system components, component supports, and associated welds occur for the SBA II and

the DBA I load combinations. The vent line, vent header, and downcomer stresses for the SBA II and DBA I load combinations are less than the allowable limits with stresses in other vent system components, component supports, and welds well within the allowable limits. The stresses in the vent system components, component supports, and welds for the IBA I, DBA II, and DBA III load combinations are also well within the allowable limits.

The results (Table 3-2.5-7) indicate that the vent line bellows differential displacements are all well within allowable limits. The maximum displacement occurs for the SBA II load combination.

The loads which cause the highest number of displacement cycles at the vent line bellows are seismic loads, SRV loads, and LOCA-related loads such as pool swell, condensation oscillation, and chugging. The bellows displacements for these loads are small compared to the maximum allowable displacement, and their effect on fatigue is negligible. Thermal loads and internal pressure loads are the largest contributors to bellows displacements. The specified number of thermal load and internal pressure load cycles is 150. Since the bellows

have a rated capacity of 1,000 cycles at maximum displacement, their adequacy for fatigue is assured.

The vent system fatigue usage factors (Table 3-2.5-8) are computed for the controlling events, which are Normal Operating plus SBA and Normal Operating plus IBA. The governing vent system component for fatigue is the vent header at the downcomer-vent header intersection. The magnitudes and cycles of downcomer lateral loads are the primary contributors to fatigue at this location.

The governing vent system weld for fatigue is the insert plate to vent line shell at the vent line-SRV piping penetration. SRV temperature and thrust loads and the number of SRV actuations are the major contributors to fatigue at this location.

Fatigue effects at other locations in the vent system are less severe than at those described above, due primarily to lower stresses.

3-2.5.2 Closure

The vent system loads described and presented in Section 3-2.2.1 are conservative estimates of the loads postulated to occur during an actual LOCA or SRV discharge event. Applying the methodology discussed in Section 3-2.4 to examine the effects of the governing loads on the vent system results in bounding values of stresses and reactions in vent system components and component supports.

The load combinations and event sequencing defined in Section 3-2.2.2 envelop the actual events postulated to occur during a LOCA or SRV discharge event. Combining the vent system responses to the governing loads and evaluating fatigue effects using this methodology results in conservative values of the maximum vent system stresses, support reactions, and fatigue usage factors for each event or sequence of events postulated to occur throughout the life of the plant.

The acceptance limits defined in Section 3-2.3 are as restrictive as those used in the original containment design documented in the plant's FSAR (in many cases, more restrictive). Comparing the resulting maximum

stresses and support reactions to these acceptance limits results in a conservative evaluation of the design margins present in the vent system and its supports. As demonstrated in the results discussed and presented in the preceding sections, all of the vent system stresses and support reactions are within these acceptance limits.

As a result, the components of the vent system described in Section 3-2.1, which are specifically designed for the loads and load combinations used in this evaluation, exhibit the margins of safety inherent in the original design of the primary containment as documented in the plant's FSAR. The NUREG-0661 requirements, as they relate to the design adequacy and safe operation of the Monticello vent system, are therefore considered to be met.

3-3.0 LIST OF REFERENCES

1. "Mark I Containment Long-Term Program," Safety Evaluation Report, NRC, NUREG-0661, July 1980.

2. "Mark I Containment Program Load Definition Report," General Electric Company, NEDO-21888, Revision 2, December 1981.

3. "Mark I Containment Program Plant Unique Load Definition," Monticello Nuclear Generating Plant, General Electric Company, NEDO-24576, Revision 1, October 1981.

4. Monticello Nuclear Generating Plant, Final Safety Analysis Report (FSAR), Northern States Power Company, Volume III, Section 12, July 1969.

5. "Mark I Containment Program Structural Acceptance Criteria Plant Unique Analysis Application Guide, Task Number 3.1.3," General Electric Company, NEDO-24583-1, October 1979.

6. ASME Boiler and Pressure Vessel Code, Section III, Division 1, 1977 Edition with Addenda up to and including Summer 1977.

7. Biggs, J. M., "Introduction to Structural Dynamics," McGraw-Hill Book Company, N.Y., 1964.